PRECLINICAL FORMULATION DEVELOPMENT AND MECHANISTIC STUDIES OF PLURONIC® P123 JS-K

by

Imit Kaur

A dissertation submitted to the faculty of
The University of Utah
in partial fulfillment of the requirements for the degree of

Doctor of Philosophy

Department of Pharmaceutics and Pharmaceutical Chemistry

The University of Utah

May 2014

The University of Utah Graduate School

STATEMENT OF DISSERTATION APPROVAL

The dissertation of **Imit Kaur**

has been approved by the following supervisory committee members:

Paul J. Shami	, Chair	**10/02/13** Date Approved
Steven E. Kern	, Member	**10/02/13** Date Approved
James N. Herron	, Member	**10/02/13** Date Approved
You Han Bae	, Member	**10/07/2013** Date Approved
Margit-Maria Janat-Amsbury	, Member	**10/03/2013** Date Approved

and by **David Grainger**, Chair/Dean of

the Department/College/School of **Pharmaceutics and Pharmaceutical Chemistry**

and by David B. Kieda, Dean of The Graduate School.

ABSTRACT

The work in this dissertation summarizes the development of a nitric oxide producing prodrug, JS-K in a polymeric Pluronic® P123 micelle formulation. This work is an attempt to advance the formulation development and provide the preclinical rationale by studying: a) formulation stability and toxicity *in vitro* and *in vivo* and plasma protein binding of the drug and the formulation *in vitro*; b) cell distribution of the free drug (JS-K) and the formulation (P123/JS-K) *in vitro*; c) mechanistic pathways triggered by JS-K and P123/JS-K leading to apoptosis and finally; d) development and validation of an analytical method for detection of the drug or formulation and biological metabolites when used in clinical settings.

Except for the mechanistic studies performed where the method employed was Western blot or fluorescence analysis, all the other studies were conducted using analytical methods developed on high performance liquid chromatography (HPLC) equipped with ultra violet (UV) detector. The available method lacked metabolite detection and sensitivity with low drug concentration. Therefore, a more robust, sensitive and elaborate method was developed using ultra performance liquid chromatography (UPLC) equipped with a UV detector. The method was also validated as per United States Pharmacopoeia (USP). The validated method could be used for studying biodistribution, pharmacokinetics and potential toxicity in clinical settings.

The major findings of the dissertation could be succinctly described by stating JS-K in the Pluronic P123 formulation was comparatively more stable than in the free-JS-K formulation. There was no major toxicity observed due to the designed formulation when tested both *in vitro* and *in vivo*. P123/JS-K showed preferential distribution in the cell nucleus, indicating some effect produced by the Pluronic® micelle. Mechanistically, not much difference was observed between JS-K and P123/JS-K and both were shown to produce stress response in leukemia cells. Both JS-K and P123/JS-K were nontoxic to CD34+ hematopoietic cells.

The work described in this dissertation is an attempt to showcase "Bench to Bedside" research in laboratory settings. An attempt has been made to incorporate all the studies required by the regulatory agencies such as US Food and Drug Administration (FDA). The studies performed and the method developed will lay the platform for future studies that are required for filing an Investigational New Drug (IND) application following current Good Manufacturing Practices (cGMP).

I would like to dedicate this dissertation to my parents,
Gurinder Pal Singh and Satwant Kaur
for their unconditional support and encouragement
and
the omnipresent Almighty for anything and everything!

TABLE OF CONTENTS

LIST OF TABLES

Table

LIST OF FIGURES

Figure

PREFACE

Work in this dissertation attempts to provide the preclinical rationale for the development of a nitric oxide (NO)-releasing prodrug, JS-K. Conventional chemotherapeutics suffer from several drawbacks, including drug resistance resulting in relapse. NO has shown activity against leukemia cells. It has also been found to induce differentiation in acute myeloid leukemia (AML) cells. JS-K, a NO donor (NOD) has shown activity against human leukemia (HL-60 cells) cells. The major limitations of the drug are its insolubility in addition to its quick degradation in blood. This is because the drug releases NO upon nucleophilic attack. The cysteines and thiols present in the blood degrade JS-K to release NO. Therefore, this dissertation focuses on the development of a JS-K formulation in polymeric Pluronic® P123 micelles. Each chapter can be considered as advancement in the JS-K development progressing steadily towards its clinical use.

Chapter 2 discusses all the formulation development studies. JS-K was incorporated in Pluronic® P123 and I started development studies from there on. The studies encompassed Pluronic® P123 characterization using established methodologies to analyze the size, shape, specific gravity, viscosity and critical micelle concentration. The studies proceeded further with cell viability assays to test toxicity *in vitro*. Following *in vitro* cytotoxicity, the formulation stability study was carried out comparing nonformulated free JS-K with JS-K incorporated in P123 (P123/JS-K). The next set of studies was carried out to test the interaction of JS-K and P123/JS-K with major blood proteins-

human serum albumin and acid glycoprotein using techniques of equilibrium dialysis and/or fluorescence quenching. For the first time, to our knowledge, a study was conducted comparing two different techniques, i.e., equilibrium dialysis and fluorescence quenching in terms of accuracy and sensitivity. Finally, an *in vivo* tumor regression study was performed in NOD/SCID *IL2Rg*^{null} mice. The drug and the formulation effectiveness were established with greater tumor regression observed in the treated group as compared to the untreated control groups.

Chapter 3 presents the cellular uptake of the free drug compared to formulated drug. HL-60 cells were used to study whole cell uptake and distribution of drug to the cytosol and to the nucleus. The drug uptake was analyzed using high performance liquid chromatography (HPLC). A sensitive JS-K detection method using an HPLC/UV detector was available for the analysis. This proved cost effective and advantageous, as the fluorescent/radio labeled JS-K was not available. Also, it would have added to the cost of analysis. The drug distribution studies established preferential distribution of P123/JS-K inside the nucleus. This result was tested in terms of the possible effect that could have been produced by the drug when distributed into the nucleus. S-glutathionylation of cytosolic proteins was compared with the nuclear protein glutathionylation when HL-60 cells were treated with JS-K or P123/JS-K. Consistent with the uptake study, nuclear protein glutathionylation was greater than cytosolic protein glutathionylation. The results in this chapter laid the foundation for the mechanistic study of JS-K as summarized in Chapter 4.

With nuclear protein glutathionylation established, it was clear that JS-K could induce glutathionylation. Such a posttranslational modification can work in favor or against the

cell function and cell survival. We hypothesized that JS-K induced posttranslational modification and JS-K-released NO could pose stress to the tumor cell, leading to apoptosis. Chapter 4 summarizes results obtained when endoplasmic reticulum (ER) stress and oxidative stress were studied. This was an extensive study as ER stress was studied on HL-60 cells, primary AML cells and hematopoietic stem cells. We studied the rise in intracellular levels of reactive oxygen/reactive nitrogen species to test oxidative stress. Both ER stress and oxidative stress were induced by JS-K or P123/JS-K in HL-60 cells. The study also showed that JS-K or P123/JS-K did not produce any ER stress in normal CD34+ hematopoietic cells, reflecting specificity of the drugs action on the tumor cells.

Chapter 5 finally lays down the method to analyze the drug in the clinical settings. Although there was a HPLC method to analyze the drug, the method lacked sensitivity. Also, the drug is prone to degradation; therefore, a method was required to test small amounts of JS-K. In this study as well, to the best of our knowledge, two sample extraction techniques were compared for the first time. We compared the direct protein precipitation method with protein precipitation followed by solid phase extraction. The UPLC method development was carried out on spiked mouse blood samples. The development study was also executed on mouse organs. The developed method was qualitatively analyzed using mass spectrometry. After the method development, method validation study was performed. USP parameters (linearity, accuracy, precision and ruggedness) were studied to validate the method. This method is important as it allows measurement of JS-K byproducts as well. This is important in the clinical setting to test for the drug or its metabolites.

This dissertation and each chapter of the dissertation justify my five wonderful years of PhD studies. I would like to express my deepest gratitude to my mentor Dr. Paul J. Shami for providing me immense support and exemplary guidance to carry forward my project smoothly. In addition, I would also like to thank him for the open, motivating and unbiased environment conducive to perform studies successfully. I would like to acknowledge his support for openness to any hypothesis or study proposed. This helped me grow as a scientist and plan and execute the research independently. Dr. Shami is a man of principles and insists on truth and honesty in research. I can say without doubt that I learned correct research ethics from him. He has constantly strived to make meaningful research available for the patients. This has inspired me and made me strong in my goal of working for "bench to bedside" research. I would like to thank Mr. Ken Kosak, senior technician at Dr. Shami's lab. He has been like a second mentor to me and has helped me immensely grow up as a scientist. My admiration for research was transformed into love for research under his guidance, as I was a fresh graduate with no lab experience. Ken was very patient and very rational in his approach. Ken is an experienced scientist and his method of mentoring is outstanding. He has been my source of inspiration throughout. I would also like to thank other members of Dr. Shami's lab. They have been instrumental in carrying out my research successfully. I would also like to thank Mrs. Susan Kosak and Mrs. Tania Shami for being wonderful guardians and looking out for me. Susan has always treated me like her daughter and has given me love and support throughout the last five years.

I would like to give a special thanks to Dr. Steven Kern for believing in me and accepting me as his last student. I would also like to thank him for giving me a lab and

project of my interest. To work in translational science was my goal and Dr. Kern understood and supported me in the project. He has also been my source of inspiration and has inspired me to multitask and work and explore different fields. I would also like to thank him for the tuition support.

I would like to thank my other committee members, Dr. James N. Herron, Dr. Margit-Maria Janat-Amsbury and Dr. You Han Bae for their unceasing scientific advice. Dr. Herron has helped me immensely with different projects. He has provided his valuable and unbiased guidance whenever needed.

I would like to express my gratitude to Dr. Dinesh Patel for the fellowship support at the Department of Pharmaceutics and Pharmaceutical Chemistry in 2008.

I would like to thank my friends in India and the United States for making my stay in the United States easy. I would like to thank them for their personal and professional support. I would express my special gratitude to Mukul Retdhania, Ankur Jain, Natasha Sharma, Priyanka Garg, Yu Tian and Li Tian. In addition, I would like to thank my cousin and his wife Mr. Jaswinder Singh and Mrs. Reena Kaur for their support and love.

I would also like to thank family friends Mr. J.B. Singh and Mrs. Maninder Kaur for loving me and supporting me here in Utah.

I would like to express my sincere thanks to my family for being supportive throughout. I would like to give a special thanks to my parents Mr. Gurinder Pal Singh and Mrs. Satwant Kaur for being with me through thick and thin. Their love, support and encouragement helped me progress forward even with the challenges encountered during my PhD studies. My father always gave me an optimistic view of the failure and my mother cheered me up with her spiritual and motivational chats. I would also like to thank

my siblings, my sister Mrs. Manpreet Kaur and my brother Mr. Mandeep Singh, for being very understanding and providing their full support. My sister has always provided me support through her inspiring phone calls, encouraging text messages and motivating letters and e-mails. My brother has always supported me personally, professionally and financially. In spite of being a busy businessman, he has always made it a point to visit me in Utah if he ever visited the United States. I can say confidently that I owe my PhD to my siblings, as they are the ones who actually instilled the importance of education in my life. I would also like to thank my brother-in-law, Mr. Tanveer Singh, and my sister-in-law, Mrs. Jaspal Kaur, for their unconditional love and support throughout. I would like to thank all the kids, Gursimar Kaur, Bhavmeet Singh, Bhavjus Singh, Tavleen Kaur and Iksimar Kaur, for loving me and cheering me up with their innocent motivational chats. I would like to thank my in-laws for believing in me and encouraging me. I would like to thank my mother-in-law Mrs. Tejinder Kaur for taking care of me and giving me love during my low times in Utah. My father-in-law Amarjit Singh has encouraged me with my PhD completion when I had dwindling faith and patience. I would also like to thank my brother-in-law Akshdeep Singh for the love and support. Finally, I would like to thank my husband Dr. Harsimar Singh for his constant support and unconditional love. He has been my real inspiration during my gloomy days. He manages to uplift my spirits even when he comes home tired from his daily schedule.

In the end, I would like to thank the *Almighty* for being with me and for me throughout. I came from a sheltered family and it would have had been impossible for me to survive all by myself.

CHAPTER 1

INTRODUCTION AND BACKGROUND

1.1 Leukemia

Leukemia is bone marrow cancer resulting from accumulation of uncontrolled, non-functional hematopoietic cells. The term can be used to describe four major types based on the type and time of accumulation of the blood cells. While chronic leukemia results from a differentiation block at a later stage of differentiation, acute leukemia stems from an earlier differentiation block. Myeloid leukemia results from accumulation of myeloid blasts while lymphoid leukemia is manifested by accumulation of lymphoid blasts (5). According to the Leukemia and Lymphoma Society, nearly 291,521 people are currently suffering from or recovering from leukemia in the USA (6). Fig. 1.1 illustrates the involvement of the stem cells and development of different types of leukemia. Table 1.1 shows the incidence of different types of leukemia.

1.1.1 Acute myeloid leukemia (AML)

1.1.1.1 Disease and incidence

AML is a blood malignancy characterized by uncontrolled expansion of myeloid blast cells in the bone marrow and peripheral blood or other tissues (7). AML is the most common adult acute leukemia (8) and progresses rapidly without treatment. This leukemia is diagnosed commonly in older patients with a median age of 67 years. In older

patients, the response to chemotherapy is lower than in younger patients, making it a particularly challenging disease in the older age group (9).

1.1.1.2 Treatment options available and the impact

Currently AML is treated with cytotoxic chemotherapeutics aimed at killing leukemic blasts. The induction therapy includes anthracycline/cytarabine combinations followed by consolidation therapy. In certain cases, autologous or allogenic hematopoietic stem cell transplantation is performed to achieve complete eradication and generate immune response (10).

1.2 Glutathione (GSH)

Glutathione or L-γ-glutamyl-L-cysteinyl-glycine is composed of three amino acids and synthesized de-novo by the action of two energy dependent enzymes, γ-glutamate-cysteine ligase and GSH synthase (11). It is the most abundant nonprotein thiol present in the cell with 85-90 % localized in the cytosol (12). GSH is an essential antioxidant and is necessary for cell survival. It is involved in a plethora of functions, including cell signaling, cell detoxification by xenobiotic efflux response, thiol-disulfide reversible reaction and providing a reservoir for the cysteine pool (13). The redox status in the cell is maintained by a delicate equilibrium between reduced GSH and the oxidized/disulfide form of GSH (GSSG). Such an equilibrium is important for providing a reducing environment for maintaining proteins in the reduced form and also allowing reversible double bond formation (14).

1.2.1 Glutathione as redox regulator

The ratio of GSH/GSSG is critical for maintaining the redox balance of the cells. Proteins are generally kept in reduced form by GSH (15). In addition to changes in GSH/GSSG levels, the cellular redox status could be changed by depletion of GSH levels due to xenobiotics/drug metabolism and reactive oxygen or reactive nitrogen species generation (16). Redox sensitive proteins have a thiol moiety on the side chain of the cysteine (Cys) residue that is sensitive to the redox status of the cell and prone to S-glutathionylation. These Cys residues can exist as thiolate anions at physiological pH and can have charge interactions with the basic amino acid residues. This makes them more prone to oxidation. While reversible oxidation can result in the formation of sulfenic acid and protein or formation of mixed disulfides, irreversible oxidation (more detrimental) results in the formation of sulfinic acid and sulfonic acid (17).

1.2.2 Glutathione and protein posttranslational modification

Protein glutathionylation is a reversible reaction (except in the cases where sulphonic acid moieties are formed) occurring under physiological conditions and under conditions of oxidative and nitrosative stress (17). It can occur between two proteins (interprotein) or within a protein (intraprotein disulfide) (18). Protein glutathionylation is determined by the availability of the cysteine residue that is dependent on its three-dimensional (3D) conformation and reactivity. Also, modification of protein thiol can affect the protein activity, depending on the cysteine residue involved. Broadly, protein glutathionylation can occur in five different ways (19):

a) Thiol-disulphide exchange

$$PSH + GSSG \rightarrow P\text{-}S\text{-}S\text{-}G + GSH$$

This reaction is mainly determined by the GSH/GSSG ratio.

PSH: protein sulfhydryl. PSSG: protein disulfide.

b) Direct oxidation

$$GSH + PSH \rightarrow PSSG$$

PSH: protein sulfhydryl. PSSG: protein disulfide.

c) Formation via intermediates: Sulfinic acid- and sulphonic acid-formed oxidized products are stable and irreversible. They are formed under oxidizing conditions.

The cysteine-sulfenic acid (SOH) can also react with GSH. It forms a reversible product. This two step reaction can be represented as:

$$PSH + H_2O_2 \rightarrow PSOH + H_2O$$

$$PSOH + GSH \rightarrow P\text{-}S\text{-}S\text{-}G + H_2O$$

PSOH: protein-sulphenic acid

d) S-nitrosothiols: Protein-S-nitrosothiols react with GSH to form S-nitrosoglutathione (GSNO) releasing free protein. The S-nitrosoglutathione then reacts with GSH again

$$PS\text{-}NO + GSH \rightarrow GSNO + Protein$$

$$GSNO + GSH \rightarrow GS\text{-}SG + HNO$$

$$GS\text{-}SG + PSH \rightarrow PS\text{-}SG + GSH$$

e) Thiyl radicals: Hydroxyl radicals (OH°) react with GSH to form thiyl radicals (GS°). The reaction of glutathionylated protein could be catalyzed by glutaredoxin.

$$PSH + HO^\circ \rightarrow PS^\circ + H_2O$$

$$PS^\circ + GS^\circ \rightarrow PS\text{-}SG$$

The primary method of formation of gluatathionylated protein is by thiol-disulfide exchange. This generally occurs when GSH/GSSG equilibrium is disturbed and the GSSG form exceeds the GSH form. Exchange occurs between the thiol group of the protein and the disulfide group of the GSSG to form protein disulfide and glutathione (20). Protein glutathionylation also results during the conditions of oxidative stress where protein sulfhydryl can directly be oxidized to protein disulfide in the reaction catalyzed by oxidants. Glutathionylated proteins can also be formed irreversibly via sulfenic acid intermediates. S-nitrosothiols and thiyl radicals can also form reversible or irreversible glutathionylated proteins (21).

1.2.3 Glutathione in cell survival

GSH has been found to be important for cell survival. In the past, studies have shown that GSH deficient cells are prone to apoptosis (22). Apoptosis or programmed cell death has been found to be modulated by GSH levels or by the posttranslational modifications of proteins induced by GSH. Early stages of apoptosis are therefore considered the hallmark of the cell death process. Oxidation of GSH to GSSG could occur due to the reactive species generated by the chemotherapeutics or metals and xenobiotics. This later leads to apoptotic response (23-26).

1.3 Glutathione-S-transferases (GST)

GST constitute a family of phase –II detoxification enzymes involved in catalytic and noncatalytic functions. They are divided into cytosolic or microsomal classes. While the microsomal GST are involved in leukotriene and prostaglandin metabolism, the cytosolic GST are divided into seven isotypes: GST α (A), GST μ (M), GST π (P), GST σ, GST θ,

GST ω and GST ζ. GST A, M and P have been found to be involved with tumor progression and chemotherapy resistance (27). The catalytic function of GST involves the catalysis of reaction between glutathione and xenobiotics and thus efflux of the conjugate by rendering it more water-soluble. The reaction takes place at the S atom of the glutathione with an electrophilic group (from the xenobiotic). The noncatalytic function of GST includes their inhibition of c-Jun-N-terminal-kinase protein (cJNK) (a stress-induced mitogen activated protein kinase (MAPK) protein), thus inhibiting apoptotic response (28). Therefore, drug resistance induced by GST could be attributed to either direct detoxification response or indirect response by inhibiting the MAP kinase pathway.

1.4 Nitric Oxide (NO)

NO is a free radical involved in a variety of physiological functions of the cell. The physiological functions of NO encompass smooth muscle relaxation, neuronal transmission and platelet aggregation. It is involved in cell signaling by inducing post-translational modifications (29). NO moieties could be incorporated into protein groups and lead to reversible or irreversible protein modification, as explained later in detail. NO is also involved in inflammation, mutagenesis and carcinogenesis (30). On the other hand, NO has also shown antitumoral properties. It can lead to apoptosis by targeting various cellular sites and bringing about posttranslational modifications such as S-Nitrosylation, S-Glutathionylation and ribosylation (2). Also, NO was found to induce differentiation in AML cells (31, 32). Thus NO enacts as the double-edged sword where the function of NO is dependent on source of NO (endogenously generated or exogenously supplied), cell type, concentration, rate of delivery and production (if

endogenous source) (4). Due to the diverse and pleiotropic effects of NO, it is important to deliver it at the target site. Fig. 1.2 shows the multiple facets of NO.

1.4.1 Nitric oxide as a free radical

Endogenously, NO is generated by three isoforms of the nitric oxide synthase (NOS): inducible NOS (iNOS), endothelial NOS (eNOS) and neuronal NOS (nNOS) (33). NO can react with oxygen to form reactive nitrogen species (RNS) or with glutathione to form S-nitrosoglutathione (GSNO called as S-nitrosylation) (34) or with heavy metals (35) or with macromolecules such as DNA (36) and proteins. NO also leads to S-thiolytion, disulfide bond formation, sulfenic, sulfinic and sulfonic acid derivatives. Under normal physiological conditions, the cells maintain a reducing environment with antioxidants (such as GSH, superoxide dismutase, Vitamins A, E and C) present. This keeps reactive oxygen and reactive nitrogen species at low levels, thus protecting the cells from oxidative damage. In a broad sense, RNS includes nitric oxide radical (NO°), peroxynitrite ($ONOO^-$) and nitrogen dioxide radical (NO_2°) (2). Alternatively, NO can also act as antioxidant and react with ROS such as superoxide (37).

1.4.2 Nitric oxide and protein modification

NO modulates cell signaling by inducing posttranslational modifications that affect protein structure, activity and function. Such modifications can be brought about by direct interaction of NO with proteins or by producing RNS. Such an addition occurs generally at the Cys residues of the proteins (38). S-nitrosylation affects cell signaling and major processes such as phosphorylation, acetylation, palmitoylation and ubiquitylation, affecting cell survival (39). Nitration of proteins also occurs at the

tyrosine residues (to form protein 3-nitrotyrosine) as a response to oxidative stress. This generally occurs through peroxynitrite generation. Such a nitration serves as a biomarker for nitrosative stress (40). The posttranslational modification induced affects the hydrophobicity, redox potential, pKa and volume of the affected protein (41, 42). NO can also induce intermolecular and intramolecular disulfide bonds affecting structure and reactivity of proteins (43).

1.4.3 Nitric oxide and glutathione

S-nitrosylation, a posttranslational modification, occurs after oxidation of NO to dinitrogen trioxide (N_2O_3) that acts as source of nitrosonim ion (NO^+). In addition to N_2O_3, other sources of NO^+ include nitrous acid (HNO_2), alkylnitrite and dinitrogen tetraoxide (N_2O_4) (44). S-Nitrosylation reactions can then proceed through reactions of NO with thiolates, thiyl radicals and transition metals (45). S-nitrosylation is enhanced with high hydrophobicity of proteins (46). It has been found that S-nitrosylation of proteins enhances glutathionylation (47). S-nitrosyltion has been found to be abnormal in pathological conditions, including cancer (46). Cys residues of proteins are prone to redox-based modifications and electrophilic substitution reactions. Glutathionylation of Cys is one such redox-based modification. S-nitroso-GSH or GSNO is the most abundant non-protein thiol in the cell and undergoes group transfer reaction to glutathionylate proteins (48). It was found that glutathionylation induced by NO is both reversible and saturable (47).

1.4.4 Nitric oxide and cell survival

Nitric oxide promotes cell growth but has also been found to induce cell senescence (1). In general, the cell survival pathways of NO are linked with protumorigenesis effects. Therefore, NO can produce both pro- and antitumorigenic effects. This has been explained in Figures 1.2 and 1.3.

1.4.5 Nitric oxide and cancer

NO has been implicated in cancer. This radical can be both procancerous and anti-cancerous, depending on the concentration, the cell type affected and the type of tumor microenvironment (49, 50). Several studies have been performed with NO or NO donors with or without chemotherapeutic agents and mixed responses have been observed (49). NO has been shown to be involved with cancer progression through tumor migration, invasion, angiogenesis and metastasis (1). Studies have suggested that NO, iNOS and sometimes eNOS are involved in solid tumors such as lung cancer, melanoma, colon cancer and pancreatic cancer (51-55). On the other hand, solid tumors have also been shown to become sensitive to chemotherapeutics when NO (by itself or in the form of NO donor) is included with regular chemotherapy or other drugs targeting cancer cells (56-60). Thus, NO can act as a chemosensitizing agent (37). Mitochondria, the energy store of the cell, gets nitrated under basal and diseased conditions (61), thus affecting cell survival. The mechanisms of protumorigenesis and antitumorigenesis effects of NO have been explained in the Fig. 1.3.

1.5 Nitric Oxide Donors (NOD) and Arylated Diazeniumdiolates (ADZD)

As explained in the text, millimolar concentrations of NO can induce apoptosis. Therefore, NO donors hold great potential as effective chemotherapeutic agents. To date, various NO donors are available clinically or are in process of development (organic nitrates, metal-NO complexes, diazeniumdiolates or drug conjugated to NO) (30, 58, 60, 62, 63). The different classes of NOD are shown in Fig. 1.4.

Generally, the nitrate and the furoxan classes of NOD have been studied in chemoprevention and the diazeniumdiolates class has been studied in chemotherapy. Therefore, with use of NOD, generally one of the purposes is achieved that includes either direct chemotherapy or use of NOD for chemoprevention or using the NOD for attenuating the side effects produced due to chemotherapy (64). Diazeniumdiolates (DZD) could be regarded as NOD acting as prodrugs releasing NO spontaneously or due to some enzymatic reactions (65, 66). Generally, a diazeniumdiolate ion (or the sodium salt) is first prepared by exposing a solution of a suitable nucleophilic compound (X-) to 5 atmospheres of NO under anaerobic conditions (67). Structural studies confirmed the substantial double bond character of the N=N linkage of many X-N(O)=NO^- ions, with the oxygen atoms being cis to one another; this and other features of their structures led to their formal designation as “diazeniumdiolates”. A structural example of such a DZD salt would be X-N(O)=NO^- Na^+, where one of the oxygen atoms (O^2) can form a salt (66).

Also, when X is a secondary amine residue, these products were found to yield 2 mol/mol NO at physiological temperature and pH, with half-lives ranging from 2 s to 20 h, depending on the type of the amine moiety attached (66).

It was further discovered that for X-N(O)=NO^- Na^+, the ionized oxygen, (O^2), can be further derivatized (i.e., alkylated) to provide additional stability to the entire compound. The addition of various moieties to the O^2 oxygen of the DZD is generally called "O^2 - alkylation", and forms the protecting/shielding group (68) as explained later in the text.

In contrast to other NO donors, DZD are easy to manage and study, as they release NO at first order rate in simple aqueous solutions or buffered solutions without requiring any redox activation. This allows the study to be carried out easily with steady NO generation (66). Also, they offer potentially site-selective NO release. Their rate and duration of NO release could be altered and modified (69). In the arylated diazeniumdiolates (ADZD), the O^2 position of the diazeniumdiolate is derivatized by an aryl shielding group to form a prodrug (70) (Fig. 1.5). ADZD are NO-generating prodrugs (JS-K, an ADZD has 2,4-dinitrophenyl as the shielding group). They are designed to be activated by GSH or other nucleophiles; the reaction can be catalyzed by GST. As explained before, GST enzymes catalyze the reaction between the S atom of GSH and the electrophilic center of xenobiotics, making the formed complex more water-soluble.

ADZD provide an electrophilic center for the GST enzyme and release NO upon attack by cellular nucleophiles, including GSH (71). As stated before, the GST-π isoform is over-expressed in several tumors and α and μ forms are expressed to a lesser extent comparatively (28). Therefore, ADZD were designed to be activated by upregulated

isoforms. Out of the several ADZD, PABA/NO (70-73) and JS-K (74-93) have been studied extensively for their anticancer effects. Molecular modeling studies showed that PABA/NO structure was designed to fit GST-π whereas the JS-K structure fits well to the GST-α and μ forms (71). In our lab, we continued our studies with JS-K.

1.6 O^2-(2,4-Dinitrophenyl) 1-[(4-ethoxycarbonyl)piperazin-1-yl]diazen-1-ium-1,2-diolate or JS-K

1.6.1 Need for development

Cancer cells have been found to be sensitive to the effect of NO (94). Also, in previous studies, it was shown that AML cells showed unusual sensitivity to NO (32, 95). Because of the above stated reasons, a library of the ADZD was tested using HL-60 human AML cells and JS-K was found to be the most potent inhibitor *in vitro* and *in vivo* with an IC_{50} ranging from 0.2-0.5 μM. JS-K is a prodrug and releases NO upon action by GSH or other cellular thiols with or without GST catalysis.

1.6.2 Chemistry

JS-K (Fig. 1.6) chemistry shows that this ADZD can release NO upon nucleophilic attack on the dinitrophenyl (DNP) ring. The DNP ring stabilizes the whole structure. During the development of the compound, structure activity relationship studies were performed and the metabolites of JS-K were studied and tested for their *in vitro* cytotoxic potential on the HL-60 cells. It was found that in addition to NO, the other metabolites, namely N-(ethoxycarbonyl)piperazine (IC_{50} 8.6 μM) and glutathione-dinitrophenyl (IC_{50} 8.4 μM) were cytotoxic as well (89). JS-K is a very labile compound and it slowly hydrolyzes to release dinitrophenol.

1.6.3 Potential chemotherapeutic

JS-K has shown toxicity towards a broad spectrum of cancer cell types. Several *in vitro* studies have been performed on various cell types to study the cytotoxic effects of JS-K, as detailed later in the text. As stated before, the initial screening of ADZD was carried out with leukemia cells. JS-K's cytotoxic effect has been tested on hematological malignancies, including myeloid leukemia (88-91), lymphoid leukemia (86) and myeloma (79). JS-K's cytotoxicity was also tested on solid tumors, including prostate (90), breast (84), lung (82), colon (76), liver (87) and glioma (93). The mechanism of JS-K action was also studied in several tumor types (Table 1.2). Conclusion of these studies was that JS-K has a broad spectrum of activity and is cytotoxic through different mechanisms, thus holding promise as a drug candidate. In our lab, JS-K *in vitro* cytotoxicity and *in vivo* tumor regression was studied using prostate cancer cells and AML cells. Although JS-K possessed cytotoxic potential in both the cancer types, higher sensitivity was observed in AML cells. It was inferred that JS-K showed higher sensitivity towards rapidly dividing liquid cancers as compared to slowly proliferating solid cancers (90).

1.6.4 Mechanism of JS-K cytotoxicity

Several studies have been performed with an attempt to delineate the mechanism of JS-K toxicity. Some common mechanisms have been reported in both solid and liquid tumor models. Table 1.2 outlines the proposed mechanisms in different tumor models. Recent literature has suggested that the relapse of AML could be attributed to the presence of a subpopulation of leukemic stem cells (LSC). Factors leading to survival of LSC could be divided into "extrinsic" factors (EF) and the "intrinsic" factors (IF) (96).

While the IF includes the cell cycle regulators, prosurvival pathways (NFκB), cell stress (oxidative, genotoxic etc) and self renewal components/pathways (β-catenin) (97), the EF encompasses the factors relating to the tumor microenvironment (bone marrow in the case of AML) and broadly includes chemokine receptors (CXCR4), adhesion molecules (CD44) and proteins involved in the maintenance of the hypoxic tumor environment (96). Mechanistic studies of JS-K have been performed with respect to both IF and EF. Although most studies were performed on tumor cells and not the tumor stem cells, the studies lay the foundation for future experiments that could be performed in tumor stem cells. The IF's such as the cell cycle regulation (86, 90), survival pathways (NFκB) (77), cell stress (79, 82, 84, 87) and self renewal pathway (86) have been explored in liquid cancers and some solid cancers. Also, the EF such as angiogenesis (78) and survival and growth factors required for the maintenance of the tumor have been studied (79). In our lab, we studied mainly the IF affected by JS-K in leukemia. An effective chemotherapeutic is required to possess broad mechanism and nontoxicity towards normal cells. In our lab and in other labs, JS-K was found to be nontoxic to normal cells. (75, 79, 84) Another important aspect of JS-K revealed its potential use in personalized medicine. In the lung cancer model, JS-K was found to be particularly toxic to a subset of a panel of various lung cancer cell lines (82). The cell lines with basally higher levels of reactive oxygen or reactive nitrogen species were most sensitive to JS-K's effect. Fig 1.7 shows factors related to AML relapse and JS-K's potential effects on those factors.

1.6.5 JS-K synergy with other drugs

With its broad mechanisms of action, JS-K was tried in combination studies. This is important for the future clinical application of the drug. The combination studies were

performed with cytarabine (ARA-C), daunorubicin and etoposide in AML. JS-K showed strong synergy with ARA-C in HL-60 cells. On the other hand, it showed antagonism with daunorubicin and etoposide (88). In another study, JS-K showed the reversal of resistance by making cells more sensitive to clinical chemotherapeutics like arsenic and platinum. JS-K also resulted in the increased accumulation of these chemotherapeutics (80). In yet another study, JS-K combination with the proteasome inhibitor Bortezomib was studied (79). The study showed that low doses of Bortezomib were synergistic with JS-K. Bortezomib is now used for the treatment of relapsed multiple myeloma (98) and refractory mantle cell lymphoma (99). One of the possible mechanisms could be the triggering of the endoplasmic reticulum (ER) stress. Bortezomib, being a proteosome inhibitor, causes ER stress (100) due to accumulation of proteins. In our lab, we studied ER stress triggered by JS-K (positive). Therefore, it could be argued that along the same lines, the combination might show synergism with JS-K in AML cells as well. Recently, Bortezomib has been tried in combination with experimental drugs *in vitro* (101) and with clinical chemotherapeutic in AML patients (102, 103). Another reason we propose for the possible synergism between JS-K and Bortezomib is the induction of oxidative stress by both drugs (100). Also, Bortezomib has been found to inhibit the NFκB survival pathway (104).

1.6.6 Pitfalls in JS-K development and alternatives

One of the major drawbacks in the use of JS-K is its extremely short half life. Half life is an important factor for JS-K development as the release of NO affects physiological function. The immediate release of NO not only prevents the drug distribution to the site of action but also could result in potential hypotension. Although

the studies performed showed no such hypotensive effects at therapeutic doses, hypotension could occur at higher doses. Another major hurdle in the JS-K development was its extreme hydrophobicity. Therefore, a polymer Pluronic® formulation of JS-K was developed. Pluronic® P123 micelles hold JS-K in the micelle core providing stabilization and solubilization.

1.7 Poloxamers

1.7.1 Polymers and drug delivery

"Polymer therapeutics" refers to the use of the polymer in evoking or modifying pharmaceutical drug availability and/or mechanism of action (105). Drug delivery of hydrophobic drugs using polymeric nanoparticles is a promising strategy. In addition to solubility of the drugs, drug incorporation also offers stability, targeting, controlled release, prolonged duration, reduced toxicity and some extent of biological activity imparted by the polymer itself (106, 107). The field has progressed significantly in the delivery of anticancer drugs. This is because of the systemic toxicity and extensive clearance due to action of drug efflux proteins on nonformulated chemotherapeutics. Therefore, polymeric systems offer the advantages of drug encapsulations and limited interaction with the healthy cells, thus enabling dose increase and reduced toxicity (108). Polymeric systems could be prepared and used according to need. They could be used for passive targeting or active targeting. They could also be designed for site-directed delivery or site-triggered delivery. They could be made pH responsive or temperature responsive (109-114). Nine polymeric anticancer (nanomedicine) drugs have been approved for clinical use so far (115).

1.7.2 Polymeric micelles/Pluronic® or poloxamers

Polymeric micelles obtained from block copolymers are nano-sized drug delivery systems possessing a hydrophilic shell (providing steric stability and targeting ability) and drug encapsulating hydrophobic core (encapsulation could be nonionic or ionic or covalent). The size range of these systems usually fall from 10-100 nm, which offers the advantage of bypassing both renal clearance and the reticuloendothelial system (116). Also, the abnormal tumor vasculature allows enhanced permeability and retention of the chemotherapeutic when encapsulated in polymeric micelles (117). Polymeric micelles have been used to deliver chemotherapeutics, imaging agents, small proteins and peptides, DNA and siRNA (111, 118-125)

Amphiphilic block copolymers can form polymeric micelles. They consist of a basic unit comprised of ethylene oxide (EO) and propylene oxide (PO) arranged as EO-PO-EO units (Fig. 1.8). The number of EO and PO can be altered, resulting in polymeric micelle of varying hydrophobicity (high PO content), chain length, hydrophilic-lipophilic balance and critical micelle concentration (105).

1.7.3 Advantages and disadvantages offered by poloxamers

Poloxamers have been used extensively as drug excipients, thus enhancing drug solubility and delivery (105). They have shown activity against drug efflux transporters due to their ability to form micelles. The unimers interact with the cancer cells and inhibit the drug efflux transporters, thus leading to sensitization of the cell to enhance drug accumulation (126, 127). The formed micelles have prolonged circulation due to their stability against dilution. As explained before, the shell and the core of the formed micelle can be designed based on the need. Due to the above advantages, poloxamers

could be considered as potential drug delivery systems with low toxicity (128). The use of Pluronic in the clinic has also highlighted some disadvantages offered by this miceller system. These include compromised drug loading capacity, poor blood stability as compared to other polymeric systems and limited information about their interaction with cells and effects produced (129).

1.7.4 Physical properties of poloxamers affecting drug delivery

The properties affecting the poloxamer structure, drug incorporation capability and bioactivity could be summarized as following:

1.7.4.1 Critical micelle concentration (CMC)

The individual block copolymers of the poloxamer possess the potential of self-assembly into micelles. The concentration at which micellization occurs is termed the critical micelle concentration or CMC. When the concentration exceeds the CMC, there exists a dynamic equilibrium between the unimers and the micelles. The chain length affects CMC as increase in the PO length reduces the CMC (130). CMC is important from a drug delivery aspect as it determines the stability of the micelle. This is explained in the following section. Also, it affects the biological response produced by the poloxamers (105).

1.7.4.2 Thermodynamic stability

The thermodynamic stability of polymeric micelles could be defined in terms of standard free energy change for the micellization process as:

$$dG = RTln(CMC)$$

The CMC of block copolymer is usually in the range of 10^{-6}-10^{-7} M, which is nearly three-four times lower when compared to small molecule surfactants. Due to this, poloxamers offer increased stability. This prevents extensive dilution of the micelles in the body fluids; thus, there is a reduced probability of these micelles to disassemble at small concentrations (128). The poloxamers also possess kinetic stability that provides protection to the micelle structure enabling a slow disassembly into unimers at extreme dilutions (131).

1.7.4.3 Micelle size

Generally, micelles preferred for pharmaceutical applications are less than 100 nm (105). The size of the micelle is an important consideration as it affects circulation in the blood and biodistribution (132).

1.8 Pluronic® P123 (P123)

P123 is an amphiphilic polymeric micelle with a molecular weight of 5750. The average number of EO and PO units are 40 and 70, respectively, with a CMC value of 4.4 μM (105). P123 possess higher stability due to longer hydrophobic block and low CMC value (133). Several studies have been performed where P123 alone or in combination with other poloxamer has been used to deliver chemotherapeutics. In one such study, Paclitaxel (PTX) was incorporated in P123 and the studies revealed higher accumulation of the drug in the tumor tissue. It also showed improved pharmacokinetic profile when compared to nonformulated PTX (134). Although P123 is not FDA approved like F127 and F68 (133), the increasing number studies performed with this poloxamer (133-139) illustrate its potential therapeutic and clinical application.

1.9 Unmet Needs

Treatment of acute myeloid leukemia is still an unmet need because of the high incidence of relapse in spite of aggressive therapy (140). Treatment failure combined with the development of drug resistance makes remission challenging. Leukemia relapse has been attributed to the presence of leukemia stem cells (LSC) or leukemia initiating cells (LIC) that were discovered over a decade ago (141). Recent data suggest that one could target LSCs by targeting surface antigens expressed on LSC or by affecting the microenvironment supporting LSC interaction or by inhibiting the signaling pathways that provides growth signals and self-renewal potential to the LSC (96).

Cancer cells acquire resistance due to development of the multidrug resistance phenotype (MDR phenotype) by activation of efflux proteins such as MRP1, ABC and BCRP; due to repair of damaged DNA; gene mutations such as that of p53 or by over-expressing detoxification enzymes such as GST. As stated by Townsend et al., one of the most effective way of targeting resistance and thus cancer is to exploit the therapeutic potential of GST. They suggest three ways to target GST. GST's could be targeted with GST inhibitors, drugs that promote GST oligomerization and thus JNK activated apoptotic pathway or by exploiting the elevated GST expression in the tumors by designing GST-activated prodrugs (28). JS-K falls into the third category.

1.10 References

1. Burke AJ, Sullivan FJ, Giles FJ, Glynn SA. The yin and yang of nitric oxide in cancer progression. Carcinogenesis. 2013;34(3):503-512.

2. Leon L, Jeannin JF, Bettaieb A. Post-translational modifications induced by nitric oxide (NO): implication in cancer cells apoptosis. Nitric Oxide. 2008;19(2):77-83.

3. Muntane J, la Mata MD. Nitric oxide and cancer. World J Hepatol. 2010;2(9):337-344.

4. Thomas DD, Ridnour LA, Isenberg JS, Flores-Santana W, Switzer CH, Donzelli S, Hussain P, Vecoli C, Paolocci N, Ambs S, Colton CA, Harris CC, Roberts DD, Wink DA. The chemical biology of nitric oxide: implications in cellular signaling. Free Radic Biol Med. 2008;45(1):18-31.

5. Wong RS, Cheong SK. Leukaemic stem cells: drug resistance, metastasis and therapeutic implications. Malays J Pathol. 2012;34(2):77-88.

6. Sung L, Aplenc R, Alonzo TA, Gerbing RB, Lehrnbecher T, Gamis AS. Effectiveness of supportive care measures to reduce infections in pediatric AML: a report from the Children's Oncology Group. Blood. 2013;121(18):3573-3577.

7. O'Donnell MR, Abboud CN, Altman J, Appelbaum FR, Arber DA, Attar E, Borate U, Coutre SE, Damon LE, Goorha S, Lancet J, Maness LJ, Marcucci G, Millenson MM, Moore JO, Ravandi F, Shami PJ, Smith BD, Stone RM, Strickland SA, Tallman MS, Wang ES, Naganuma M, Gregory KM. Acute myeloid leukemia. J Natl Compr Canc Netw. 2012;10(8):984-1021.

8. Medeiros BC, Othus M, Estey EH, Fang M, Appelbaum FR. Impact of body-mass index on the outcome of adult patients with acute myeloid leukemia. Haematologica. 2012;97(9):1401-1404.

9. Yanada M, Naoe T. Acute myeloid leukemia in older adults. Int J Hematol. 2012;96(2):186-193.

10. Roboz GJ. Current treatment of acute myeloid leukemia. Curr Opin Oncol. 2012;24(6):711-719.

11. Meng Q, Peng Z, Chen L, Si J, Dong Z, Xia Y. Nuclear Factor-kappaB modulates cellular glutathione and prevents oxidative stress in cancer cells. Cancer Lett. 2010;299(1):45-53.

12. Raza H. Dual localization of glutathione S-transferase in the cytosol and mitochondria: implications in oxidative stress, toxicity and disease. FEBS J. 2011;278(22):4243-4251.

13. Singh S, Khan AR, Gupta AK. Role of glutathione in cancer pathophysiology and therapeutic interventions. J Exp Ther Oncol. 2012;9(4):303-316.

14. Montero AJ, Jassem J. Cellular redox pathways as a therapeutic target in the treatment of cancer. Drugs. 2011;71(11):1385-1396.

15. Dalle-Donne I, Rossi R, Giustarini D, Colombo R, Milzani A. S-glutathionylation in protein redox regulation. Free Radic Biol Med. 2007;43(6):883-898.

16. Chakravarthi S, Jessop CE, Bulleid NJ. The role of glutathione in disulphide bond formation and endoplasmic-reticulum-generated oxidative stress. EMBO Rep. 2006;7(3):271-275.

17. Dalle-Donne I, Rossi R, Giustarini D, Colombo R, Milzani A. S-glutathionylation in protein redox regulation. Free Radic Biol Med. 2007;43(6):883-898.

18. Cumming RC, Andon NL, Haynes PA, Park M, Fischer WH, Schubert D. Protein disulfide bond formation in the cytoplasm during oxidative stress. J Biol Chem. 2004;279(21):21749-21758.

19. Ghezzi P, Di Simplicio P. Glutathionylation pathways in drug response. Curr Opin Pharmacol. 2007;7(4):398-403.

20. Dalle-Donne I, Milzani A, Gagliano N, Colombo R, Giustarini D, Rossi R. Molecular mechanisms and potential clinical significance of S-glutathionylation. Antioxid Redox Signal. 2008;10(3):445-473.

21. Ghezzi P. Regulation of protein function by glutathionylation. Free Radic Res. 2005;39(6):573-580.

22. Markovic J, Garcia-Gimenez JL, Gimeno A, Vina J, Pallardo FV. Role of glutathione in cell nucleus. Free Radic Res. 2010;44(7):721-733.

23. Townsend DM. S-glutathionylation: indicator of cell stress and regulator of the unfolded protein response. Mol Interv. 2007;7(6):313-324.

24. Higuchi Y. Glutathione depletion-induced chromosomal DNA fragmentation associated with apoptosis and necrosis. J Cell Mol Med. 2004;8(4):455-464.

25. Bhalla S, Gordon LI, David K, Prachand S, Singh AT, Yang S, Winter JN, Guo D, O'Halloran T, Platanias LC, Evens AM. Glutathione depletion enhances arsenic trioxide-induced apoptosis in lymphoma cells through mitochondrial-independent mechanisms. Br J Haematol. 2010;150(3):365-369.

26. Guha P, Dey A, Sen R, Chatterjee M, Chattopadhyay S, Bandyopadhyay SK. Intracellular GSH depletion triggered mitochondrial Bax translocation to accomplish resveratrol-induced apoptosis in the U937 cell line. J Pharmacol Exp Ther. 2011;336(1):206-214.

27. Sau A, Pellizzari Tregno F, Valentino F, Federici G, Caccuri AM. Glutathione transferases and development of new principles to overcome drug resistance. Arch Biochem Biophys. 2010;500(2):116-122.

28. Townsend DM, Tew KD. The role of glutathione-S-transferase in anti-cancer drug resistance. Oncogene. 2003;22(47):7369-7375.

29. Moncada S, Palmer RM, Higgs EA. Nitric oxide: physiology, pathophysiology, and pharmacology. Pharmacolo Rev. 1991;43(2):109-142.

30. Weinberg JB. Nitric Oxide and Life or Death of Human Leukemia Cells. In: Bonavida B (editor). Nitric Oxide (NO) and Cancer, Cancer Drug Discovery: Springer Science+Business Media; 2010; p. 147-167.

31. Magrinat G, Mason SN, Shami PJ, Weinberg JB. Nitric oxide modulation of human leukemia cell differentiation and gene expression. Blood. 1992;80(8):1880-1884.

32. Shami PJ, Moore JO, Gockerman JP, Hathorn JW, Misukonis MA, Weinberg JB. Nitric oxide modulation of the growth and differentiation of freshly isolated acute non-lymphocytic leukemia cells. Leuk Res. 1995;19(8):527-533.

33. Hickok JR, Vasudevan D, Jablonski K, Thomas DD. Oxygen dependence of nitric oxide-mediated signaling. Redox Biol. 2013;1(1):203-209.

34. Nikitovic D, Holmgren A. S-nitrosoglutathione is cleaved by the thioredoxin system with liberation of glutathione and redox regulating nitric oxide. J Biol Chem. 1996;271(32):19180-19185.

35. Valko M, Morris H, Cronin MT. Metals, toxicity and oxidative stress. Curr Med Chem. 2005;12(10):1161-1208.

36. Folkes LK, O'Neill P. Modification of DNA damage mechanisms by nitric oxide during ionizing radiation. Free Radic Biol Med. 2013;58:14-25.

37. Sullivan R, Graham CH. Chemosensitization of cancer by nitric oxide. Curr Pharm Des. 2008;14(11):1113-1123.

38. Hess DT, Matsumoto A, Kim SO, Marshall HE, Stamler JS. Protein S-nitrosylation: purview and parameters. Nat Rev Mol Cell Biol. 2005;6(2):150-166.

39. Hess DT, Stamler JS. Regulation by S-nitrosylation of protein post-translational modification. J Biol Chem. 2012;287(7):4411-4418.

40. Radi R. Protein tyrosine nitration: biochemical mechanisms and structural basis of functional effects. Acc Chem Res. 2013;46(2):550-559.

41. Koide S, Sidhu SS. The importance of being tyrosine: lessons in molecular recognition from minimalist synthetic binding proteins. ACS Chem Biol. 2009;4(5):325-334.

42. Yokoyama K, Uhlin U, Stubbe J. Site-specific incorporation of 3-nitrotyrosine as a probe of pKa perturbation of redox-active tyrosines in ribonucleotide reductase. J Am Chem Soc. 2010;132(24):8385-8397.

43. Arnelle DR, Stamler JS. NO+, NO, and NO- donation by S-nitrosothiols: implications for regulation of physiological functions by S-nitrosylation and acceleration of disulfide formation. Arch Biochem Biophys. 1995;318(2):279-285.

44. Pfeiffer S, Mayer, B. and Hemmens, B. Nitric Oxide: Chemical Puzzles Posed by a Biological Messenger. Angew Chem Int Ed. (1999);38(12):1714–1731.

45. Smith BC, Marletta MA. Mechanisms of S-nitrosothiol formation and selectivity in nitric oxide signaling. Curr Opin Chem Biol. 2012;16(5-6):498-506.

46. Anand P, Stamler JS. Enzymatic mechanisms regulating protein S-nitrosylation: implications in health and disease. J Mol Med (Berl). 2012;90(3):233-244.

47. West MB, Hill BG, Xuan YT, Bhatnagar A. Protein glutathiolation by nitric oxide: an intracellular mechanism regulating redox protein modification. Faseb J. 2006;20(10):1715-1717.

48. Singh SP, Wishnok JS, Keshive M, Deen WM, Tannenbaum SR. The chemistry of the S-nitrosoglutathione/glutathione system. Proc Natl Acad Sci U S A. 1996;93(25):14428-14433.

49. Sinha BK, Bhattacharjee S, Chatterjee S, Jiang J, Motten AG, Kumar A, Espey MG, Mason RP. Role of nitric oxide in the chemistry and anticancer activity of etoposide (VP-16,213). Chem Res Toxicol. 2013;26(3):379-387.

50. Hickok JR, Thomas DD. Nitric oxide and cancer therapy: the emperor has NO clothes. Curr Pharm Des. 2010;16(4):381-391.

51. Ambs S, Bennett WP, Merriam WG, Ogunfusika MO, Oser SM, Harrington AM, Shields PG, Felley-Bosco E, Hussain SP, Harris CC. Relationship between p53 mutations and inducible nitric oxide synthase expression in human colorectal cancer. J Natl Cancer Inst. 1999;91(1):86-88.

52. Glynn SA, Boersma BJ, Dorsey TH, Yi M, Yfantis HG, Ridnour LA, Martin DN, Switzer CH, Hudson RS, Wink DA, Lee DH, Stephens RM, Ambs S. Increased NOS2 predicts poor survival in estrogen receptor-negative breast cancer patients. J Clin Invest. 2010;120(11):3843-3854.

53. Ridnour LA, Barasch KM, Windhausen AN, Dorsey TH, Lizardo MM, Yfantis HG, Lee DH, Switzer CH, Cheng RY, Heinecke JL, Brueggemann E, Hines HB, Khanna C, Glynn SA, Ambs S, Wink DA. Nitric oxide synthase and breast cancer: role of TIMP-1 in NO-mediated Akt activation. PLoS One. 2012;7(9):e44081.

54. Lampson BL, Kendall SD, Ancrile BB, Morrison MM, Shealy MJ, Barrientos KS, Crowe MS, Kashatus DF, White RR, Gurley SB, Cardona DM, Counter CM. Targeting eNOS in pancreatic cancer. Cancer Res. 2012;72(17):4472-4482.

55. Godoy LC, Anderson CT, Chowdhury R, Trudel LJ, Wogan GN. Endogenously produced nitric oxide mitigates sensitivity of melanoma cells to cisplatin. Proc Natl Acad Sci U S A. 2012;109(50):20373-20378.

56. Rothweiler F, Michaelis M, Brauer P, Otte J, Weber K, Fehse B, Doerr HW, Wiese M, Kreuter J, Al-Abed Y, Nicoletti F, Cinatl J, Jr. Anticancer effects of the nitric oxide-modified saquinavir derivative saquinavir-NO against multidrug-resistant cancer cells. Neoplasia. 2010;12(12):1023-1030.

57. Donia M, Maksimovic-Ivanic D, Mijatovic S, Mojic M, Miljkovic D, Timotijevic G, Fagone P, Caponnetto S, Al-Abed Y, McCubrey J, Stosic-Grujicic S, Nicoletti F. In vitro and in vivo anticancer action of Saquinavir-NO, a novel nitric oxide-derivative of the protease inhibitor saquinavir, on hormone resistant prostate cancer cells. Cell Cycle. 2011;10(3):492-499.

58. Duan S, Cai S, Yang Q, Forrest ML. Multi-arm polymeric nanocarrier as a nitric oxide delivery platform for chemotherapy of head and neck squamous cell carcinoma. Biomaterials. 2012;33(11):3243-3253.

59. Deng L, Zhang E, Chen C. Synergistic interaction of beta-galactosyl-pyrrolidinyl diazeniumdiolate with cisplatin against three tumor cells. Arch Pharm Res. 2013;36(5):619-625.

60. Rigas B, Williams JL. NO-donating NSAIDs and cancer: an overview with a note on whether NO is required for their action. Nitric Oxide. 2008;19(2):199-204.

61. Castro L, Demicheli V, Tortora V, Radi R. Mitochondrial protein tyrosine nitration. Free Radic Res. 2011;45(1):37-52.

62. Wink DA, Cook JA, Christodoulou D, Krishna MC, Pacelli R, Kim S, DeGraff W, Gamson J, Vodovotz Y, Russo A, Mitchell JB. Nitric oxide and some nitric oxide donor compounds enhance the cytotoxicity of cisplatin. Nitric Oxide. 1997;1(1):88-94.

63. Nath N, Chattopadhyay M, Kodela R, Tian S, Vlismas P, Boring D, Crowell JA, Kashfi K. Modulation of stress genes expression profile by nitric oxide-releasing aspirin in Jurkat T leukemia cells. Biochem Pharmacol. 2010;79(12):1759-1771.

64. S. Anand and Thatcher GRJ. Nitric Oxide-Releasing Molecules for Cancer Therapy and Chemoprevention. In: Bonavida B, editor. Nitric Oxide (NO) and Cancer. New York: Springer; 2010. p. 361-385.

65. Keefer LK. Nitric oxide (NO)- and nitroxyl (HNO)-generating diazeniumdiolates (NONOates): emerging commercial opportunities. Curr Top Med Chem. 2005;5(7):625-636.

66. Keefer LK. Fifty years of diazeniumdiolate research. From laboratory curiosity to broad-spectrum biomedical advances. ACS Chem Biol. 2011;6(11):1147-1155.

67. Keefer LK, Nims RW, Davies KM, Wink DA. "NONOates" (1-substituted diazen-1-ium-1,2-diolates) as nitric oxide donors: convenient nitric oxide dosage forms. Methods Enzymol. 1996;268:281-293.

68. Keefer LK. Nitric oxide (NO)- and nitroxyl (HNO)-generating diazeniumdiolates (NONOates): emerging commercial opportunities. Curr Top Med Chem. 2005;5(7):625-636.

69. Keefer LK. Progress toward clinical application of the nitric oxide-releasing diazeniumdiolates. Annu Rev Pharmacol Toxicol. 2003;43:585-607.

70. Chakrapani H, Wilde TC, Citro ML, Goodblatt MM, Keefer LK, Saavedra JE. Synthesis, nitric oxide release, and anti-leukemic activity of glutathione-activated nitric oxide prodrugs: Structural analogues of PABA/NO, an anti-cancer lead compound. Bioorg Med Chem. 2008;16(5):2657-2664.

71. Findlay VJ, Townsend DM, Saavedra JE, Buzard GS, Citro ML, Keefer LK, Ji X, Tew KD. Tumor cell responses to a novel glutathione S-transferase-activated nitric oxide-releasing prodrug. Mol Pharmacol. 2004;65(5):1070-1079.

72. Kumar V, Hong SY, Maciag AE, Saavedra JE, Adamson DH, Prud'homme RK, Keefer LK, Chakrapani H. Stabilization of the nitric oxide (NO) prodrugs and anticancer leads, PABA/NO and Double JS-K, through incorporation into PEG-protected nanoparticles. Mol Pharm. 2010;7(1):291-298.

73. Townsend DM, Findlay VJ, Fazilev F, Ogle M, Fraser J, Saavedra JE, Ji X, Keefer LK, Tew KD. A glutathione S-transferase pi-activated prodrug causes kinase activation concurrent with S-glutathionylation of proteins. Mol Pharmacol. 2006;69(2):501-508.

74. Chakrapani H, Goodblatt MM, Udupi V, Malaviya S, Shami PJ, Keefer LK, Saavedra JE. Synthesis and in vitro anti-leukemic activity of structural analogues of JS-K, an anti-cancer lead compound. Bioorg Med Chem Lett. 2008;18(3):950-953.

75. Chakrapani H, Kalathur RC, Maciag AE, Citro ML, Ji X, Keefer LK, Saavedra JE. Synthesis, mechanistic studies, and anti-proliferative activity of glutathione/glutathione S-transferase-activated nitric oxide prodrugs. Bioorg Med Chem. 2008;16(22):9764-9771.

76. Edes K, Cassidy P, Shami PJ, Moos PJ. JS-K, a nitric oxide prodrug, has enhanced cytotoxicity in colon cancer cells with knockdown of thioredoxin reductase 1. PLoS One. 2010;5(1):e8786.

77. Kitagaki J, Yang Y, Saavedra JE, Colburn NH, Keefer LK, Perantoni AO. Nitric oxide prodrug JS-K inhibits ubiquitin E1 and kills tumor cells retaining wild-type p53. Oncogene. 2009;28(4):619-624.

78. Kiziltepe T, Anderson KC, Kutok JL, Jia L, Boucher KM, Saavedra JE, Keefer LK, Shami PJ. JS-K has potent anti-angiogenic activity in vitro and inhibits tumour angiogenesis in a multiple myeloma model in vivo. J Pharm Pharmacol. 2010;62(1):145-151.

79. Kiziltepe T, Hideshima T, Ishitsuka K, Ocio EM, Raje N, Catley L, Li CQ, Trudel LJ, Yasui H, Vallet S, Kutok JL, Chauhan D, Mitsiades CS, Saavedra JE, Wogan GN, Keefer LK, Shami PJ, Anderson KC. JS-K, a GST-activated nitric oxide generator, induces DNA double-strand breaks, activates DNA damage response pathways, and induces apoptosis in vitro and in vivo in human multiple myeloma cells. Blood. 2007;110(2):709-718.

80. Liu J, Li C, Qu W, Leslie E, Bonifant CL, Buzard GS, Saavedra JE, Keefer LK, Waalkes MP. Nitric oxide prodrugs and metallochemotherapeutics: JS-K and CB-3-100 enhance arsenic and cisplatin cytolethality by increasing cellular accumulation. Mol Cancer Ther. 2004;3(6):709-714.

81. Liu J, Malavya S, Wang X, Saavedra JE, Keefer LK, Tokar E, Qu W, Waalkes MP, Shami PJ. Gene expression profiling for nitric oxide prodrug JS-K to kill HL-60 myeloid leukemia cells. Genomics. 2009;94(1):32-38.

82. Maciag AE, Chakrapani H, Saavedra JE, Morris NL, Holland RJ, Kosak KM, Shami PJ, Anderson LM, Keefer LK. The nitric oxide prodrug JS-K is effective against non-small-cell lung cancer cells in vitro and in vivo: involvement of reactive oxygen species. J Pharmacol Exp Ther. 2011;336(2):313-320.

83. Maciag AE, Saavedra JE, Chakrapani H. The nitric oxide prodrug JS-K and its structural analogues as cancer therapeutic agents. Anticancer Agents Med Chem. 2009;9(7):798-803.

84. McMurtry V, Saavedra JE, Nieves-Alicea R, Simeone AM, Keefer LK, Tari AM. JS-K, a nitric oxide-releasing prodrug, induces breast cancer cell death while sparing normal mammary epithelial cells. Int J Oncol. 2011;38(4):963-971.

85. Nandurdikar RS, Maciag AE, Citro ML, Shami PJ, Keefer LK, Saavedra JE, Chakrapani H. Synthesis and evaluation of piperazine and homopiperazine analogues of JS-K, an anti-cancer lead compound. Bioorg Med Chem Lett. 2009;19(10):2760-2762.

86. Nath N, Chattopadhyay M, Pospishil L, Cieciura LZ, Goswami S, Kodela R, Saavedra JE, Keefer LK, Kashfi K. JS-K, a nitric oxide-releasing prodrug, modulates ss-catenin/TCF signaling in leukemic Jurkat cells: evidence of an S-nitrosylated mechanism. Biochem Pharmacol. 2010;80(11):1641-1649.

87. Ren Z, Kar S, Wang Z, Wang M, Saavedra JE, Carr BI. JS-K, a novel non-ionic diazeniumdiolate derivative, inhibits Hep 3B hepatoma cell growth and induces c-Jun phosphorylation via multiple MAP kinase pathways. J Cell Physiol. 2003;197(3):426-434.

88. Shami PJ, Maciag AE, Eddington JK, Udupi V, Kosak KM, Saavedra JE, Keefer LK. JS-K, an arylating nitric oxide (NO) donor, has synergistic anti-leukemic activity with cytarabine (ARA-C). Leuk Res. 2009;33(11):1525-1529.

89. Shami PJ, Saavedra JE, Bonifant CL, Chu J, Udupi V, Malaviya S, Carr BI, Kar S, Wang M, Jia L, Ji X, Keefer LK. Antitumor activity of JS-K [O2-(2,4-dinitrophenyl) 1-[(4-ethoxycarbonyl)piperazin-1-yl]diazen-1-ium-1,2-diolate] and related O2-aryl diazeniumdiolates in vitro and in vivo. J Med Chem. 2006;49(14):4356-4366.

90. Shami PJ, Saavedra JE, Wang LY, Bonifant CL, Diwan BA, Singh SV, Gu Y, Fox SD, Buzard GS, Citro ML, Waterhouse DJ, Davies KM, Ji X, Keefer LK. JS-K, a glutathione/glutathione S-transferase-activated nitric oxide donor of the diazeniumdiolate class with potent antineoplastic activity. Mol Cancer Ther. 2003;2(4):409-417.

91. Shami PJ LH, Kosak KM, Saavedra KM, Keefer LK, Cao TM. . JS-K, an arylating nitric oxide (NO) generator, shows no toxicity towards normal hematopoietic cells. In: Proceedings of the 2007 meeting of the American Association of Cancer Research; 2007.

92. Udupi V, Yu M, Malaviya S, Saavedra JE, Shami PJ. JS-K, a nitric oxide prodrug, induces cytochrome c release and caspase activation in HL-60 myeloid leukemia cells. Leuk Res. 2006;30(10):1279-1283.

93. Weyerbrock A, Osterberg N, Psarras N, Baumer B, Kogias E, Werres A, Bette S, Saavedra JE, Keefer LK, Papazoglou A. JS-K, a glutathione S-transferase-activated nitric oxide donor with antineoplastic activity in malignant gliomas. Neurosurgery. 2012;70(2):497-510.

94. Hibbs JB, Jr., Taintor RR, Vavrin Z, Rachlin EM. Nitric oxide: a cytotoxic activated macrophage effector molecule. Biochem Biophys Res Commun. 1988;157(1):87-94.

95. Shami PJ, Sauls DL, Weinberg JB. Schedule and concentration-dependent induction of apoptosis in leukemia cells by nitric oxide. Leukemia. 1998;12(9):1461-1466.

96. Konopleva MY, Jordan CT. Leukemia stem cells and microenvironment: biology and therapeutic targeting. J Clin Oncol. 2011;29(5):591-599.

97. Jordan CT. The leukemic stem cell. Best Pract Res Clin Haematol. 2007;20(1):13-18.

98. Kane RC, Bross PF, Farrell AT, Pazdur R. Velcade: U.S. FDA approval for the treatment of multiple myeloma progressing on prior therapy. The Oncologist. 2003;8(6):508-513.

99. Kane RC, Dagher R, Farrell A, Ko CW, Sridhara R, Justice R, Pazdur R. Bortezomib for the treatment of mantle cell lymphoma. Clin Cancer Res. 2007;13(18 Pt 1):5291-5294.

100. Fribley A, Zeng Q, Wang CY. Proteasome inhibitor PS-341 induces apoptosis through induction of endoplasmic reticulum stress-reactive oxygen species in head and neck squamous cell carcinoma cells. Mol Cell Biol. 2004;24(22):9695-9704.

101. Stapnes C, Doskeland AP, Hatfield K, Ersvaer E, Ryningen A, Lorens JB, Gjertsen BT, Bruserud O. The proteasome inhibitors bortezomib and PR-171 have antiproliferative and proapoptotic effects on primary human acute myeloid leukaemia cells. Br J Haematol. 2007;136(6):814-828.

102. Attar EC, De Angelo DJ, Supko JG, D'Amato F, Zahrieh D, Sirulnik A, Wadleigh M, Ballen KK, McAfee S, Miller KB, Levine J, Galinsky I, Trehu EG, Schenkein D, Neuberg D, Stone RM, Amrein PC. Phase I and pharmacokinetic study of bortezomib in combination with idarubicin and cytarabine in patients with acute myelogenous leukemia. Clin Cancer Res. 2008;14(5):1446-1454.

103. Attar EC, Amrein PC, Fraser JW, Fathi AT, McAfee S, Wadleigh M, Deangelo DJ, Steensma DP, Stone RM, Foster J, Neuberg D, Ballen KK. Phase I dose escalation study of bortezomib in combination with lenalidomide in patients with myelodysplastic syndromes (MDS) and acute myeloid leukemia (AML). Leuk Res. 2013.

104. Jiang XJ, Huang KK, Yang M, Qiao L, Wang Q, Ye JY, Zhou HS, Yi ZS, Wu FQ, Wang ZX, Zhao QX, Meng FY. Synergistic effect of panobinostat and bortezomib on chemoresistant acute myelogenous leukemia cells via AKT and NF-kappaB pathways. Cancer Lett. 2012;326(2):135-142.

105. Kabanov AV, Batrakova EV, Alakhov VY. Pluronic block copolymers as novel polymer therapeutics for drug and gene delivery. J Control Release. 2002;82(2-3):189-212.

106. Zhang L, Radovic-Moreno AF, Alexis F, Gu FX, Basto PA, Bagalkot V, Jon S, Langer RS, Farokhzad OC. Co-delivery of hydrophobic and hydrophilic drugs from nanoparticle-aptamer bioconjugates. ChemMedChem. 2007;2(9):1268-1271.

107. Tiwari G, Tiwari R, Sriwastawa B, Bhati L, Pandey S, Pandey P, Bannerjee SK. Drug delivery systems: An updated review. Int J Pharm Investig. 2012;2(1):2-11.

108. Gabizon AA. Selective tumor localization and improved therapeutic index of anthracyclines encapsulated in long-circulating liposomes. Cancer Res. 1992;52(4):891-896.

109. Erik Brewer JC, and Anthony Lowman. Emerging Technologies of Polymeric Nanoparticles in Cancer Drug Delivery. J Nanomater. 2011;2011:1-10.

110. Mebarek N, Aubert-Pouessel A, Gerardin C, Vicente R, Devoisselle JM, Begu S. Polymeric micelles based on poly(methacrylic acid) block-containing copolymers with different membrane destabilizing properties for cellular drug delivery. Int J Pharm. 2013;454(2):611-620.

111. Duan X, Xiao J, Yin Q, Zhang Z, Yu H, Mao S, Li Y. Smart pH-Sensitive and Temporal-Controlled Polymeric Micelles for Effective Combination Therapy of Doxorubicin and Disulfiram. ACS Nano. 2013;7(7):5858-5869.

112. Cajot S, Van Butsele K, Paillard A, Passirani C, Garcion E, Benoit JP, Varshney SK, Jerome C. Smart nanocarriers for pH-triggered targeting and release of hydrophobic drugs. Acta Biomater. 2012;8(12):4215-4223.

113. Van Butsele K, Morille M, Passirani C, Legras P, Benoit JP, Varshney SK, Jerome R, Jerome C. Stealth properties of poly(ethylene oxide)-based triblock copolymer micelles: a prerequisite for a pH-triggered targeting system. Acta Biomater. 2011;7(10):3700-3707.

114. Chen YC, Liao LC, Lu PL, Lo CL, Tsai HC, Huang CY, Wei KC, Yen TC, Hsiue GH. The accumulation of dual pH and temperature responsive micelles in tumors. Biomaterials. 2012;33(18):4576-4588.

115. Taurin S, Nehoff H, Greish K. Anticancer nanomedicine and tumor vascular permeability; Where is the missing link? J Control Release. 2012;164(3):265-275.

116. Miyata K CR, Kataoka K. Polymeric micelles for nano-scale drug delivery. Reac Funct Pol. 2011;71:227-234.

117. Oerlemans C, Bult W, Bos M, Storm G, Nijsen JF, Hennink WE. Polymeric micelles in anticancer therapy: targeting, imaging and triggered release. Pharm Res. 2010;27(12):2569-2589.

118. Cabral H, Murakami M, Hojo H, Terada Y, Kano MR, Chung UI, Nishiyama N, Kataoka K. Targeted therapy of spontaneous murine pancreatic tumors by

polymeric micelles prolongs survival and prevents peritoneal metastasis. Proc Natl Acad Sci U S A. 2013.

119. Chen Y, Zhang W, Gu J, Ren Q, Fan Z, Zhong W, Fang X, Sha X. Enhanced antitumor efficacy by methotrexate conjugated Pluronic mixed micelles against KBv multidrug resistant cancer. Int J Pharm. 2013;452(1-2):421-433.

120. Drbohlavova J, Chomoucka J, Adam V, Ryvolova M, Eckschlager T, Hubalek J, Kizek R. Nanocarriers for anticancer drugs - new trends in nanomedicine. Curr Drug Metab. 2013;14(5):547-564.

121. Zeng S, Xiong MP. Trilayer micelles for combination delivery of rapamycin and siRNA targeting Y-box binding protein-1 (siYB-1). Biomaterials. 2013;34(28):6882-6892.

122. Cheng C, Convertine AJ, Stayton PS, Bryers JD. Multifunctional triblock copolymers for intracellular messenger RNA delivery. Biomaterials. 2012;33(28):6868-6876.

123. Schnitzler T, Herrmann A. DNA block copolymers: functional materials for nanoscience and biomedicine. Acc Chem Res. 2012;45(9):1419-1430.

124. Robin MP, Mabire AB, Damborsky JC, Thom ES, Winzer-Serhan UH, Raymond JE, O'Reilly RK. New functional handle for use as a self-reporting contrast and delivery agent in nanomedicine. J Am Chem Soc. 2013;135(25):9518-9524.

125. Rapoport N. Ultrasound-mediated micellar drug delivery. Int J Hyperthermia. 2012;28(4):374-385.

126. Shaik N, Giri N, Elmquist WF. Investigation of the micellar effect of pluronic P85 on P-glycoprotein inhibition: cell accumulation and equilibrium dialysis studies. J Pharm Sci. 2009;98(11):4170-4190.

127. Katragadda U, Teng Q, Rayaprolu BM, Chandran T, Tan C. Multi-drug delivery to tumor cells via micellar nanocarriers. Int J Pharm. 2011;419(1-2):281-286.

128. Adams ML, Lavasanifar A, Kwon GS. Amphiphilic block copolymers for drug delivery. J Pharm Sci. 2003;92(7):1343-1355.

129. Kim S, Shi Y, Kim JY, Park K, Cheng JX. Overcoming the barriers in micellar drug delivery: loading efficiency, in vivo stability, and micelle-cell interaction. Expert Opin Drug Deliv. 2010;7(1):49-62.

130. Trong LC, Djabourov M, Ponton A. Mechanisms of micellization and rheology of PEO-PPO-PEO triblock copolymers with various architectures. J Colloid Interface Sci. 2008;328(2):278-287.

131. Halperin A, and S. Alexander. Polymeric micelles: their relaxation kinetics. Macromolecules 1989;22(5):2403-2412.

132. Kabanov AV, Batrakova EV, Alakhov VY. Pluronic block copolymers for overcoming drug resistance in cancer. Adv Drug Deliv Rev. 2002;54(5):759-779.

133. Choo ESG, Bin Yu, and Junmin Xue. Synthesis of poly (acrylic acid)(PAA) modified Pluronic P123 copolymers for pH-stimulated release of Doxorubicin. J Colloid Interface Sci 2011;358(2):462-470.

134. Han LM, Guo J, Zhang LJ, Wang QS, Fang XL. Pharmacokinetics and biodistribution of polymeric micelles of paclitaxel with Pluronic P123. Acta Pharmacol Sin. 2006;27(6):747-753.

135. Liu Z, Liu D, Wang L, Zhang J, Zhang N. Docetaxel-loaded pluronic p123 polymeric micelles: in vitro and in vivo evaluation. International J Mol Sci. 2011;12(3):1684-1696.

136. Wei Z, Hao J, Yuan S, Li Y, Juan W, Sha X, Fang X. Paclitaxel-loaded Pluronic P123/F127 mixed polymeric micelles: formulation, optimization and in vitro characterization. Int J Pharm. 2009;376(1-2):176-185.

137. Wei Z, Yuan S, Hao J, Fang X. Mechanism of inhibition of P-glycoprotein mediated efflux by Pluronic P123/F127 block copolymers: Relationship between copolymer concentration and inhibitory activity. Eur J Pharm Biopharm. 2012;S0939-6411(12)00312-00318.

138. Yang Z, Sahay G, Sriadibhatla S, Kabanov AV. Amphiphilic block copolymers enhance cellular uptake and nuclear entry of polyplex-delivered DNA. Bioconjug Chem. 2008;19(10):1987-1994.

139. Zhang W, Shi Y, Chen Y, Yu S, Hao J, Luo J, Sha X, Fang X. Enhanced antitumor efficacy by paclitaxel-loaded pluronic P123/F127 mixed micelles against non-small cell lung cancer based on passive tumor targeting and modulation of drug resistance. Eur J Pharm Biopharm. 2010;75(3):341-353.

140. ten Cate B, de Bruyn M, Wei Y, Bremer E, Helfrich W. Targeted elimination of leukemia stem cells; a new therapeutic approach in hemato-oncology. Curr Drug Targets. 2010;11(1):95-110.

141. Krause DS, Van Etten RA. Right on target: eradicating leukemic stem cells. Trends Mol Med. 2007;13(11):470-481.

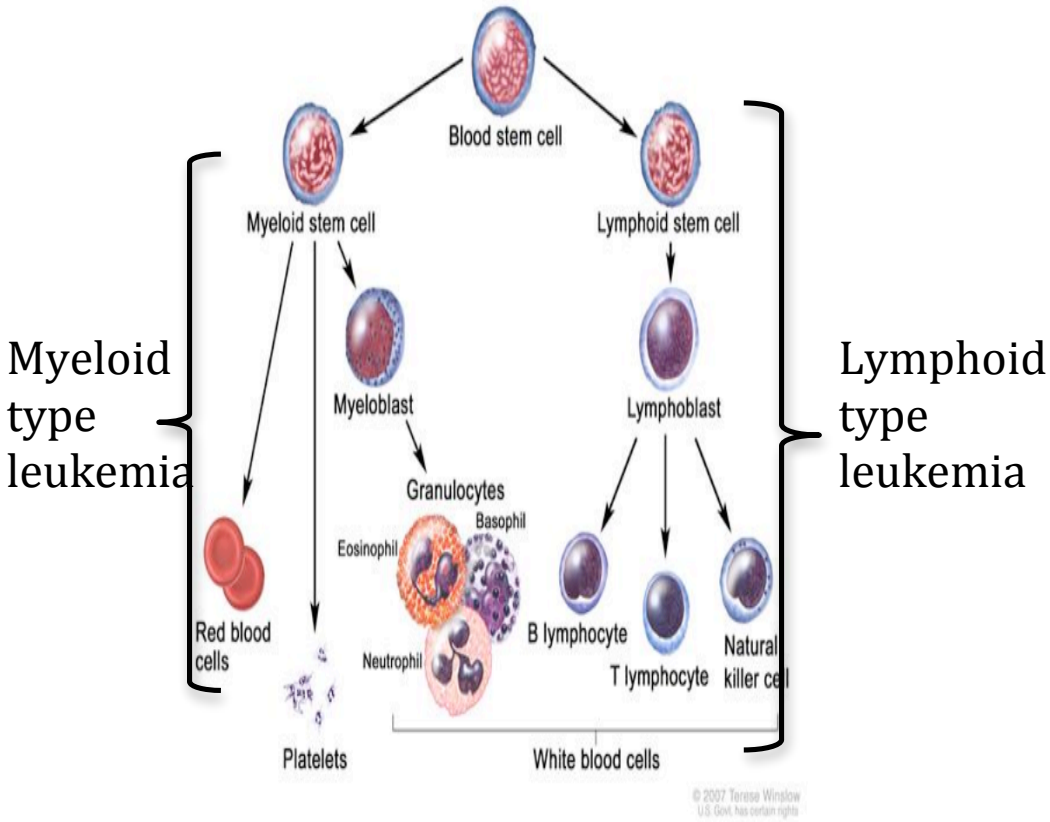

Fig. 1.1: Etiology of Leukemia. In myeloid leukemias, the differentiation block occurs along the myeloid lineage while in lymphoid leukemias this occurs along the lymphoid lineage. See text for detail. Adapted from cancer.gov.

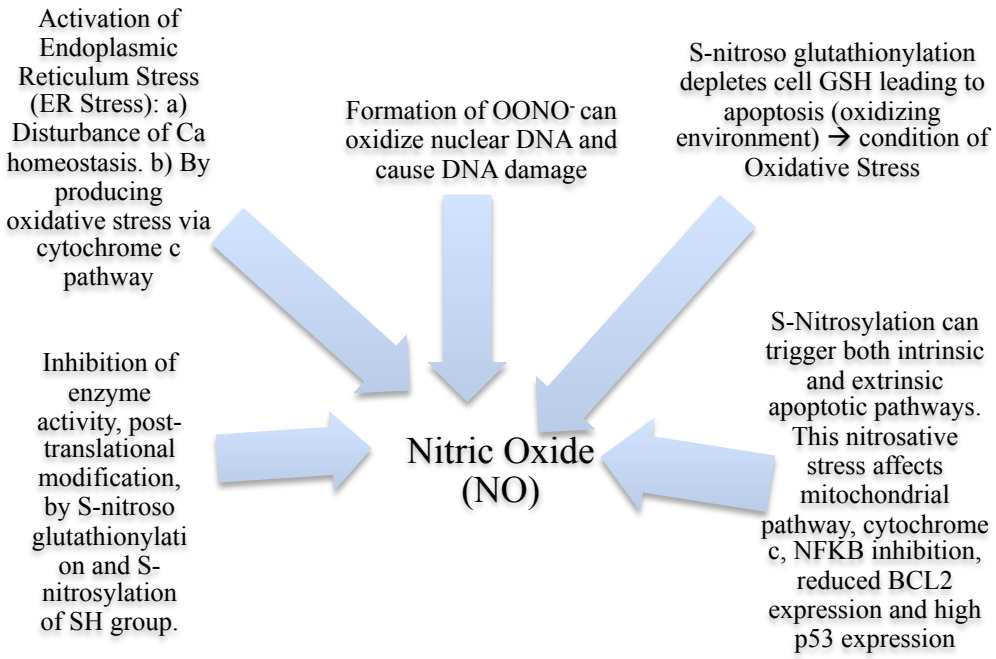

Fig. 1.2: Multiple facets of Nitric Oxide. Data from (1-4).

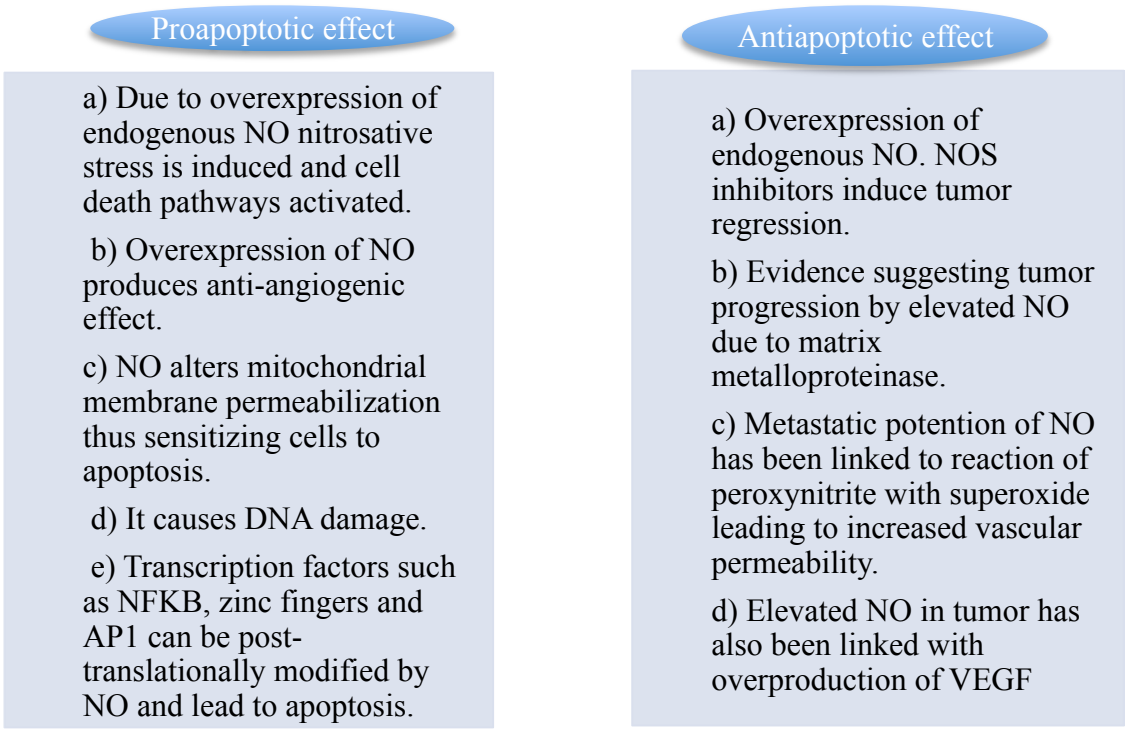

Fig. 1.3: Pro- and antiapoptotic effects produced by NO. Data modified from (1, 2).

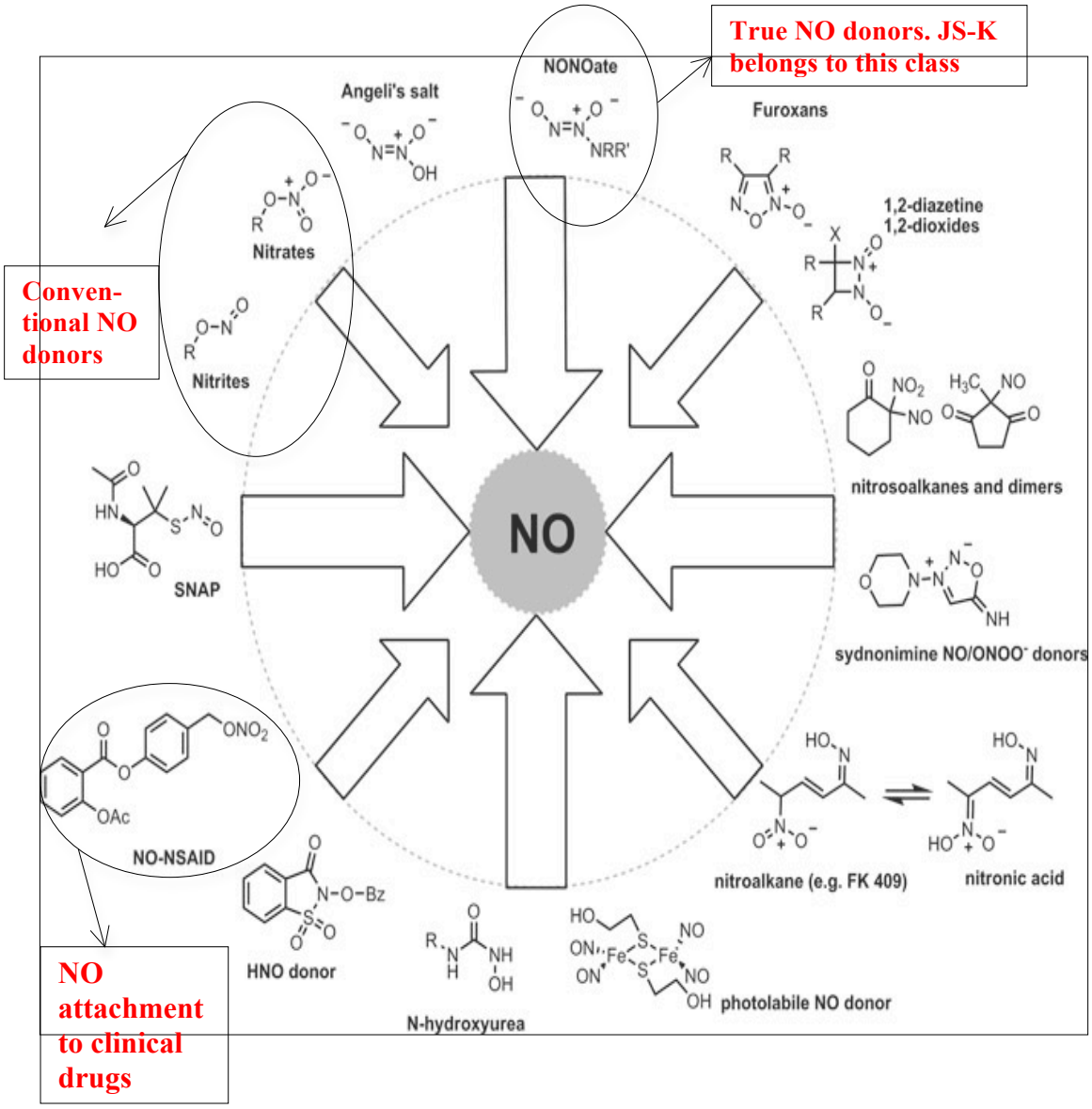

Fig. 1.4: Different classes of nitric oxide donors. Adapted from G.R.J. Thatcher, S. Anand. Nitric Oxide-Releasing Molecules for Cancer Therapy and Chemoprevention. In B. Bonavida (ed.), Nitric Oxide (NO) and Cancer, Vol. Part VII, Springer, New York, 2010, pp. 362.

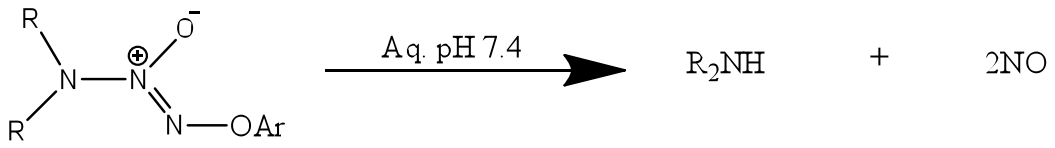

Fig. 1.5: NO release from ADZD

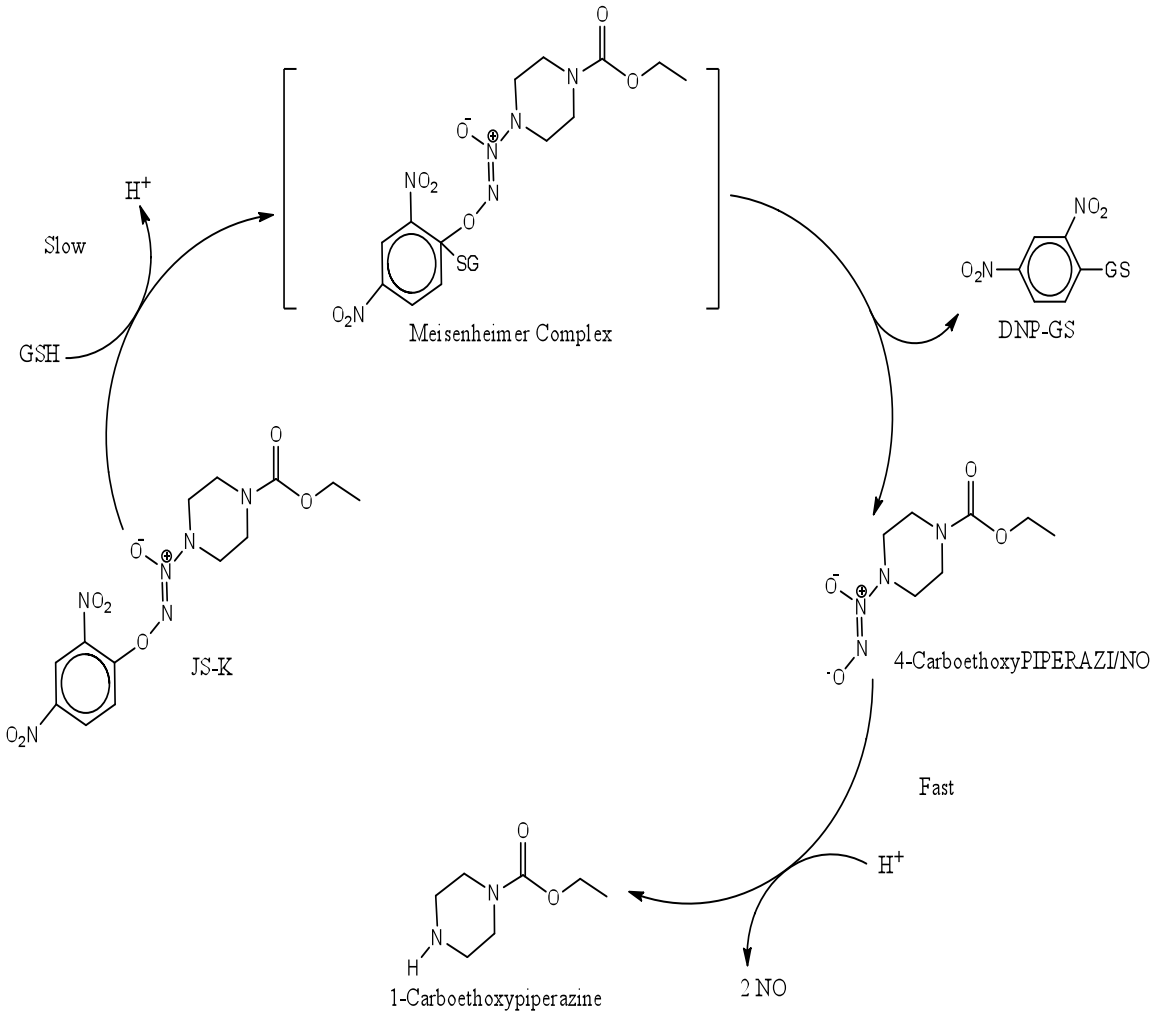

Fig. 1.6: Structure and activation of JS-K

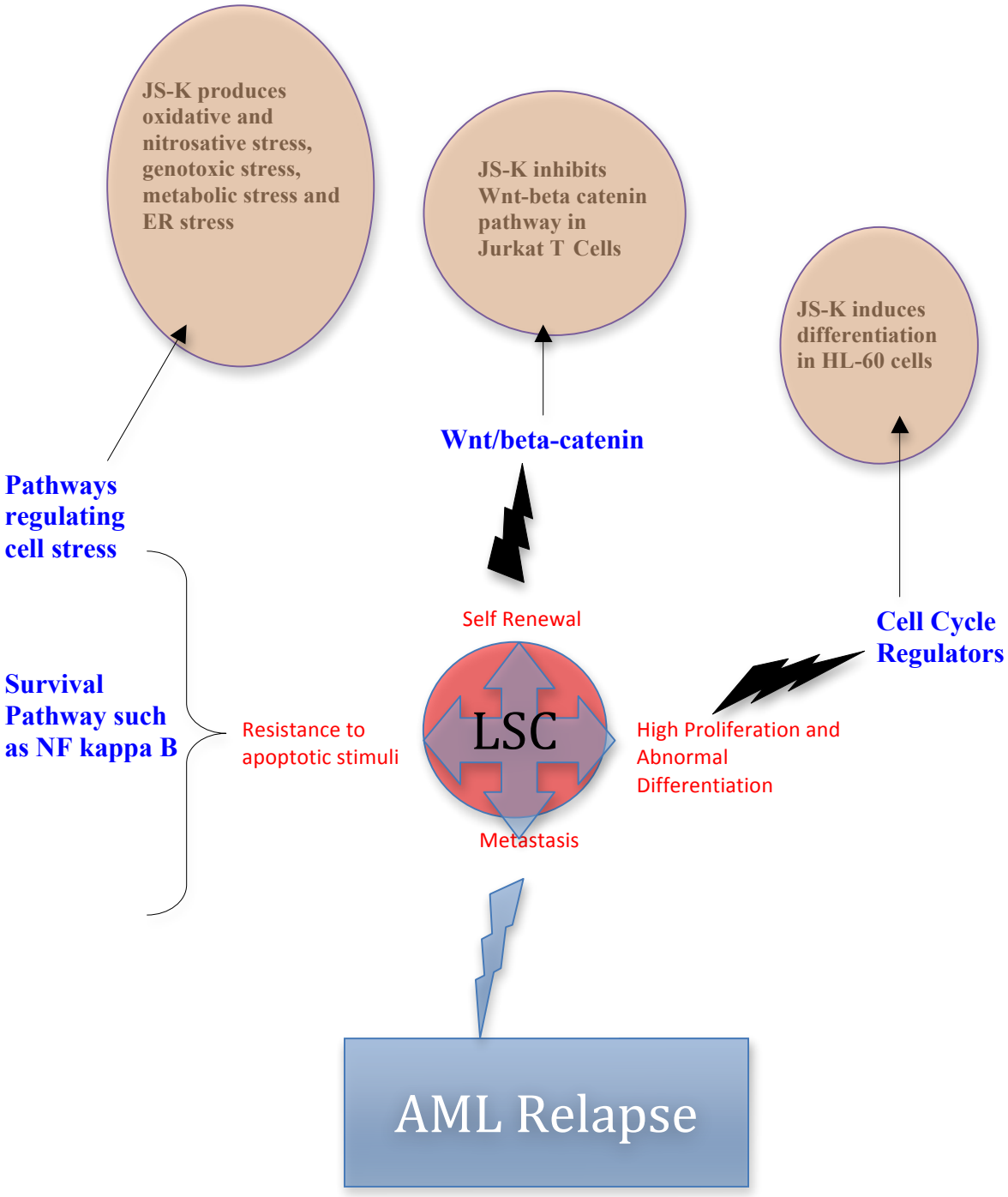

Fig. 1.7: Targets of JS-K's action in hematological malignancies. AML relapse could be attributed to survival of leukemic stem cells (LSC). Factors supporting LSC survival are in red, pathways related to those factors are in blue and the effect produced by JS-K is in balloons.

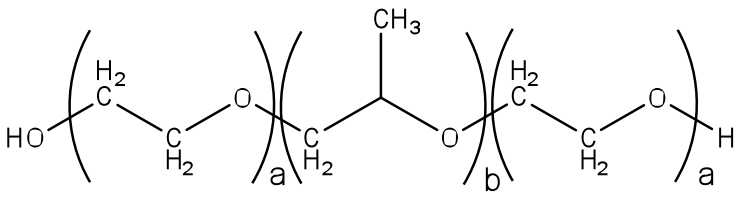

Fig. 1.8: Basis structure of block copolymer. Number of "a" and "b" units differs in the different types of block copolymers.

Table 1.1: Estimated number of new cases of different Leukemia in United States (2013)			
Type	Total	Male	Female
Acute lymphoblastic leukemia	6,070	3,350	2,720
Chronic lymphocytic leukemia	15,680	9,720	5,960
Acute myeloid leukemia	14,590	7,820	6,770
Chronic myeloid leukemia	5,920	3,420	2,500
Other leukemia	6,350	3,570	2,780
Total estimated new cases	48,610	27,880	20,730
Source: Cancer Facts and Figures 2013, American Cancer Society; 2013, cancer.org			

Table 1.2: JS-K studies performed in various tumor types and the mechanism of action proposed in each study				
JS-K formulation	Tumor type	*In vitro* cell line/ IC_{50}	*In vivo*	Proposed MOA
Free JS-K	Acute Myeloid Leukemia (AML)	HL-60 cells-0.2-0.5 µM U937 cells-	NOD/SCID mice implanted s.c. with HL-60 cells. Mice treated at dose of 4 µmol/kg every alternate dose. >50% tumor reduction observed in JS-K treated mice when compared to controls. The excised tumors showed extensive necrosis (90).	a) Intrinsic (caspase 3 & 9) and extrinsic apoptotic pathway (caspase 8) (92) b) Differentiation of leukemia (HL-60 cells) cells (90). c) Oxidative stress d) ER stress

Table 1.2 continued

JS-K formulation	Tumor type	*In vitro* cell line/ IC_{50}	*In vivo*	Proposed MOA
P123/JS-K	AML	HL-60 cells, U937 cells		a) Oxidative stress b) ER stress
JS-K	Acute Lymphoblastic Leukemia (ALL) (86)	Jurkat T cells (JTC). IC_{50} = 9 μM (48 hrs)		a) JS-K modulated the b-catenin pathway by reducing b-catenin/TCF-4 inhibitory activity. b) Nuclear b-catenin S-nitrosylation was observed.

Table 1.2 continued

JS-K formulation	Tumor type	*In vitro* cell line/ IC_{50}	*In vivo*	Proposed MOA
JS-K	Multiple Myeloma (79)	MM.1S, RPMI8226, OPM1 and OPM2: IC_{50}- 0.3-1.2 μM (48 hrs)	Human xenograft mouse model was established. The mice were treated at a dose of 4 μmol/kg thrice/week Survival of JS-K treated mice was significantly higher than the controls. Also, the excised tumors showed apoptosis in JSK treated mice	a) Up to 2.5 μM JS-K was found to be non toxic in healthy peripheral blood mononuclear cells. b) Induction of apoptosis through PARP, caspase 8 and 9 cleavage (time course and dose dependent study (0.6-2.5 μM). This study was carried out in MM.1S cells. c) JS-K treatment overcame the survival advantages conferred by growth factors such as IL-6 and IGF-1. d) Cytotoxicity produced by JS-K is mediated by NO• e) JS-K produces genotoxicity by inducing DNA double strand breaks and activating DNA damage response. f) JS-K caused activation of JNK protein.

Table 1.2 continued

JS-K formulation	Tumor type	*In vitro* cell line/ IC_{50}	*In vivo*	Proposed MOA
JS-K 0.5 or 1 μM	Breast Cancer	MDA-MB-231 cells or MCF-7/COX-2 cells or MDA-MBA-231/F10 cells (F10) (84)		a) Anti-invasive effects by affecting mitogen-activated protein kinase (MAPK) and by increasing TIMP-2 production. b) 0.5 μM JS-K did not affect p38, ERK or JNK phosphorylation in any cell line except F10. c) 1 μM JS-K decreased p38 phosphorylation in all cells and ERK phosphorylation in F10 cells. d) Confirmed the involvement of NO• for producing apoptotic effects
JS-K	Prostate cancer	PPC 1 cells. High IC_{50} as compared to liquid leukemia cells (90).	NOD/SCID mice implanted s.c. with HL-60 cells. Mice treated at dose of 4 μmol/kg thrice/week. Significant tumor reduction observed in JS-K treated mice when compared to controls	a) Extensive necrosis in the excised tumors was observed.

Table 1.2 continued

JS-K formulation	Tumor type	*In vitro* cell line/ IC_{50}	*In vivo*	Proposed MOA
JS-K and P123/JS-K.	Non small cell lung cancer (NSCLC) (82)	H194 or H177 cells.	Athymic NCr-nu/nu mice were injected with H194 or H177 cells and treated with P123/JS-K at a dose of 6μ mol/kg thrice/week.	a) JS-K showed cytotoxicity towards a subset of human NSCLC. The most sensitive cells lines showed higher level of basal reactive oxygen/nitrogen species. b) Study confirmed release of NO by JS-K. c) Study showed that ROS/RNS levels increased in the cells after JS-K treatment suggesting oxidative stress. Also, with basal levels of ROS/RNS present in the cell system, JS-K increased the levels of ROS/RNS. d) Intrinsic apoptotic pathway activated. e) JS-K caused DNA damage.
JS-K	Hepatoma (87)	Hep-3b cells. IC_{50}: 8 μM (72 hrs)		a) Activation of MAPK pathway by inducing ERK, p38 and JNK phosphorylation. b) JS-K induced MAPK activation is NO mediated.

Table 1.2 continued

JS-K formulation	Tumor type	*In vitro* cell line/ IC_{50}	*In vivo*	Proposed MOA
JS-K	Glioma (93)	U87 glioma cells and primary glioma cells. IC 50 < 15 µmol/L	U87 xenograft model was established in rats and treated with 6 mg/kg/d s.c. for 7 days. Substantial tumor attenuation observed in JS-K treated rats. Necrosis was also observed.	a) NO release from U87 cells after JS-K treatment.
JS-K	Multiple Myeloma (78)	Human umbilical vein endothelial cells (HUVEC) (IC_{50} 0.5 µM after 3 days) and OPM1 multiple myeloma cells.	NIH III mice were implanted s.c. with OPM1 cells and treated with 4 µM JS-K thrice a week. Tumor explants from treated mice showed reduced angiogenesis when compared to control.	a) JS-K inhibited cord formation and endothelial cell migration in HUVEC thus indicating anti-angiogenic activity in vitro.

Table 1.2 continued

JS-K formulation	Tumor type	*In vitro* cell line/ IC_{50}	*In vivo*	Proposed MOA
JS-K	----	Retinal pigment epithelial cells (RPE)- IC_{50}-2 µM (77)		a) Inhibition of ubiquitin-E1 thioester. b) Increases cellular p53 levels

CHAPTER 2

DEVELOPMENT AND CHARACTERIZATION OF A PLURONIC® P123 FORMULATION FOR THE NITRIC OXIDE-GENERATING AGENT JS-K[2]

2.1 Abstract

O^2-(2,4-dinitrophenyl)1-[(4-ethoxycarbonyl)piperazin-1-yl]diazen-1-ium-1,2-diolate] or JS-K is a nitric oxide-producing prodrug belonging to the class of arylated diazeniumdiolates. JS-K has shown promising antitumor activity *in vitro* and *in vivo*. The major obstacle in clinical use of JS-K is its challenging solubility and stability. We have developed a Pluronic® P123 formulation for JS-K. The present study aims to characterize and compare Pluronic® P123-formulated JS-K (P123/JS-K) with free JS-*K in vitro* and *in vivo*.

We analyzed micelle size using dynamic light scattering, shape by transmission electron microscopy and critical micelle concentration using UV analysis. We performed our efficacy study *in vitro* and *in vivo* by cytotoxicity analysis on HL-60 and U937 myeloid leukemia cells. We also implanted HL-60 cells in NOD/SCID *IL2Rγ*^{null} mice and performed a tumor regression study. We also assessed JS-K or P123/JS-K stability by

---

[2] Adapted from manuscript: Development and characterization of a Pluronic® formulation for the nitric oxide-generating agent JS-K. Imit Kaur, Moises Terrazas, Ken M. Kosak, James N Herron, Steven E. Kern, Kenneth M. Boucher and Paul J. Shami. Submitted to Nanomedicine.

analyzing JS-K or P123/JS-K recovery from RPMI media/10% FBS, human plasma, human whole blood and 4 mM glutathione. Finally, we analyzed plasma protein binding of JS-K or P123/JS-K using equilibrium dialysis and fluorescence quenching. We analyzed binding constant, Stern Volmer constant and thermodynamic parameters including enthalpy, entropy and free energy.

We conclude that Pluronic® P123 solubilizes JS-K and stabilizes it as indicated by higher recovery from physiological media. The Pluronic® formulation also showed different protein binding characteristics as compared to free drug. Finally, P123/JS-K showed higher tumor regression when compared to free JS-K.

2.2 Introduction

Acute myeloid leukemia (AML) is the second most common type of adult leukemia. Estimated new cases and deaths from AML in the United States in 2010 were 12,330 and 8,950, respectively (1). The success of conventional chemotherapeutic agents is frequently limited by the development of drug resistance and severe toxicity of current treatments (2).

Nitric oxide (NO), a biologically occurring pleiotropic molecule, is involved in a plethora of physiological, biological and pathological functions (3), (4). NO has shown promising therapeutic activity against multiple diseases, including cardiovascular and pulmonary diseases (5).

NO has shown *in vitro* tumoricidal activity (6). It can lead to apoptosis by targeting various cellular sites and bringing about posttranslational modifications such as *S*-nitrosylation, *S*-glutathionylation, DNA nitration or deamination and ADP ribosylation (7). NO induces differentiation in acute myeloid leukemia (AML) cells (8). Due to

instability of the NO radical and its hypotensive effects, NO cannot be administered directly or in high doses. NO donors such as diazeniumdiolates generate NO spontaneously. They induce apoptosis and differentiation in AML cells (9). However, these compounds cannot be used clinically for the treatment of malignant diseases because of the pleiotropic effects of NO, and particularly NO-induced vasodilatation through activation of the soluble guanylate cyclase/cGMP pathway (10). Alternatively, arylated diazeniumdiolates react with glutathione (GSH) to release NO. Although the reaction can occur spontaneously, it is catalyzed by the glutathione S-transferases (GST). GSTs are often elevated in malignant cells (11). O^2-(2,4-dinitrophenyl)1-[(4-ethoxycarbonyl)piperazin-1-yl]diazen-1-ium-1,2-diolate] or JS-K (Fig. 2.1), an arylated diazeniumdiolate, has potent antileukemic activity *in vitro* and *in vivo* (12), (13), (14). In *in vivo* murine models, JS-K was also found to be effective against prostate cancer (11), hepatoma (15), multiple myeloma (13) and non-small cell lung cancer (14). JS-K also possesses anti-angiogenic activity both *in vitro* and *in vivo* (16). In multiple myeloma and breast cancer studies, JS-K did not affect the growth of normal human peripheral blood mononuclear cells (13) and normal mammary epithelial cells (17).

Pluronic® block copolymers are widely used for the solubilization of hydrophobic chemotherapeutic agents. These are amphiphilic molecules arranged as A-B-A blocks of hydrophilic poly(ethylene oxide) (PEO or A) and hydrophobic poly(propylene oxide) (PPO or B). The block copolymers possess different hydrophilic-lipophilic balance (HLB) due to varying concentrations of ethylene oxide and propylene oxide units. HLB is important for critical micelle concentration (CMC), i.e., the concentration above which these copolymers self-assemble into micelles in an aqueous solution (18), (19).

Plasma protein binding is an important parameter of the drug development process that needs to be established to predict drug distribution characteristics. Drug bound to plasma proteins acts as a reservoir or drug depot and is not available for its effect. Only the free drug molecules are available at the target site (20). Therefore, in preclinical settings, it is important to determine the plasma protein binding characteristics of an active pharmaceutical ingredient (API) to assess safety, efficacy and bioavailability (21). Two major plasma proteins involved in drug binding are human serum albumin (HSA) and alpha1-acid glycoprotein (AGP) (22). Plasma protein binding could be analyzed via conventional equilibrium dialysis technique or the comparatively new technique of fluorescence quenching.

In the present study, a novel Pluronic® P123 micelle formulation of JS-K was developed and preliminary preclinical studies were carried out. We performed *in vitro* cytotoxicity analysis and also an *in vivo* tumor regression study in a mouse model. The Pluronic® micelle was characterized in its size, shape, surface charge and critical micelle concentration. Finally, we performed serum-binding analysis and compared two different techniques of binding, namely equilibrium dialysis and fluorescence quenching. While both the techniques provided valuable information in terms of binding characteristics, we were able to assess thermodynamic parameters associated with drug-protein binding using fluorescence quenching.

2.3 Materials and Methods

2.3.1 Materials

JS-K was synthesized as previously described (23) and provided by Dr. Joseph Saavedra (SAIC Frederick). Pluronic® polymers were obtained from BASF (Florham

Park, NJ). Human serum albumin (HSA) and alpha 1 acid glycoprotein (AGP) used for protein binding studies were from Sigma (St. Louis, MO). Low binding SpectraPor dialysis membrane [MWCO: 12,000-14,000] was from Spectrum Laboratories Inc (Los Angeles, CA). All the other chemicals were from Sigma (St. Louis, MO) unless otherwise indicated.

2.3.2 Cell culture

Human myeloid leukemia HL-60 cells and human monocytic leukemia cells U937 (ATCC, Manassas, VA) were cultured in RPMI-1640 supplemented with 10% fetal bovine serum (FBS), penicillin/streptomycin and mycozap. Cells were cultured at 37°C in a 5% CO_2 humidified atmosphere. Five micromolar JS-K stocks in dimethyl sulfoxide (DMSO) were serially diluted in phosphate buffered saline (PBS) before addition to the cultures. The final concentration of DMSO added to the cultures was 0.1% or less. For each experiment, JS-K was added at the time of culture initiation, cells were harvested at the indicated time points, washed in PBS and assays conducted.

2.3.3 Preparation of JS-K loaded P123 micelles

11.25% of P123 micelle stock solution was prepared in deionized water. The solution was further diluted to 2.25% in PBS (pH 6.5). 1 mM micelle JS-K (P123/JS-K) was prepared by heating 980 µL of 2.25% P123 at 50°C and adding 20 µL of 50 mM JS-K stock in DMSO. The weight loading of drug in P123 micelles was 1.7%. Further dilution was made in PBS (pH 6.5).

2.3.4 P123 JS-K drug retention and loading

JS-K was loaded in P123, P105 and F127 Pluronic® polymers. The proportion of JS-K to Pluronic® polymer in solution was 3.84% by weight. The JS-K micelle preparations were dialyzed for 5.5 h or 17 h. The different Pluronic® formulations (before and after dialysis) were incubated with HL-60 cells for three days. The MTS cytoxicity analysis was performed (see below).

2.3.5 *In vitro* cytotoxic activity

The *in vitro* cytotoxic activity of JS-K, P123/JS-K micelles and blank P123 micelles was assessed by MTS assay (Promega, Madison, WI) in HL-60 and U-937 cells. Briefly, cells were seeded in a 96-well plate at a density of 10^4 cells per well per 100µL. Cells were treated with 0, 0.09 µM, 0.2 µM, 0.4 µM, 0.6 µM and 0.8 µM of free JS-K or P123/JS-K or blank P123 in triplicates. After incubating for 72 h, 20 µL of MTS reagent was added to each well and incubated further for 1.5 h. Absorbance was read at 490 nm in a microplate reader (Modulus Microplate, Turner Biosystems). Untreated cells were taken as 100% viable. A media blank was used to correct for background absorbance. Results were expressed as a growth percent of control and IC_{50} values were derived from growth vs. drug concentration curves.

2.3.6 P123 Pluronic® micelle formulation of JS-K

JS-K stocks (50 mM) in DMSO were mixed with stocks of Pluronic® P123 polymers prepared in PBS. Micellization was allowed to occur spontaneously with gentle heating (50°C). The proportion of JS-K to P123 in solution was 1.7% by weight. For experiments with free JS-K, DMSO stocks of JS-K (50 mM) were diluted to a final concentration of

JS-K of 1 mM in PBS/80% DMSO in stability experiments or PBS/40% DMSO for protein binding experiments or only PBS for other experiments.

2.3.7 P123/JS-K formulation characterization

2.3.7.1 Particle size measurement

Particle mean size measurements were performed using the dynamic light scattering method using a MalvernNano zeta sizer. The size analysis was performed on blank P123 micelles (2.25%) in PBS and JS-K incorporated P123 micelles (final loading 1.7%).

2.3.7.2 Transmission electron microscopy (TEM) analysis

The morphology of P123 micelles was studied by TEM after negative staining with phosphotungstic acid solution (2% w/v). 1 mM of JS-K formulation in 2.25% of P123 micelle was prepared. TEM images were obtained only with P123/JS-K micelles as the empty micelles were found to be comparatively less stable without drug.

2.3.7.3 Critical micelle concentration (CMC)

CMC of Pluronic® P123 micelles was analyzed using the Iodine UV-absorption spectra method using iodine as hydrophobic probe as previously reported (24). Briefly, KI/I_2 solution was prepared by dissolving 0.5 g Iodine (I_2) and 1 g Potassium Iodide (KI) in 50 mL water for injection (WFI). P123 concentrations ranging from 0.000005% to 0.1% were prepared in WFI. To each 5 mL solution, 25µL of KI/I_2 solution was added. The vials were covered with foil to avoid photo-degradation. The samples were incubated for nearly 12 h at room temperature. The measurements were performed at 366 nm using a UV-vis spectrometer (Ultrospec 2000, Pharmacia Biotech). Triplicate readings were performed for each sample. CMC value was analyzed by plotting absorbance vs log%

Pluronic® weight and was interpreted at the point where a sharp increase in absorbance was observed. The data were analyzed by a piece-wise linear model with a single change in slope. A grid search method was used to determine the optimal change point. The statistical analysis was performed using R statistical computing software version 2.15.0 (Vienna, Austria).

2.3.8 P123/JS-K formulation stability in physiological media

The stability of JS-K formulated in DMSO was compared to JS-K formulated in P123 Pluronic® micelle in various physiological media. JS-K recovery in either formulation was tested in 4 mM GSH (formulated in PBS; pH 7.4); RPMI media, human plasma and human whole blood. At the indicated time points, aliquots from the relevant test solution were collected in 95% Acetonitrile/Formate in water (ACN/Formate in water) in polypropylene vials. The extracts were spin filtered (0.2 μm, low binding nylon filters) for 2 min. JS-K levels were measured by HPLC using an isocratic mobile phase consisting of 25% 0.025 M ammonium formate (pH 4.2), 25% ACN and 50% methanol at a flow rate of 1 mL/min for 6-8 min.

2.3.9 P123/JS-K protein binding studies

The two most common proteins in the blood are human serum albumin (HSA) and alpha 1 acid glycoprotein (AGP). While HSA preferentially binds with acidic drugs, AGP binds mainly with basic or neutral drugs (25). We studied interaction of free drug and micelle formulated drug with these two proteins by fluorescence quenching of tryptophan present in these proteins. Free or P123-formulated JS-K was prepared at

concentrations 20 μM-700 μM or 100μM-700μM for temperature controlled fluorometric studies.

We compared the equilibrium dialysis technique with fluorescence quenching in our preliminary experiments. Both preliminary experiments were carried out at room temperature. The purpose of these experiments was to test the sensitivity and closeness of results obtained from either of the technique. Also, with the dialysis technique, since higher drug volumes were used for extended hours, free JS-K precipitation was observed and therefore, saturation/equilibrium was not attained. Dialysis was carried out using Spectra/Por dialysis membranes (MWCO:12,000-14,000) which were activated for 30 min. in HPLC grade water and rinsed before use. The membranes were held in a 20 mL glass vial. The glass vial was covered with aluminum foil so as to prevent photo-degradation of JS-K. The drug preparation (JS-K in DMSO or JS-K in P123) with 4% final HSA was added in the dialysis bag and a similar sink (i.e., HSA and DMSO or P123) was created in the glass vial. The whole apparatus was kept at constant stirring position and the samples were collected from both sides of the membrane after 2, 4, 6 and 8 h. We found that for P123/JS-K, equilibrium was achieved after 2 h. For free JS-K, we could not achieve equilibrium due to possible degradation of the drug over time. Therefore, 2 h of equilibrium dialysis was selected for both formulations. The samples were then soaked for 30 min. in 95% acetonitrile/5% ammonium formate in water (pH~3) and then spin filtered (0.2 micron, low binding nylon) for 2 min. JS-K levels in the bag and the glass vial were measured by HPLC or UPLC. For quantitation, AUC values were calculated. Percent recovery from each fraction was calculated based on the total initial amount of JS-K added. The association and dissociation constants were calculated using

the SigmaPlot (Systat, Chicago, IL) software with the in-built equation for Ligand Binding.

For the fluorometric analysis, the formulation was prepared as described above. Final protein concentration was 4% for HSA and 0.09% for AGP. Drug and protein were added in 96-well black opaque plates to avoid the inner filter effect. Fluorescence was read at an excitation of 280 nm and emission of 360 nm. Necessary blank fluorescence was read and subtracted as background from the fluorescence of interest. For the temperature-controlled studies, plates were incubated at the desired temperature in a PCR thermal controller (PTC-100™, MJ Research, Inc) for 30 min. and read within 10 min. on the fluorescent reader (Synergy 4, BioTek) previously adjusted to the same temperature. Fluorometric analysis was carried out using the Stern Volmer equation. In case of HSA, Ksv and Ka were obtained at 298, 303 and 310 K. The thermodynamic parameters such as enthalpy, entropy and free energy were calculated to assess the nature of binding involved.

2.3.10 *In vivo* studies of JS-K and P123/JS-K

To study the *in vivo* antineoplastic potency of JS-K and P123/JS-K, NOD/SCID *IL2Rg*^{null} mice were injected subcutaneously with 2.5 x 10^6 HL-60 cells. When tumors became palpable, treatment with JS-K (4 µmol/kg) or P123/JS-K (4 µmol/kg or 5 µmol/kg) or P123 only (volume equivalent to a P123/JS-K dose of 5 µmol/kg) was started. Dose selection was made based on the prior exploratory experiments. Historically, we have shown that 4 µmol/kg dose of free JS-K could be administered without producing any hypotensive effects (11). We were able to escalate the dose with P123/JS-K without any observable hypotensive effects. Treatments were administered

intravenously every other day. For the no treatment group, only body weight and tumor size were measured. Mouse weight and tumor size were measured every other day using a Vernier caliper. Tumor volume was calculated using the formula: width x length x [(width + length)/2] x 0.5236. Animals were sacrificed after 8 treatments using isofluorane inhalation and tumors were collected for histochemical analysis. The protocol was approved by the University of Utah Institutional Animal Care and Use Committee.

2.3.11 High performance liquid chromatography and ultra performance liquid chromatography

HPLC to measure JS-K levels was conducted on a Water's Alliance HPLC system controlled by Empower software. We used an isocratic mobile phase consisting of A = 30% 0.02 M ammonium formate (pH 3), 40% acetonitrile (ACN) and 30% methanol and D = 100% methanol. Flow rate was kept constant at 1 mL/min for 6-8 min. During chromatographic separation, JS-K was monitored by absorbance at 300 nm. The method results in a standard detection curve over a linear range of 6.1 – 49.1 ng with a lower limit of quantitation of 6.4 ng. Very low amounts of JS-K were measured using Water's UPLC Empower 2 software. The samples were run on gradient of 0.02 M formic acid, pH ~2.7 and 100% acetonitrile at a flow rate of 0.6 mL/min.

2.3.12 Statistical analysis

The omnibus null hypothesis of no difference in mean tumor volume between any of the groups was tested using one-way analysis of variance. Tukey's Honest Significant Difference test was used to adjust the p-values for the individual differences for multiple comparisons. Statistical analysis was performed using R statistical computing software

version 2.13.0 (Vienna, Austria). At specific time points, individual tumor volumes were compared using the Student's t-test assuming a 2-tailed distribution with unequal variance. Differences were considered significant for *P* values below 0.05.

We also performed statistical analysis using trapezoid method. For each mice group cumulative area under the curve (AUC) of the tumor volume was calculated starting from the first treatment to the last eighth treatment. Cumulative AUC (for the last treatment) of each group was used for running one-way analysis of variance. Differences were considered significant for *P* values below 0.05.

2.4 Results

2.4.1 P123 JS-K drug retention and loading

We performed some preliminary experiments to analyze the efficacy of JS-K loading in different pluronic systems and cytotoxicity produced by different poloxamers. JS-K was loaded in P123, P105 and F127 as explained in the methods section. We tested the cytoxicity of three different Pluronic micelles. The three micelles tested have different HLB values (F127>P105>P123) (26). The micelles were dialyzed and tested for cytotoxicity as explained in the materials and methods section. The order of efficacy obtained against HL-60 cells after dialysis was P123>P105>F127 (results not shown). To determine the extent of JS-K loading and retention in micelles, JS-K was loaded in P123. The proportion of JS-K to Pluronic® polymer in solution was 10% by weight. The percent of JS-K retained after 2 h of dialysis was determined by HPLC. Percent retention of JS-K in P123 was 75 ± 10%. These preliminary experiments showed that JS-K in a micellar formulation is retained after dialysis.

2.4.2 P123 micelle JS-K in vitro cytotoxicity

P123 micelle JS-K (1.7% JS-K/P123 by weight) *in vitro* cytotoxicity was analyzed using two different acute myeloid leukemia cell lines, HL-60 and U-937. Both the cell lines are for AML with different phenotypes. While HL-60 cells are myeloid derived, U-937 cells are monocytic. We used two different cell lines two analyze the sensitivity of AML cells with variable phenotypes against JS-K or P123/JS-K treatment. In HL-60 cells, IC_{50} values obtained from free JS-K treatment are similar to IC_{50} value obtained from P123/JS-K formulation. P123 control showed negligible toxicity. In U-937 cells, IC_{50} value obtained from P123/JS-K is slightly lower than JS-K. The results indicate Pluronics® have negligible toxicity themselves and do not affect toxicity imparted by JS-K. The results are shown in Table 2.1.

2.4.3 P123 micelle JS-K characterization

P123/JS-K formulation was characterized by particle size measurement, surface charge and morphology. These studies are important as particle size affects biodistribution and elimination. The mean diameter of blank P123 micelles was 29.2 ± 1.36 nm. We observed a slight reduction in size on JS-K incorporation, suggesting stabilization of micelles (Table 2.2). TEM images suggested that P123/JS-K micelles are spherical in shape (Fig. 2.2). TEM images of blank micelles could not be obtained due to the dynamic character of the Pluronics® changing from unimers to micelles. JS-K incorporation stabilized the micelles.

2.4.4 Critical micelle concentration (CMC) determination

CMC is an important characterization parameter that influences micellar stability and solubilization characteristics. To measure CMC, we used a hydrophobic probe– Iodine (I_2) as explained in the methods section. I_2 gets solubilized in the hydrophobic micelle core. An excess KI solution aids conversion of triatomic I_3^-- to I_2, maintaining the saturated solution of I_2 (24). The absorption intensity of I_2 was plotted against different weight percent of Pluronic® and CMC value was obtained from the point on the curve where an abrupt increase in absorbance was observed (Fig. 2.3). We obtained an average CMC value of 5.6 ± 1.3 μM (average and SEM of two independent experiments with three replicates each). This value is compatible with the value reported by Kabanov et al. for P123 (26).

2.4.5 Stability of P123/JS-K in different physiological and biological media

We compared the stability of unformulated JS-K and P123/JS-K in blood, glutathione, plasma and RPMI/10% FBS media. As shown in Table 2.3, the P123 formulation extended the percentage recovery of JS-K as compared to the free drug. This likely reflect shielding of JS-K from proteins and nucleophiles by Pluronic® micelles. Also, the table highlights the recovery affected by the different suspending media. Although all treatments were carried out for 60 min., but the drug was not recovered from some of the suspending media like whole blood. The HPLC method used for JS-K quantification was sensitive to intact JS-K detection only. Therefore, only intact drug was measured. JS-K degraded to its metabolites was not detected by the HPLC method.

2.4.6 HSA and AGP binding with JS-K and P123/JS-K

2.4.6.1 Equilibrium dialysis

The equilibrium dialysis study was carried out to investigate the interaction of JS-K or P123/JS-K with HSA as explained in the material and methods section. JS-K showed affinity for HSA and the equilibrium time was obtained at 2 h. Although at that time point, some drug degradation/precipitation was seen with free JS-K, it was important to stick to 2 h for the achievement of steady state condition. We measured drug levels from both "in the dialysis bag" and "out of the bag" as explained before to determine the binding constant. The values were derived using the ligand binding equation. The results are reported in the Table 2.4.

2.4.6.2 Fluorescence quenching study at room temperature

In preliminary work, both HSA and AGP quenching by JS-K and P123/JS-K was analyzed at room temperature. A Stern Volmer plot was generated for both formulations and proteins. Equation 1 was used to obtain the Stern Volmer quenching constant:

$$\frac{Fo}{F} = 1 + Ksv[Q] \qquad (1)$$

(where Fo: Fluorescence in the absence of external quencher; F: Quenched Fluorescence; Q: Conc. of quencher/drug; Ksv: Stern Volmer Constant).

Figures 2.4 and 2.5 show the Stern Volmer plots of HSA and AGP, respectively. The quenching data were used to determine the binding constant with HSA and compare the value obtained with equilibrium dialysis. Table 2.4 shows the binding parameters obtained by two techniques and the Stern Volmer constants obtained for HSA and AGP.

As shown in Table 2.4, the binding constants obtained from the two techniques are acceptably close. This confirmed the sensitivity and accuracy of both techniques. For the subsequent experiments, we chose fluorescence quenching over equilibrium dialysis because the former is a rapid and sensitive technique. It also requires less material (μL as compared to mL for dialysis) and is relatively quicker than dialysis. This is particularly important for our studies, as nonformulated JS-K is prone to degradation.

2.4.6.3 Determination of quenching mechanism

Fluorescence quenching was performed at 25°C, 30°C and 37°C as explained in the material and methods section in order to obtain the Stern Volmer constant at different temperatures. As shown in Table 2.5, a temperature effect was observed. With increase in temperature, the Stern Volmer constant is reduced. Such an inverse relationship with temperature could explain the quenching behavior (Figures 2.6 and 2.7). Fluorescence quenching could be caused by a number of factors leading to molecular interactions such as excited state reactions, ground state complex formation and collisional quenching. The decrease in Ksv value with a higher temperature suggests a static quenching mechanism (27), i.e., formation of complex between JS-K and HSA or P123/JS-K and HSA. The quenching rate constant (Kq) was calculated to further confirm formation of complex and static quenching mechanisms. The quenching rate constant can be calculated using the equation:

$$Kq = \frac{Ksv}{\tau_o} \qquad (2)$$

τ_o is the average lifetime of HSA molecule in absence of JS-K (quencher) or any other drug. It represents the average lifetime a molecule spends in the excited state.

The value of τ_o of HSA is 10^{-8} s (28). The Kq values calculated are shown in Table 2.5. The Kq values obtained are higher than the maximum scatter collision quenching for HSA, i.e., $2x10^{10}$ L $mol^{-1}s^{-1}$.

We also performed a fluorescence study with HSA and P123 only. Interestingly, instead of quenching, fluorescence enhancement was observed (results not shown).

2.4.6.4 Analysis of binding constants

The association binding constant (Ka) was calculated using a modified Stern Volmer equation:

$$\frac{Fo}{dF} = \frac{1}{fK(Q)} + \frac{1}{f} \qquad (3)$$

where Fo = original unquenched fluorescence of HSA; dF = difference in the fluorescence in the absence and presence of JS-K or P123/JS-K at the concentration Q; f = fraction of initial fluorescence accessible to quencher.

Binding constants obtained at different temperatures are shown in Table 2.5.

2.4.6.5 Thermodynamic constants analysis

Thermodynamic parameters are important for the determination of binding forces involved between the protein and the drug. The forces involved could be noncovalent bonds including hydrophobic interactions; electrostatic interactions; Van der Waals forces and/or hydrogen bonds. The thermodynamic parameters were evaluated using the Van't Hoff equation:

$$\log Ka = -\frac{dH}{2.303RT} + \frac{dS}{2.303R} \qquad (4)$$

$$dG = dH - TdS \qquad (5)$$

The enthalpy change (dH) and entropy change (dS) were calculated from the slope and intercept of the binding constant vs. temperature curve, respectively. Free energy (dG) was calculated from the derived enthalpy and entropy at different temperatures. The results are shown in Table 2.6.

2.4.7 *In vivo* tumor regression analysis

We tested the *in vivo* efficacy of free JS-K and P123/JS-K using HL-60 cells implanted in NOD/SCID *IL2Rg*^{null} as detailed in the methods section. Five groups were compared as follows: no treatment control, P123 control, free JS-K at 4 μmol/kg, P123/JS-K at 4 μmol/kg and P123/JS-K at 5 μmol/kg. There were 12 to 13 animals per variable. Mice were treated intravenously every other day for a total of 8 doses. Tumor volume curves for each variable are shown in Fig. 2.8. When the curves were compared using two way analysis of variance (ANOVA) method, they were not statistically different. However, when comparing tumor volumes using the Student's t-test at day 13, free JS-K at 4 μmol/kg and P123/JS-K at 5 μmol/kg induced a statistically significant reduction in tumor volume as compared to controls. Interestingly, at day 16, the difference between free JS-K-treated mice and controls was no longer significant. However, at day 16, P123/JS-K at 4 or 5 μmol/kg induced a statistically significant reduction in tumor volume. At day 16, tumor volume measurements were as follows (average and SEM): No treatment: 1.57 ± 0.22 cm^3, P123 control: 1.62 ± 0.20 cm^3, free JS-K (4 μmol/kg): 1.29 ± 0.23 cm^3, P123/JS-K (4 μmol/kg): 0.89 ± 0.07 cm^3, P123/JS-K (5 μmol/kg): 0.81 ± 0.06 cm^3. Differences between P123/JS-K at 4 or 5 μmol/kg were not statistically significant. In the other set of analysis performed, we calculated the

cumulative area under the curve for tumor volumes plotted against the day of treatment. At day 16, we obtained statistically significant tumor reduction when all the treated groups were compared to control or no treatment. However, differences between P123/JS-K at 4 or 5 μmol/kg were not statistically significant. We could not carry the experiment beyond day 16 based on tumor volume guidelines of the IACUC.

2.5 Discussion

In this chapter, we describe a formulation for the prospective anticancer agent JS-K. Pluronic® block copolymers have been widely used as these are comparatively nontoxic and offer ease of preparation (29). Polymeric micelles do not offer high loading capacity, but seemed to work well for our purposes. In preliminary studies, we compared Pluronics® F127, P105 and P123. All three Pluronics® are different with respect to their physical characteristics, HLB value and solubility (26). The results indicated that for JS-K, P123 was the best choice in terms of stability and enhancing solubility of this extremely hydrophobic drug. JS-K in P123 micelles was more stable than in the other 2 formulations and P123 by itself did not have significant toxicity. Although most of our studies were performed on HL-60 cells, we also tested P123/JS-K in U-937 cells at the same drug loading percentage and obtained similar *in vitro* cytotoxicity results.

We conducted studies to characterize P123/JS-K since it is a clinical candidate. As evident from the size measurements, not much difference in the size was observed before and after incorporation of JS-K. Also, the TEM images of P123/JS-K reflect stability achieved by incorporation of JS-K. It has been suggested that for Pluronic® micelles, at concentrations significantly above the CMC, micelle stability diminishes (30). Our studies support this observation as we were unable to get TEM images of blank micelles,

but with JS-K incorporation, spherical micelles were observed. JS-K, being extremely hydrophobic, stabilized the dynamic nature of the micelles with physical interactions. We also measured the CMC of the Pluronic® P123 using the KI/I2 method. The value we obtained is in agreement with what has been obtained by others (24, 26).

Upon testing, free JS-K and P123/JS-K in various physiological media P123/JS-K showed enhanced recovery and extended stability as compared to JS-K alone. Human plasma, RPMI/FBS media and PBS were chosen as matrices of different complexity. Stability of JS-K was also tested in the presence of GSH because JS-K is cleaved in the presence of GSH. Higher stability of JSK in plasma as compared to whole blood could be attributed to higher GSH in blood as compared to plasma (31, 32). The relative stabilization of JS-K with P123 micelles could be attributed to shielding of JS-K in the micelle, thus preventing interaction with GSH.

A drug's interaction with serum proteins is an important PK/PD parameter that needs to be studied as this provides the basis for dosage regimen and other related PK analyses. The two major serum proteins are HSA and AGP. While it is generally observed that acidic drugs tend to bind with HSA and basic drugs tend to bind with AGP, the hypothesis is not absolute (33). We studied interaction of JS-K with HSA and AGP and P123/JS-K with HSA and AGP. We tried to compare our results obtained from equilibrium dialysis with the results obtained from spectrometric analysis. Equilibrium dialysis is an old and reliable technique but suffers from drawbacks such as requirement of high volumes, extensive time for equilibrium, volume shift and extensive preliminary studies. Nevertheless, it is the most widely used method and is still used to analyze plasma protein binding of various drugs (22). We initially performed the equilibrium

dialysis study for 8 h. For such a long time, P123/JS-K was relatively stable but free JS-K degradation was observed. In the P123/JS-K system, equilibrium was observed within 2 h. Complete equilibrium was not obtained for free JS-K probably due to drug instability. Nevertheless, the 2 h point was selected for the equilibrium dialysis for both formulations. Using SigmaPlot, we analyzed the binding constant and possible number of binding sites using an in-built ligand binding equation. As free JS-K is prone to degradation, we validated our results using spectrophotometric analysis. Also, none of the binding analysis techniques provide complete information. Therefore, a combination of two different techniques can provide valuable datasets (22). With the use of fluorescence quenching, we were able to analyze the Stern Volmer constant, binding constant and thermodynamic constants such as enthalpy, entropy and free energy. Fluorescence quenching of tryptophan upon binding of drug can yield useful information. This technique is fast and reliable, and requires less sample (28), (34), (35). In a complex system where the drug (JS-K) is incorporated inside the micelle core, protein binding can take place between JS-K and tryptophan residues of protein, P123/JS-K micelle and the tryptophan residues and finally between the unimers/ micelles and the tryptophan residues. As observed from the results, the association constant (Ka) obtained from the two techniques is slightly different. Comparing equilibrium constants at room temperature, for P123/JS-K, Ka obtained from equilibrium dialysis and fluorescence quenching was close whereas nearly ten times higher Ka was calculated for free JS-K when fluorescence quenching analysis was performed. This difference could be explained by considering the stability of free JS-K. While P123/JS-K was allowed to attain equilibrium, free JS-K might have degraded during the experiment. Although it could be

argued that the stern volmer plot obtained has various data points that could be considered as outliers, we consider it due to the lack of technique optimization. The results were promising and therefore, a more optimized temperature controlled study was performed. When a temperature controlled study was performed with fluorescence quenching technique, both the formulations showed increase in binding constant or binding strength with temperature although the increase observed for free JS-K was more marked than P123/JS-K (Figures 2.6 and 2.7). This could be explained by reduced binding property of Pluronic® polymers. In order to be effective, the drug should be released from the polymer to produce its therapeutic effect. How early JS-K is released from the micelle core needs to be established. The thermodynamic parameters obtained from the fluorescence quenching study holds significance as well. The negative free energy possessed by both free JS-K and P123/JS-K binding with HSA at different temperatures indicates a spontaneous reaction that is thermodynamically favorable. Again, both free JS-K and P123/JS-K possess positive enthalpy and entropy but the values are about ten times higher with free JS-K interaction with serum protein. Although it is hard to speculate, the relevance of such an observation as the specific heat capacity is not considered, but according to studies carried out by Ross and Subramanian (36), the positive value of both enthalpy and entropy indicate hydrophobic interactions.

Protein binding analysis can also be extended to hypothesize JS-K stability and interaction with HSA. As the protein binding is occurring, it could be hypothesized that JS-K stability can be enhanced with HSA interaction. A depot can be formed between JS-K and HSA. Some studies have shown interaction of NO residues (such as nitrosothiols) with albumin (37, 38). Also, the major metabolite of JS-K, S-glutathione-2,4-

dinitrophenyl can also interact with albumin via glutathione moiety. Therefore, either JS-K as a whole or the metabolites of JS-K can interact with albumin to form a depot of either whole JS-K or the metabolites of JS-K that are instrumental in producing cytotoxic effects of the drug.

The *in vivo* tumor regression study carried out justifies the use of the Pluronic® formulation of JS-K showing significant tumor regression after 8 treatments. It is interesting that both JS-K and P123/JS-K showed nearly equal tumor regression up to seven injections but P123/JS-K treated mice showed maximum regression after 8 treatments. One could speculate that the P123 formulation allowed JS-K accumulation in the tumor to a greater extent and that a critical threshold of antineoplastic activity was reached as a result. Another point is that the micelles prevented the drug from interacting with proteins and as a result allowed more drug to interact with leukemic cells. Finally, the micelles probably enhanced penetration of the drug in the leukemic cells as we have previously demonstrated (39). It would have been informative to be able to carry the experiment beyond that time point. However, ethical guidelines precluded us from doing so.

2.6 Conclusions

Overall, our study demonstrated that JS-K formulated in Pluronic® P123 has a more favorable *in vitro* and *in vivo* profile. The polymeric micelle formulation stabilizes the drug and diminishes its interaction with plasma proteins. The binding is thermodynamically favorable and points towards hydrophobic interactions. We also conclude that P123/JS-K is likely more therapeutically effective than free JS-K.

2.7 Future Perspectives

JS-K has potential as a cancer chemotherapeutic agent. Its solubility and stability challenges can be overcome with a micelle formulation strategy. Such a strategy could potentially allow its full clinical development.

2.8 References

1. Facts 2012. The Leukemia and Lymphoma Society. 2012.

2. Pokrajac M, Miljkovic B, Simic D, Brzakovic B, Galetin A. Comparative pharmacokinetics and bioavailability of two cotrimoxazole preparations. Die Pharmazie. 1998;53(7):470-472.

3. Moncada S, Palmer RM, Higgs EA. Nitric oxide: physiology, pathophysiology, and pharmacology. Pharmacol Rev. 1991;43(2):109-142.

4. Nathan C. Nitric oxide as a secretory product of mammalian cells. Faseb J. 1992;6(12):3051-3064.

5. Burgaud JL, Riffaud JP, Del Soldato P. Nitric-oxide releasing molecules: a new class of drugs with several major indications. Curr Pharm Des. 2002;8(3):201-213.

6. Hibbs JB, Jr., Taintor RR, Vavrin Z, Rachlin EM. Nitric oxide: a cytotoxic activated macrophage effector molecule. Biochem Biophys Res Commun. 1988;157(1):87-94.

7. Leon L, Jeannin JF, Bettaieb A. Post-translational modifications induced by nitric oxide (NO): implication in cancer cells apoptosis. Nitric Oxide. 2008;19(2):77-83.

8. Magrinat G, Mason SN, Shami PJ, Weinberg JB. Nitric oxide modulation of human leukemia cell differentiation and gene expression. Blood. 1992;80(8):1880-1884.

9. Shami PJ, Sauls DL, Weinberg JB. Schedule and concentration-dependent induction of apoptosis in leukemia cells by nitric oxide. Leukemia. 1998;12(9):1461-1466.

10. Liu J, Malavya S, Wang X, Saavedra JE, Keefer LK, Tokar E, Qu W, Waalkes MP, Shami PJ. Gene expression profiling for nitric oxide prodrug JS-K to kill HL-60 myeloid leukemia cells. Genomics. 2009;94(1):32-38.

11. Shami PJ, Saavedra JE, Wang LY, Bonifant CL, Diwan BA, Singh SV, Gu Y, Fox SD, Buzard GS, Citro ML, Waterhouse DJ, Davies KM, Ji X, Keefer LK. JS-K, a glutathione/glutathione S-transferase-activated nitric oxide donor of the diazeniumdiolate class with potent antineoplastic activity. Mol Cancer Ther. 2003;2(4):409-417.

12. Shami PJ, Saavedra JE, Bonifant CL, Chu J, Udupi V, Malaviya S, Carr BI, Kar S, Wang M, Jia L, Ji X, Keefer LK. Antitumor activity of JS-K [O2-(2,4-dinitrophenyl) 1-[(4-ethoxycarbonyl)piperazin-1-yl]diazen-1-ium-1,2-diolate] and related O2-aryl diazeniumdiolates in vitro and in vivo. J Med Chem. 2006;49(14):4356-4366.

13. Kiziltepe T, Hideshima T, Ishitsuka K, Ocio EM, Raje N, Catley L, Li CQ, Trudel LJ, Yasui H, Vallet S, Kutok JL, Chauhan D, Mitsiades CS, Saavedra JE, Wogan GN, Keefer LK, Shami PJ, Anderson KC. JS-K, a GST-activated nitric oxide generator, induces DNA double-strand breaks, activates DNA damage response pathways, and induces apoptosis in vitro and in vivo in human multiple myeloma cells. Blood. 2007;110(2):709-718.

14. Maciag AE, Chakrapani H, Saavedra JE, Morris NL, Holland RJ, Kosak KM, Shami PJ, Anderson LM, Keefer LK. The nitric oxide prodrug JS-K is effective against non-small-cell lung cancer cells in vitro and in vivo: involvement of reactive oxygen species. J Pharmacol Exp Ther. 2011;336(2):313-320.

15. Ren Z, Kar S, Wang Z, Wang M, Saavedra JE, Carr BI. JS-K, a novel non-ionic diazeniumdiolate derivative, inhibits Hep 3B hepatoma cell growth and induces c-Jun phosphorylation via multiple MAP kinase pathways. J Cell Physiol. 2003;197(3):426-434.

16. Kiziltepe T, Anderson KC, Kutok JL, Jia L, Boucher KM, Saavedra JE, Keefer LK, Shami PJ. JS-K has potent anti-angiogenic activity in vitro and inhibits tumour angiogenesis in a multiple myeloma model in vivo. J Pharm Pharmacol. 2010;62(1):145-151.

17. Simeone AM, McMurtry V, Nieves-Alicea R, Saavedra JE, Keefer LK, Johnson MM, Tari AM. TIMP-2 mediates the anti-invasive effects of the nitric oxide-releasing prodrug JS-K in breast cancer cells. Breast Cancer Res. 2008;10(3):R44.

18. Batrakova EV, Kabanov AV. Pluronic block copolymers: evolution of drug delivery concept from inert nanocarriers to biological response modifiers. J Control Release. 2008;130(2):98-106.

19. Cho K, Wang X, Nie S, Chen ZG, Shin DM. Therapeutic nanoparticles for drug delivery in cancer. Clin Cancer Res. 2008;14(5):1310-1316.

20. Bi S, Yantao S, Chunyu Q, Hanqi Z, and Chunming L. Binding of several anti-tumor drugs to bovine serum albumin: Fluorescence study. J Lumin. 2009;129(5):541-547.

21. Aggarwal P, Hall JB, McLeland CB, Dobrovolskaia MA, McNeil SE. Nanoparticle interaction with plasma proteins as it relates to particle biodistribution, biocompatibility and therapeutic efficacy. Adv Drug Deliv Rev. 2009;61(6):428-437.

22. Vuignier K, Schappler J, Veuthey JL, Carrupt PA, Martel S. Drug-protein binding: a critical review of analytical tools. Anal Bioanal Chem. 2010;398(1):53-66.

23. Udupi V, Yu M, Malaviya S, Saavedra JE, Shami PJ. JS-K, a nitric oxide prodrug, induces cytochrome c release and caspase activation in HL-60 myeloid leukemia cells. Leuk Res. 2006;30(10):1279-1283.

24. Wei Z, Hao J, Yuan S, Li Y, Juan W, Sha X, Fang X. Paclitaxel-loaded Pluronic P123/F127 mixed polymeric micelles: formulation, optimization and in vitro characterization. Int J Pharm. 2009;376(1-2):176-185.

25. Noni Husain RAA, and Isiah M. Warner. Spectroscopic analysis of the binding of doxorubicin to human .alpha.-1 acid glycoprotein. J Phys Chem. 1993;97 (41):10857-10861.

26. Kabanov AV, Batrakova EV, Alakhov VY. Pluronic block copolymers as novel polymer therapeutics for drug and gene delivery. J Control Release. 2002;82(2-3):189-212.

27. Shi Y, Liu H, Xu M, Li Z, Xie G, Huang L, Zeng Z. Spectroscopic studies on the interaction between an anticancer drug ampelopsin and bovine serum albumin. Spectrochim Acta A Mol Biomol Spectrosc. 2012;87:251-257.

28. Kandagal PB, Ashoka S, Seetharamappa J, Shaikh SM, Jadegoud Y, Ijare OB. Study of the interaction of an anticancer drug with human and bovine serum albumin: spectroscopic approach. J Pharm Biomed Anal. 2006;41(2):393-399.

29. Gaucher G, Dufresne MH, Sant VP, Kang N, Maysinger D, Leroux JC. Block copolymer micelles: preparation, characterization and application in drug delivery. J Control Release. 2005;109(1-3):169-188.

30. Cho HJ, Yoon HY, Koo H, Ko SH, Shim JS, Lee JH, Kim K, Kwon IC, Kim DD. Self-assembled nanoparticles based on hyaluronic acid-ceramide (HA-CE) and Pluronic(R) for tumor-targeted delivery of docetaxel. Biomaterials. 2011;32(29):7181-7190.

31. Eve Unt CK, Ivi Vaher and Mihkel Zilmer Red blood cell and whole blood glutathione redox status in endurance-trained men following a ski marathon. J Sports Sci Med. 2008;7:344-349.

32. Wu G, Fang YZ, Yang S, Lupton JR, Turner ND. Glutathione metabolism and its implications for health. J Nutr. 2004;134(3):489-492.

33. Tesseromatis C, Alevizou A. The role of the protein-binding on the mode of drug action as well the interactions with other drugs. Eur J Drug Metab Pharmacokinet. 2008;33(4):225-230.

34. Mahesha HG, Singh SA, Srinivasan N, Rao AG. A spectroscopic study of the interaction of isoflavones with human serum albumin. FEBS J. 2006;273(3):451-467.

35. Cui F, Qin L, Zhang G, Liu Q, Yao X, Lei B. Interaction of anthracycline disaccharide with human serum albumin: investigation by fluorescence spectroscopic technique and modeling studies. J Pharm Biomed Anal. 2008;48(3):1029-1036.

36. Ross PD, Subramanian S. Thermodynamics of protein association reactions: forces contributing to stability. Biochemistry. 1981;20(11):3096-3102.

37. Quinlan GJ, Martin GS, Evans TW. Albumin: biochemical properties and therapeutic potential. Hepatology. 2005;41(6):1211-1219.

38. Kashiba-Iwatsuki M, Miyamoto M, Inoue M. Effect of nitric oxide on the ligand-binding activity of albumin. Arch Biochem Biophys. 1997;345(2):237-242.

39. Kaur I, Terrazas M, Kosak KM, Kern SE, Boucher KM, Shami PJ. Cellular distribution studies of the nitric oxide-generating antineoplastic prodrug O(2) -(2,4-dinitrophenyl)1-((4-ethoxycarbonyl)piperazin-1-yl)diazen-1-ium-1,2-diolate formulated in Pluronic P123 micelles. J Pharm Pharmacol. 2013;65(9):1329-1336.

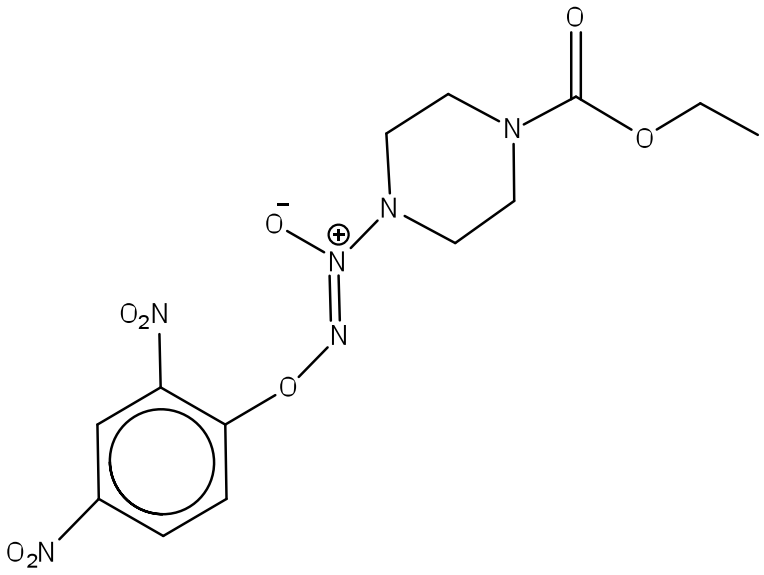

Fig. 2.1: Structure of JS-K

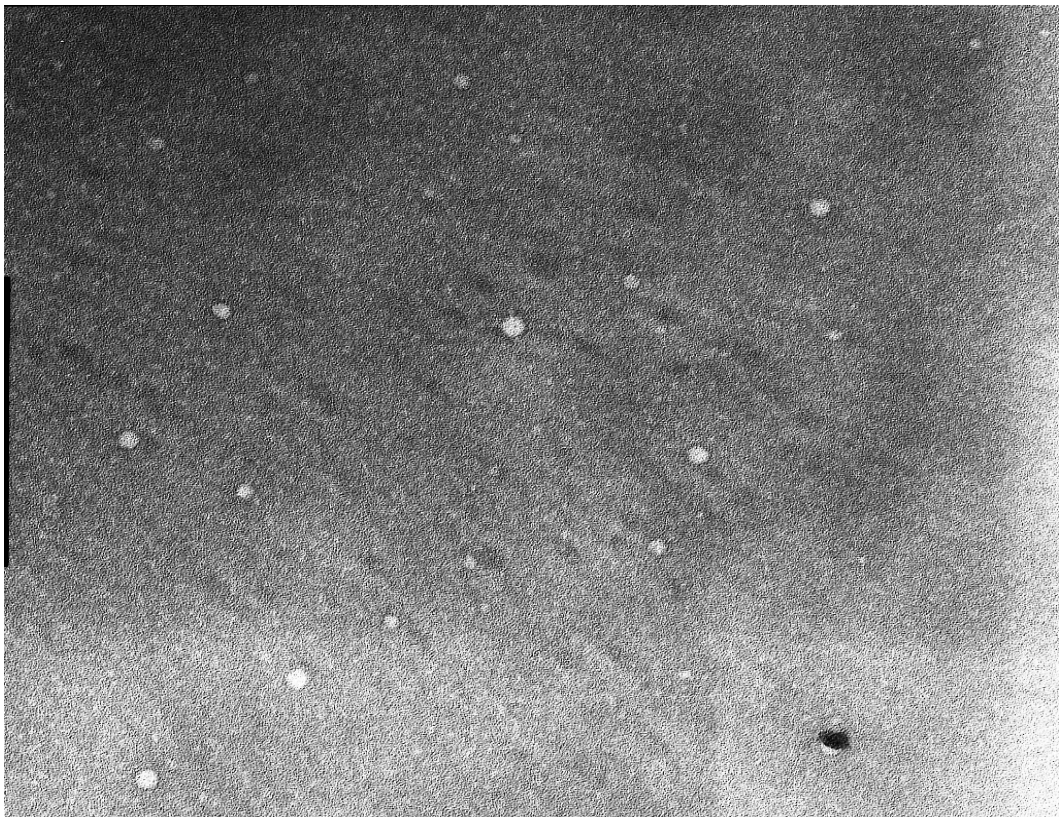

Fig. 2.2: TEM image (magnification 667x) of 1mM JS-K loaded in 2.25% P123 micelles.

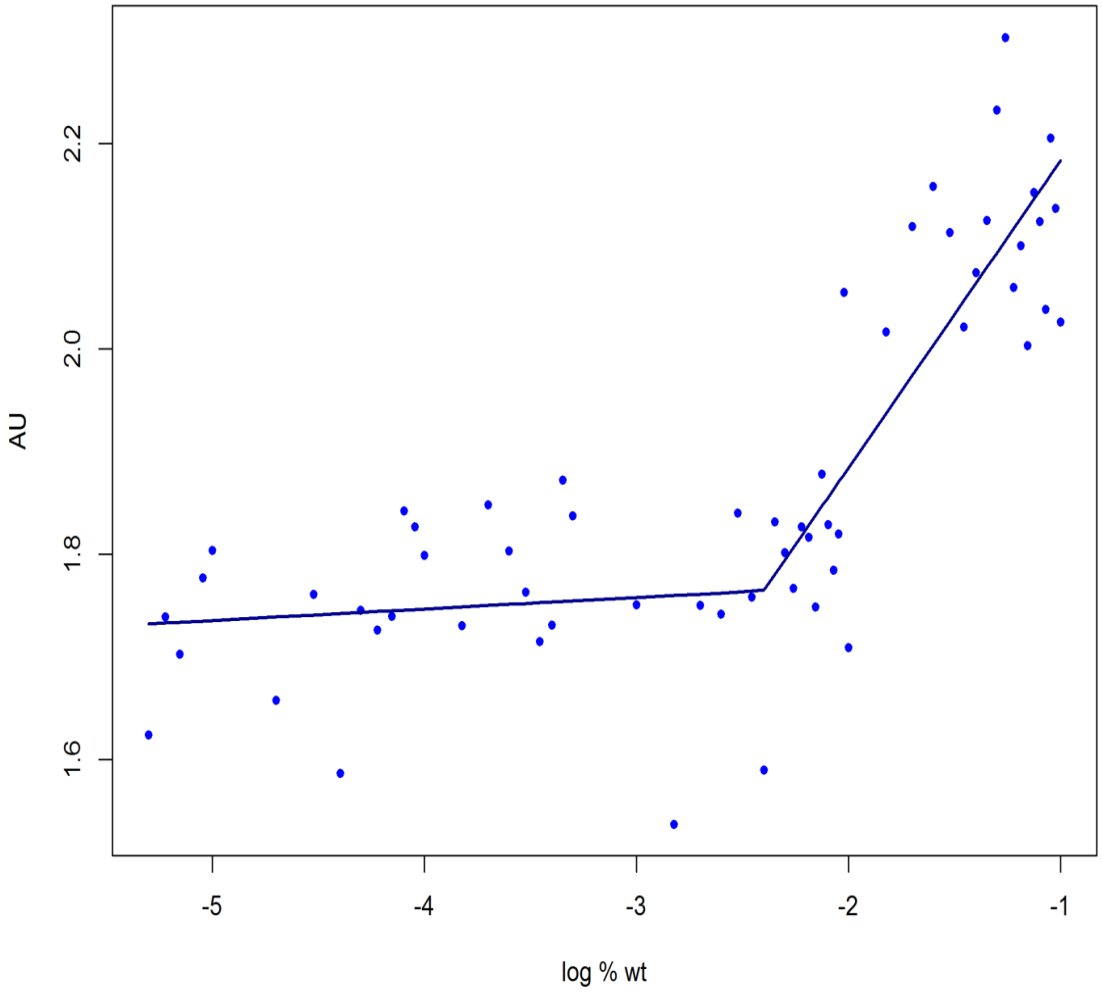

Fig. 2.3: Critical micelle concentration (CMC) value of Pluronic® P123 as determined by plotting Absorbance (AU) with log Pluronic® % weight/volume. The CMC was obtained from the break point calculated on R statistical software. CMC was calculated from the average of two independent experiments with each concentration prepared in triplicates.

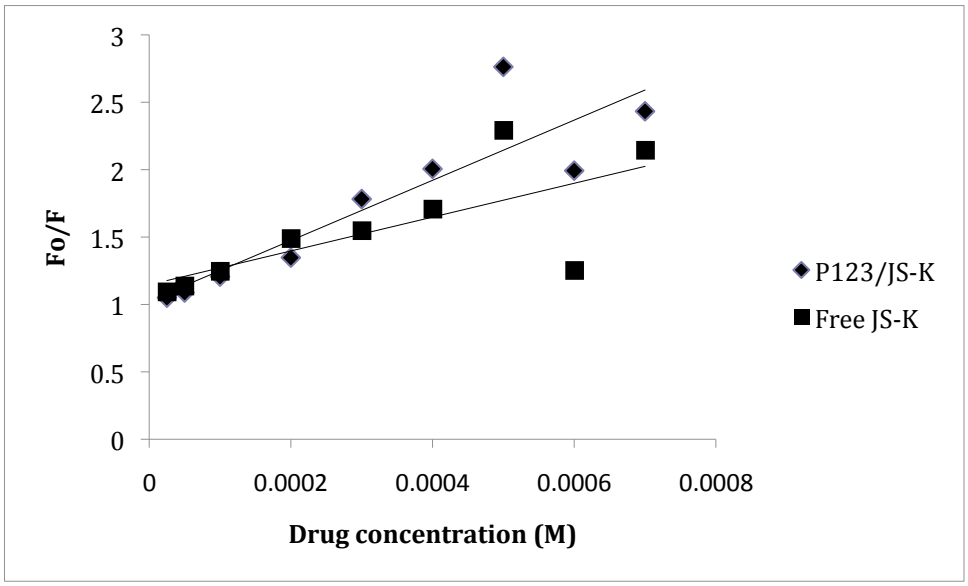

Fig. 2.4: Stern Volmer Plot for JS-K and HSA or P123/JS-K and HSA at room temperature
y-axis: Fluorescence of HSA/Fluorescence of drug; **x-axis**: JS-K or P123/JS-K concentration. Plots obtained from averages of 3 independent experiments.

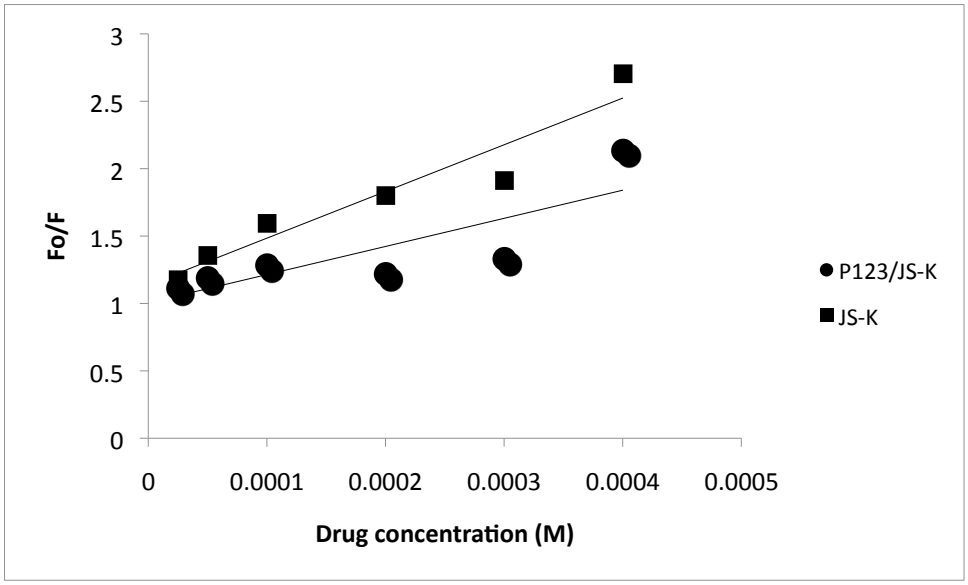

Fig. 2.5: Stern Volmer plot for JS-K and AGP or P123/JS-K and AGP at room temperature.
y-axis : Fluorescence of HSA/Fluorescence of drug; **x-axis**: JS-K or P123/JS-K concentration. Plots obtained from averages of 3 independent experiments.

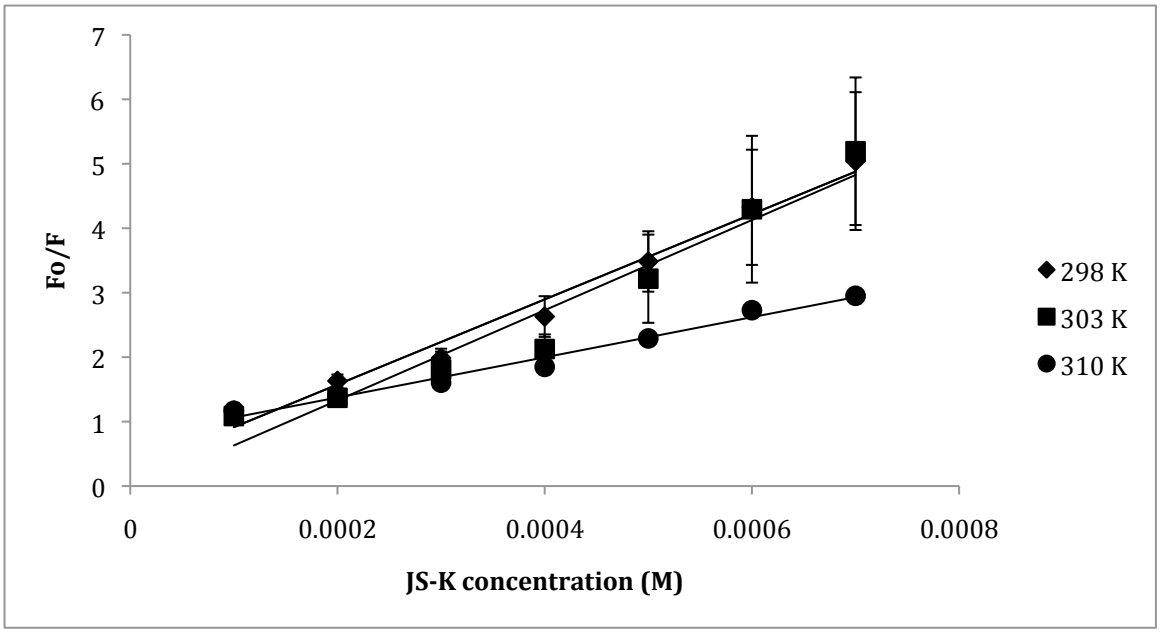

Fig. 2.6: Stern volmer plot for JS-K and HSA at 298, 303 and 310 K. Each point and standard error of mean (SEM) is a representative of two independent experiments with nine replicates.

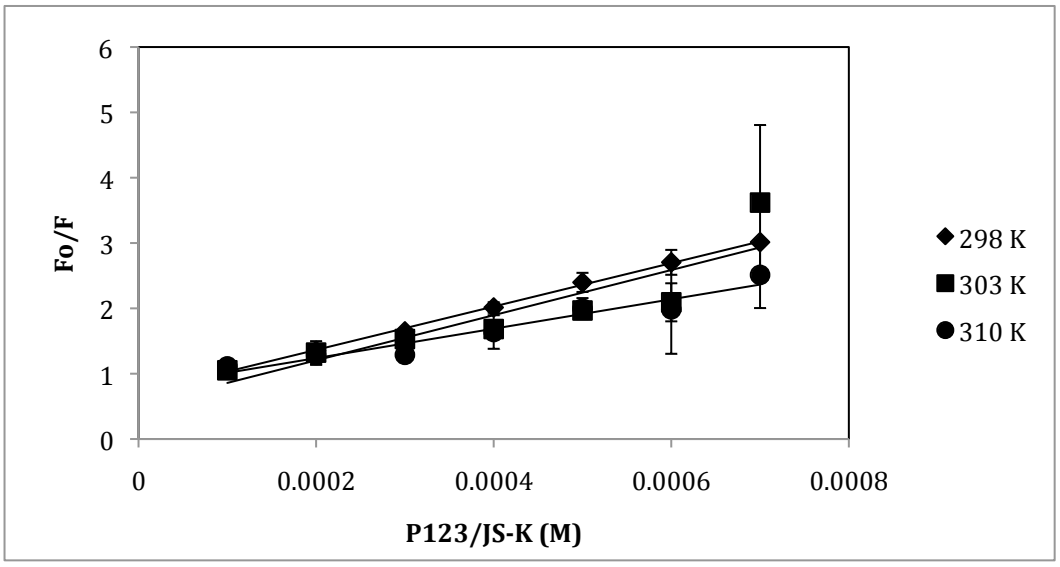

Fig. 2.7: Stern volmer plot for P123/JS-K at temperatures 298, 303 and 310 K. Each point and standard error of mean (SEM) is a representative of two independent experiments with nine replicates.

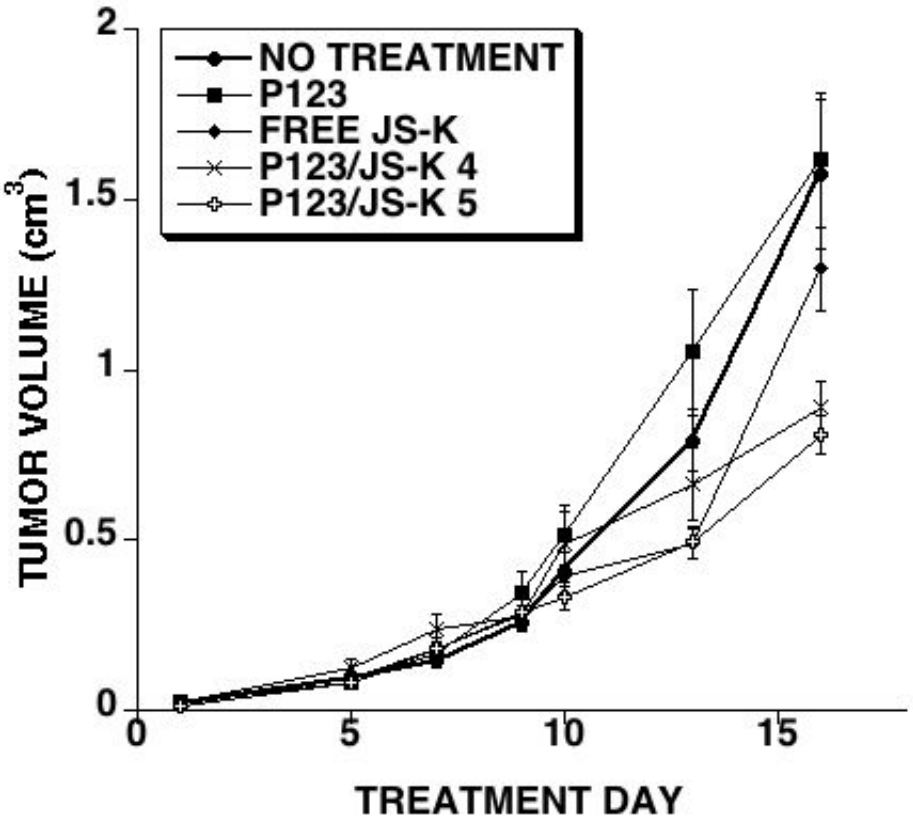

Fig. 2.8: *In vivo* tumor regression analysis: NOD/SCID *IL2Rg*^{null} mice were injected with HL-60 cells subcutaneously. Treatments started after tumors became palpable. A total of 8 injections were given. Treatment groups consisted of no treatment control, Pluronic® P123 treatment control, free JS-K injected at 4 μmol/kg, P123/JS-K injected at 4 μmol/kg, or P123/JS-K injected at 5 μmol/kg. See text for details.

Table 2.1: MTS cytotoxicity assay on HL-60 and U-937 cells comparing JS-K and P123/JS-K.		
System	Formulation	IC_{50} ± SEM* (μM)
HL-60 Cells	P123/JS-K	0.24 ± 0.059
	JS-K	0.24 ± 0.055
	P123 control	--
U-937 Cells	P123/JS-K	0.3 ± 0
	JS-K	0.4 ± 0
	P123 control	--
*Average and standard error mean of at least two separate experiments. Each experiment was performed in triplicates.		

Table 2.2: Size measurement of blank micelles and P123 loaded with JS-K at different percentages. The size of micelles decreases with increased loading.

System	Weight % drug loading	Size ± SEM (nm)*
Blank P123	0	29.24 ± 1.36
P123/JS-K	0.17	27.8 ± 4.9
	1.7	17.6 ± 1.21

*Averages and SEM of atleast two separate measurements. Each measurement with 20 iterations.

Table 2.3: Stability studies of JS-K. Percent recovery of JS-K or P123/JS-K calculated at the indicated time points. Percent Recovery of P123/JS-K is higher than JS-K, indicating drug stabilization.

Solution (time)	JS-K (% recovery±SEM*)	P123/JS-K (% recovery± SEM*)	p**
RPMI 1640/10% FBS (60 min.)	23 ± 0.4	48 ± 4	0.0015
Human plasma (60 min.)	39 ± 1	59 ±1.5	0.012
Whole blood (10 min.)	0 ± 0	6 ± 0	0.0284
4 mM GSH (5 min.)	8.5 ± 4.6	51 ± 10.8	0.003

*Average and SEM of atleast two independent experiments. **The Students t-test was used to obtain P values comparing both formulations. Results were considered statistically significant for $P < 0.05$.

Table 2.4: Binding Constants (Ka) obtained from equilibrium dialysis and fluorescence quenching and Stern Volmer constant (Ksv) obtained from fluorescence quenching at room temperature. Concentration of drugs used in both studies ranged from 0.7 mM-0.025 mM.

Formulation	Ka (equilibrium dialysis) (M^{-1}±SEM)*	Ksv (fluorescence quenching) with HSA (M^{-1})***	Ka (fluoroscence quenching) (M^{-1})***	Ksv (fluorescence quenching) with AGP (M^{-1})***
JS-K	$3.4 \times 10^3 \pm 2.2$ Ns** = 2.2; R^2 = 0.84	1.2×10^3 R^2 = 0.59	15×10^3 R^2 = 0.77	3×10^3 R^2 = 0.91
P123/JS-K	$3.0 \times 10^3 \pm 3.6$ Ns** = 1.9; R^2 = 0.89	2.2×10^3 R^2 = 0.805	3.5×10^3 R^2 = 0.99	2×10^3 R^2 = 0.67

* Average and Standard error of mean (SEM) of atleast three independent experiments. ** Ns=No. of binding sites. *** Average of at least three independent experiments.

Table 2.5: Stern Volmer quenching constant (Ksv) and HSA association binding constant (Ka) of JS-K and P123/JS-K at three temperatures: 298, 303 and 310 K.

Formulation	Temperature (K)	Ksv* ($x10^3$ M^{-1})	Kq* ($x10^{11}$ $M^{-1}s^{-1}$)	Ka* (M^{-1})
JS-K	298	6.6 $R^2 = 0.983$	6.6	57.3 $R^2 = 0.96$
	303	6.9 $R^2 = 0.94$	6.9	226.14 $R^2 = 0.98$
	310	3.1 $R^2 = 0.98$	3.1	1052.3 $R^2 = 0.99$
P123/JS-K	298	3.3 $R^2 = 0.99$	3.3	608.2 $R^2 = 0.988$
	303	3.4 $R^2 = 0.79$	3.4	615.2 $R^2 = 0.986$
	310	2.2 $R^2 = 0.93$	2.2	681.2 $R^2 = 0.840$

* Calculated from the slope of the curve plotted. Two independent experiments were performed with nine replicates at each concentration.
R^2 = goodness of fit

Table 2.6: Thermodynamic parameters for HSA and JS-K or HSA and P123/JS-K at three temperatures- 298, 303 and 310 K.

Formulation	Temperature (K)	Ka (M^{-1})	dG^o (kJ mol^{-1})	dH^o (kJ mol^{-1})	dS^o (J mol^{-1} K^{-1})
JS-K	298	57.3 $R^2 = 0.96$	-10.14	185.46 $R^2 = 0.99$	656.39 $R^2 = 0.99$
	303	226.14 $R^2 = 0.98$	-13.42		
	310	1052.3 $R^2 = 0.99$	-18.02		
P123/JS-K	298	608.2 $R^2 = 0.988$	-15.93	7.4 $R^2 = 0.88$	78.3 $R^2 = 0.88$
	303	615.2 $R^2 = 0.986$	-16.32		
	310	681.2 $R^2 = 0.840$	-16.87		

Calculated from the slope of the curve plotted. Two independent experiments were performed with nine replicates at each concentration.
R^2 = goodness of fit.

CHAPTER 3

CELLULAR DISTRIBUTION STUDIES OF THE NITRIC OXIDE-GENERATING ANTINEOPLASTIC PRODRUG JS-K, FORMULATED IN PLURONIC P123 MICELLES[3]

3.1 Abstract

Objective: Nitric oxide (NO) possesses anti-tumor activity. It induces differentiation and apoptosis in acute myeloid leukemia (AML) cells. The NO prodrug O^2-(2,4-dinitrophenyl)1-[(4-ethoxycarbonyl)piperazin-1-yl]diazen-1-ium-1,2-diolate, or JS-K, has potent antileukemic activity. JS-K is also active *in vitro* and *in vivo* against multiple myeloma, prostate cancer, non-small cell lung cancer, glioma and liver cancer. Using the Pluronic® P123 polymer, we have developed a micelle formulation for JS-K in order to increase its solubility and stability. The goal of the current study was to investigate the cellular trafficking of JS-K in AML cells.

Methods: We investigated the intracellular distribution of JS-K (free drug) and JS-K formulated in P123 micelles (P123/JS-K) using HL-60 AML cells. We also studied the *S*-

---

[3] Reprinted with kind permission from John Wiley and Sons: Journal of Pharmacy and Pharmacology, Cellular distribution studies of the nitric oxide generating antineoplastic prodrug JS-K, formulated in Pluronic P123 micelles. Volume 65 (9), 2013, 1329-1336, Imit Kaur, Moises Terrazas, Ken M. Kosak, Steven E. Kern, Kenneth M. Boucher and Paul J. Shami.

glutathionylating effects of JS-K on proteins in the cytoplasmic and nuclear cellular fractions.

Key findings: Both free JS-K and P123/JS-K accumulate primarily in the nucleus. Both free JS-K and P123/JS-K induced *S*-glutathionylation of nuclear proteins, although the effect produced was more pronounced with P123/JS-K. Minimal *S*-glutathionylation of cytoplasmic proteins was observed.

Conclusions: We conclude that a micelle formulation of JS-K increases its accumulation in the nucleus. Post-translational protein modification through *S*-glutathionylation may contribute to JS-K's anti-leukemic properties.

3.2 Introduction

Nitric oxide (NO) is a naturally occurring biological molecule with multiple functions in the vascular, neurologic and immune systems (1). It has direct cytotoxic effects on tumor cells (2). It can lead to apoptosis by targeting various cellular sites and bringing about post-translational modifications of proteins through mechanisms such as *S*-nitrosylation, *S*-glutathionylation and ADP ribosylation (3). NO has also been found to trigger apoptosis by inducing endoplasmic reticulum stress (4). We have previously shown that NO induces differentiation in acute myeloid leukemia (AML) cells (5). Also, diazeniumdiolates generate NO spontaneously and induce apoptosis in AML cells (6). However, these compounds cannot be used clinically for the treatment of malignant diseases because of the pleiotropic effects of NO, and particularly NO-induced vasodilatation through activation of the soluble guanylate cyclase/cGMP pathway (1). An alternative strategy relies on the use of prodrugs that target NO to the malignant cells. Arylated diazeniumdiolates react with glutathione (GSH) to release NO. The reaction is

catalyzed by glutathione *S*-transferases (GST) (7). This drug design exploits upregulation of GST in malignant cells (8). Our initial screen of arylated diazeniumdiolates revealed that O^2-(2,4-dinitrophenyl)1-[(4-ethoxycarbonyl)piperazin-1-yl]diazen-1-ium-1,2-diolate] or JS-K (Fig. 3.1) has potent anti-leukemic activity *in vitro* and *in vivo* (7). JS-K inhibits the growth of HL-60 myeloid leukemia cells with a 50% growth inhibitory concentration (IC_{50}) of 0.25 – 0.5 μM (7). In *in vivo* murine models, JS-K was also found to be effective against prostate cancer (7), hepatoma (9), multiple myeloma (10), non-small cell lung cancer (11) and glioma (12). JS-K also possesses anti-angiogenic activity both *in vitro* and *in vivo* (13). JS-K was shown to be selectively toxic towards tumor cells in multiple myeloma and breast cancer models. It did not affect the growth of normal human peripheral blood mononuclear cells (10) or normal mammary epithelial cells (14). Thus, JS-K is a promising candidate for development as an anti-neoplastic agent with a broad spectrum of activity.

In preliminary studies, JS-K was found to have challenging pharmacologic properties that hinder its clinical development. These include poor solubility in aqueous media and reactivity with blood components resulting in a short half- life ($t_{1/2}$). To solve these problems, we have developed a nanoscale formulation of JS-K using Pluronic® micelles. Pluronic® tri-block copolymers (poloxamers) are amphiphilic polymers composed of ethylene oxide (EO) and propylene oxide (PO) arranged in the sequence EOx-POy-EOx (15). Depending on the length of the EO and PO blocks, Pluronic® polymers form nanoscale micelles at different critical micelle concentrations (CMC) (16). These micelles have a hydrophobic core that traps sparingly soluble molecules and a hydrophilic shell that allows solubilization of the latter in aqueous media. Pluronic®

polymers are excellent candidates to solubilize anti-cancer agents because they have low toxicity, circumvent the multi-drug resistance phenotype and lead to higher intra-tumoral drug accumulation through the enhanced permeability and retention (EPR) effect (15-18). After screening multiple Pluronic® polymer candidates, we have developed a formulation for JS-K using the P123 Pluronic®. The purpose of the current study was to compare the intracellular trafficking of free JS-K as opposed to JS-K formulated in Pluronic® P123 micelles (P123/JS-K). Results show that Pluronic® P123 micelles increase the penetration of JS-K in HL-60 AML cells. We also observed that JS-K induces *S*-glutathionylation of nuclear proteins.

3.3 Materials and Methods

3.3.1 Materials

JS-K was synthesized at Richman Chemical (Lower Gwynedd, PA) as previously described (19). Pluronic® P123 polymers were obtained from BASF (Florham Park, NJ). All other chemicals were from Sigma (St. Louis, MO) unless otherwise noted.

3.3.2 Cells and culture conditions

Human myeloid leukemia HL-60 cells (ATCC, Rockville, MD) were cultured in RPMI-1640 supplemented with 10% fetal bovine serum (FBS) and penicillin/streptomycin. Cells were cultured at 37 ºC in a 5% CO_2 humidified atmosphere. For experiments in different media, cells were suspended in phosphate buffered saline (PBS) with or without 10% FBS, or RPMI/10% FBS as indicated in the individual experiment. For each experiment, JS-K was added at the time of culture

initiation, cells were harvested at the indicated time points, washed in PBS and assays conducted.

3.3.3 Pluronic® micelle formulation of JS-K

JS-K stocks (50 mM) in DMSO were mixed with stocks of Pluronic® P123 polymers prepared in PBS. Micellization was allowed to occur spontaneously with gentle heating at 55-60°C. The Pluronic® stock concentration was 2.25%. The proportion of JS-K to P123 in solution was 1.7% by weight. pH of the Pluronic® solution of JS-K was maintained at 6.5. The final concentration of JS-K in the Pluronic® solution was 1 mM. For comparison, experiments were conducted with free JS-K. In the latter case, a DMSO stock (50 mM) of JS-K was serially diluted in PBS to a final concentration of JS-K of 1 mM in PBS/60%DMSO. For the cellular uptake and cell distribution studies, the final JS-K concentration in culture with either formulation was 50 μM. This high concentration was used in order to ensure detection of measurable levels of JS-K within the limitations of our assays. For the *S*-glutathionylation assays (see below), the final concentration of JS-K in culture using either formulation was 5 μM.

3.3.4 High performance liquid chromatography (HPLC)

HPLC analysis to measure JS-K levels was conducted on a Waters Alliance HPLC system consisting of a 2695 Separation Module, a 2996 Photodiode Array Detector using a Waters XTerra MS C18 chromatography column (4.6 X 150 mm; 3.5 mm particle size), controlled by Empower software. We used an isocratic mobile phase consisting of A= 30% 0.02 M ammonium formate (pH 3), 40% acetonitrile (ACN) and 30% methanol, and D = 100% methanol. Flow rate was kept constant at 1mL/min for 6 min. During

chromatographic separation, JS-K was monitored by absorbance at 300 nm. The method results in a standard detection curve over a linear range of 6.1-49.1 ng with a lower limit of detection of 6.4 ng.

3.3.5 Cellular uptake and nuclei isolation

HL-60 cells (5 x 10^6 cells per mL) were cultured in 6 well tissue culture plates. Free or P123/JS-K was added to HL-60 cells at final concentrations of 50 mM. At the indicated time points, cells were collected by centrifugation and washed with PBS at pH 6.5. Cells were then lysed in lysis buffer. For whole cell lysates the lysis buffer consisted of 1% SDS formate. The lysis buffer for cytosolic and nuclear extraction consisted of 40 mM sodium citrate, 1% Triton X-100 adjusted to pH 6.5 or lower in order to increase the stability of JS-K. The lysed samples were then vortexed for few seconds and refrigerated for 30 min. at 4ºC. Nuclei were then separated from the cytosol by centrifugation for 10 min. at 600g. The efficiency of the nuclear isolation was verified by microscopic inspection of cytospins of the nuclear and cytoplasmic fractions stained with Wright/Giemsa stain. The isolated cellular fractions were then extracted with acetonitrile (60%)/formate (40%) for measurements of JS-K levels by HPLC as described above.

3.3.6 Glutathionylation assays

In order to evaluate protein *S*-glutathionylation, HL-60 cells (5x10^6 cells/mL) were treated with free JS-K or P123/JS-K or P123 only or DMSO only at a concentration of 5 μM for 30 min. Cytosolic and nuclear protein isolation was performed using the Qproteome Nuclear Protein Isolation Kit (Qiagen, Valencia, CA) following the manufacturer's protocol with the exception of excluding dithiothreitol (DTT) in order not

to confound results of the *S*-glutathionylation assay. Protein concentration of the samples was determined using the Bradford assay. Proteins were separated by SDS-PAGE on 4-12% polyacrylamide gel under non-reducing conditions. Proteins were transferred to polyvinylidene fluoride (PVDF) membranes. After blocking in 5% nonfat dry milk in tris-buffered saline with 0.2% tween (TBST), the membrane was incubated overnight at 4°C with anti-glutathione monoclonal antibody (1:1000, Virogen, Watertown, MA). Blots were developed by incubating the membrane with horseradish peroxidase conjugated secondary antibody (1:5000, Jackson Immuno Research Laboratories, INC, Westgrove, PA) and analyzed by enhanced chemiluminescence (GE Healthcare, Piscataway, NJ).

3.3.7 Statistical analysis

Two-way analysis of variance (ANOVA) was performed using SigmaPlots (Systat Software Inc, Chicago, IL). Results obtained for free JS-K or P123/JS-K were compared at different time points. Post-hoc analysis was performed using the Holm Sidak test. Differences were considered statistically significant for *P* values below 0.05.

3.4 Results

3.4.1 Cellular uptake studies

We started by performing exploratory experiments to compare the recovery of JS-K from whole cell extracts when the drug was formulated in P123 micelles (P123/JS-K) as opposed to the unformulated compound (dissolve in PBS/DMSO). Cells were incubated in PBS or RPMI/10%FBS and JS-K added at a concentration of 50 μM for both formulations. After 15, 30 and 60 min., JS-K recovery from whole cell extracts was

conducted as detailed in the *Methods*. JS-K recovery was higher with the P123 micelles than with the free drug (data not shown for these exploratory experiments). Since with these exploratory experiments it seemed that the P123 formulation enhanced the cellular penetration of JS-K, we next sought to determine if it affected its intracellular distribution.

We initially conducted the experiments with cells incubated in PBS in order to avoid the confounding effect of proteins or other elements in full media. For both formulations, recovery of JS-K from nuclei was higher than from the cytosol. However, P123 micelles increased the recovery of JS-K from nuclei. When cells were incubated in PBS, the percent recovery of free JSK from nuclei at 15, 30, 60 and 120 min. was 5.03±2.7; 5.00±3.2; 10.83±6.1 and 0.58±0.2, respectively (Fig. 3.2). Under the same conditions and at the same time points, the percent recovery of P123-formulated JS-K from nuclei was 9.05±4; 20.00±8.1; 21.15±3.6 and 27.73±4.9, respectively (Fig. 3.2). The differences between the 2 formulations were statistically significant when they were compared ($P = <0.001$), but the differences between the different time points of the same formulation were not significant. Also, the differences between the two formulations were statistically significant at 30 and 120 min. On the other hand, percent recovery of free JS-K from cytosol at 15, 30, 60 and 120 min. was 1.47±0.5; 0.87±0.5; 1.4±0.5 and 1.74±0.8, respectively (Fig. 3.2). Under the same conditions and at the same time points, the percent recovery of P123-formulated JS-K from cytosol was 2.73±1.5; 0.83±0.2; 1.22±0.4 and 0.95±0.3 (Fig. 3.2). It is notable that with free JS-K, nuclear recovery peaked at 60 min. and was negligible afterwards. On the other hand, when JS-K was formulated in P123 micelles, nuclear recovery peaked at 120 min.

As the recovery from the cytosol was negligible when the cells were incubated in PBS, the cytosolic fraction was not tested for JS-K recovery in subsequent studies. In order to determine the effect of proteins in the culture medium on JS-K recovery, we then measured JS-K levels when the cells were incubated in PBS/10% FBS. When cells were incubated in PBS/10% FBS, the percent recovery of free JS-K from nuclei at 30, 60 and 120 min. was 3.55±2.1, 3.15±1.5 and 2.13±1.1, respectively (Fig. 3.3). Under the same conditions and at the same time points, the percent recovery of P123/JS-K from nuclei was 20.74±7.2; 12.70±3.7 and 16.03±3.9, respectively (Fig. 3.3). The differences between the 2 formulations were statistically significant ($P<0.001$) but the differences between the different time points of the same formulation were not significant. When the formulations were compared at different time points, the differences were statistically significant at 30 and 120 min.

In order to determine the effect of full media on JS-K recovery, we repeated the experiments when the cells were incubated in RPMI/10% FBS. When cells were incubated in RPMI/10% FBS, the percent recovery of free JS-K from nuclei at 15, 30, 60 and 120 min. was 0.38±0.17; 0.45±0.23; 0.43±0.25 and 0.2±0.11, respectively (Fig. 3.4). Under the same conditions and at the same time points, the percent recovery of P123/JS-K was 2.93±1.65, 4.68±1.62, 9.30±1.58 and 11.90±4.4, respectively (Fig. 3.4). Overall JS-K recovery from nuclei was lower than with the less complex matrices, but again, recovery was higher with P123/JS-K. The two formulations showed statistically significant differences ($P<0.001$) but the differences between the different time points of the same formulation were not significant. When the formulations were compared at different time points, the differences were statistically significant at 60 and 120 min.

3.4.2 S-Glutathionylation studies

Protein *S*-glutathionylation is a well-established mechanism that controls protein function at the post-translational level (20,21). In that respect, NO has been shown to be a potent *S*-glutathionylating agent (3). We therefore sought to determine whether JS-K had the same effect in HL-60 cells. Based on our results showing increased levels of JS-K in the nucleus we also investigated whether JS-K had a differential *S*-glutathionylation effect on nuclear as opposed to cytoplasmic proteins. HL-60 cells were treated with JS-K at a concentration of 5 μM for 30 min. upon which nuclear and cytoplasmic proteins were isolated for assays of *S*-glutathionylation. Results showed that free JS-K induced minimal increase in the *S*-glutathionylation of cytosolic proteins (Fig. 3.5). The effect was similar when JS-K was formulated in P123 micelles (Fig. 3.5). When the soluble fraction of nuclear proteins was analyzed, free JS-K did not induce significant *S*-glutathionylation. However, for the same protein fraction, P123/JS-K induced significant *S*-glutathionylation (Fig. 3.6). When the insoluble fraction of nuclear proteins was analyzed, both free and P123-formulated JS-K induced significant *S*-glutathionylation. The effect was slightly more pronounced with the P123 formulation (Fig. 3.6).

3.5 Discussion

In the current work we evaluated the cellular distribution of JS-K in HL-60 leukemia cells. When free JS-K was added to the leukemic cells, there was minimal drug recovery from the different cellular compartments. However, higher levels of JS-K were recovered from the nucleus. When JS-K was formulated in P123 micelles, recovery of JS-K was substantially increased. Again, the highest amounts of JS-K were recovered from the nucleus. Several factors could explain these observations. JS-K reacts with GSH to form

the secondary products dinitro-phenyl *S*-glutathione and the diazeniumdiolate 4-carbethoxypiperazi-NO, which releases NO. Intracellular GSH levels are found mainly concentrated in the cytoplasm (22). One could therefore speculate that higher levels of JS-K were recovered from the nucleus because most of the JS-K in the cytoplasm reacted with GSH. However, the fact that JS-K was measured in the nucleus indicates that it does get transported into that compartment either passively or actively.

When formulated in P123 micelles, JS-K was recovered at higher levels than when the drug was formulated in PBS/DMSO. It is to be noted that for these assays, we used high concentrations of JS-K (50 μM) in order to be able to measure drug levels using the assay we developed. Previous work has shown that the solubility limit of JS-K in aqueous solutions was around 10 μM (7). Consequently, a possible reason for which there was greater cellular recovery of JS-K with the P123 formulation is that, by increasing the solubility of JS-K in the culture media, P123 allowed more drug to reach the cells. However, P123 micelles enhance recovery of JS-K in particular from the nucleus. This may be due to the fact that the micelles temporarily shield JS-K and prevent it from reacting with cytoplasmic GSH and proteins in the cytoplasm. Furthermore, P123 micelles by themselves may enhance the penetration of JS-K into the nucleus. Indeed, Rapoport et al. studied the effect of Pluronic® P105 on the cellular distribution of the lipophilic drug Ruboxyl. They showed that Ruboxyl accumulates in the nucleus at P105 concentrations as high as 1% (23). It is therefore likely that a similar effect occurs when JS-K is formulated with P123 micelles.

The recovery of JS-K from the different cellular compartments diminished when the cells were incubated with complex media such as PBS/10%FBS and RPMI/10%FBS.

This could be due to the fact that the stability of JS-K diminishes as it is exposed to proteins and other components of the media. P123 micelles yield to increased recovery of JS-K from the cells as compared to free JS-K in these media. Again, this is likely due to "protection" of JS-K by the micelles.

From a mechanistic standpoint, we show that JS-K induces *S*-glutathionylation of mainly nuclear proteins. Such a post-translational modification can have important implications. An oxidative cellular environment is linked with cell death whereas a reducing environment promotes cell survival (24). Depletion of cellular GSH pool has been associated with apoptosis (22). Nuclear GSH depletion also triggers apoptosis (25). The transcription factor nuclear factor-kB (NF-kB) promotes AML survival (24). *S*-glutathionylation of this protein can prevent its nuclear translocation, thus promoting apoptosis. NO inhibits directly the DNA binding activity of NF-kB (26). Whether, as an NO donor, JS-K affects AML cell survival through *S*-glutathionylation of NF-kB remains to be proven. We found that in HL-60 cells, *S*-glutathionylation is less marked on cytoplasmic proteins. This may be due to increased levels of GSH in the cytoplasm with resultant competition for reaction with JS-K.

As demonstrated above, P123 micelles increase the stability of JS-K. Micelles also enhance nuclear translocation of JS-K with observable post-translational modification of nuclear proteins through *S*-glutathionylation. Post-translational modifications such as *S*-glutathionylation and *S*-nitrosylation can have important consequences. These modifications can enhance or repress the activity of proteins and cause apoptosis (3). They can also cause activation of the unfolded protein response (UPR) due to accumulation of misfolded *S*-glutathionylated or *S*-nitrosylated proteins and result in

endoplasmic reticulum (ER) stress (27,28). If ER stress is strong and prolonged, apoptosis ensues (29). Induction of ER stress could therefore contribute to JS-K's cytotoxic activity.

S-glutathionylation of nuclear proteins by JS-K raises the possibility that the drug may be exerting some of its effect through a mechanism involving post-translational modification of these proteins. These proteins likely include transcription factors (soluble nuclear proteins) and histones (insoluble nuclear proteins). The latter finding raises the possibility that JS-K may affect leukemia cell growth through an epigenetic mechanism as has recently been reported for NO (30). Townsend et al. have shown that the JS-K analogue PABA-NO is a potent *S*-glutathionylating agent. They further demonstrated that one of the principal proteins that are *S*-glutathionylated by PABA-NO is Protein Disulphide Isomerase (28). Identification of proteins that are *S*-glutathionylated by JS-K will require further investigation.

3.6 Conclusions

We show here that JS-K likely affects leukemic cell viability by multiple mechanisms, including post-translational modification of nuclear proteins. While the drug by itself accumulates in different cellular compartments, a Pluronic® micelle formulation affects its cellular trafficking and leads to enhanced accumulation in the nucleus. JS-K-induced protein *S*-glutathionylation raises the possibility that it exerts part of its effect through the post-translational modification of key proteins that are yet to be identified. JS-K shows promise for medicinal applications as an anti-neoplastic agent.

3.7 Authorship Contributions

Research design: Kaur, Kosak, Kern and Shami

Conducted experiments: Kaur and Terrazas

Data analysis: Kaur, Kosak, Kern, Boucher and Shami

Wrote the manuscript: Kaur and Shami

3.8 Acknowledgements

This work was supported by grant RO1 CA129611 from the National Cancer Institute.

3.9 Disclosures

Paul Shami is Scientific Founder, Chief Medical Officer and Chairman of the Board of Directors of JSK Therapeutics Inc.

3.10 References

1. Moncada S, Palmer RM, Higgs EA. Nitric oxide: physiology, pathophysiology, and pharmacology. Pharmacol Rev. 1991;43(2):109-142.

2. Nathan C. Nitric oxide as a secretory product of mammalian cells. Faseb J. 1992;6(12):3051-3064.

3. Yim CY, Bastian NR, Smith JC, Hibbs JB, Jr., Samlowski WE. Macrophage nitric oxide synthesis delays progression of ultraviolet light-induced murine skin cancers. Cancer Res. 1993;53(22):5507-5511.

4. Hibbs JB, Jr., Taintor RR, Vavrin Z, Rachlin EM. Nitric oxide: a cytotoxic activated macrophage effector molecule. Biochem Biophys Res Commun. 1988;157(1):87-94.

5. Nathan CF, Hibbs JB, Jr. Role of nitric oxide synthesis in macrophage antimicrobial activity. Curr Opin Immunol. 1991;3(1):65-70.

6. Leon L, Jeannin JF, Bettaieb A. Post-translational modifications induced by nitric oxide (NO): implication in cancer cells apoptosis. Nitric Oxide. 2008;19(2):77-83.

7. Gotoh T, Mori M. Nitric oxide and endoplasmic reticulum stress. Arterioscler Thromb Vasc Biol. 2006;26(7):1439-1446.

8. Magrinat G, Mason SN, Shami PJ, Weinberg JB. Nitric oxide modulation of human leukemia cell differentiation and gene expression. Blood. 1992;80(8):1880-1884.

9. Shami PJ, Sauls DL, Weinberg JB. Schedule and concentration-dependent induction of apoptosis in leukemia cells by nitric oxide. Leukemia. 1998;12(9):1461-1466.

10. Saavedra JE, Shami PJ, Wang LY, Davies KM, Booth MN, Citro ML, Keefer LK. Esterase-sensitive nitric oxide donors of the diazeniumdiolate family: in vitro antileukemic activity. J Med Chem. 2000;43(2):261-269.

11. Liu J, Malavya S, Wang X, Saavedra JE, Keefer LK, Tokar E, Qu W, Waalkes MP, Shami PJ. Gene expression profiling for nitric oxide prodrug JS-K to kill HL-60 myeloid leukemia cells. Genomics. 2009;94(1):32-38.

12. van der Kolk DM, Vellenga E, Muller M, de Vries EG. Multidrug resistance protein MRP1, glutathione, and related enzymes. Their importance in acute myeloid leukemia. Adv Exp Med Biol. 1999;457:187-198.

13. Shami PJ, Saavedra JE, Wang LY, Bonifant CL, Diwan BA, Singh SV, Gu Y, Fox SD, Buzard GS, Citro ML, Waterhouse DJ, Davies KM, Ji X, Keefer LK. JS-K, a glutathione/glutathione S-transferase-activated nitric oxide donor of the diazeniumdiolate class with potent antineoplastic activity. Mol Cancer Ther. 2003;2(4):409-417.

14. Ren Z, Kar S, Wang Z, Wang M, Saavedra JE, Carr BI. JS-K, a novel non-ionic diazeniumdiolate derivative, inhibits Hep 3B hepatoma cell growth and induces c-Jun phosphorylation via multiple MAP kinase pathways. J Cell Physiol. 2003;197(3):426-434.

15. Kiziltepe T, Hideshima T, Ishitsuka K, Ocio EM, Raje N, Catley L, Li CQ, Trudel LJ, Yasui H, Vallet S, Kutok JL, Chauhan D, Mitsiades CS, Saavedra JE, Wogan GN, Keefer LK, Shami PJ, Anderson KC. JS-K, a GST-activated nitric oxide generator, induces DNA double-strand breaks, activates DNA damage response pathways, and induces apoptosis in vitro and in vivo in human multiple myeloma cells. Blood. 2007;110(2):709-718.

16. Maciag AE, Chakrapani H, Saavedra JE, Morris NL, Holland RJ, Kosak KM, Shami PJ, Anderson LM, Keefer LK. The nitric oxide prodrug JS-K is effective against non-small-cell lung cancer cells in vitro and in vivo: involvement of reactive oxygen species. J Pharmacol Exp Ther. 2011;336(2):313-320.

17. Weyerbrock A, Osterberg N, Psarras N, Baumer B, Kogias E, Werres A, Bette S, Saavedra JE, Keefer LK, Papazoglou A. JS-K, a glutathione S-transferase-activated nitric oxide donor with antineoplastic activity in malignant gliomas. Neurosurgery. 2012;70(2):497-510.

18. Kiziltepe T, Anderson KC, Kutok JL, Jia L, Boucher KM, Saavedra JE, Keefer LK, Shami PJ. JS-K has potent anti-angiogenic activity in vitro and inhibits tumour angiogenesis in a multiple myeloma model in vivo. J Pharm Pharmacol. 2010;62(1):145-151.

19. McMurtry V, Saavedra JE, Nieves-Alicea R, Simeone AM, Keefer LK, Tari AM. JS-K, a nitric oxide-releasing prodrug, induces breast cancer cell death while sparing normal mammary epithelial cells. Int J Oncol. 2011;38(4):963-971.

20. Kabanov AV, Batrakova EV, Alakhov VY. Pluronic block copolymers for overcoming drug resistance in cancer. Adv Drug Deliv Rev. 2002;54(5):759-779.

21. Duncan R. The dawning era of polymer therapeutics. Nat Rev Drug Discov. 2003;2(5):347-360.

22. Kozlov MY M-NN, Batrakova EV and Kabanov AV. Relationship between Pluronic Block Copolymer Structure, Critical Micellization Concentration and Partitioning Coefficients of Low Molecular Mass Solutes. Macromolecules. 2000;33(9):3305-3313.

23. Miyata K CR, Kataoka K. Polymeric micelles for nano-scale drug delivery. React Funct Polym. 2011;71:227-234.

24. Oh KT, Bronich TK, Kabanov AV. Micellar formulations for drug delivery based on mixtures of hydrophobic and hydrophilic Pluronic block copolymers. J Control Release. 2004;94(2-3):411-422.

25. Saavedra JE, Srinivasan A, Bonifant CL, Chu J, Shanklin AP, Flippen-Anderson JL, Rice WG, Turpin JA, Davies KM, Keefer LK. The secondary amine/nitric oxide complex ion R(2)N[N(O)NO](-) as nucleophile and leaving group in S9N)Ar reactions. J Org Chem. 2001;66(9):3090-3098.

26. Antonio Martínez-Ruiz SL. Signalling by NO-induced protein S-nitrosylation and S-glutathionylation:Convergences and divergences. Cardiovascular Res. 2007;75:220–228.

27. Townsend DM. S-glutathionylation: indicator of cell stress and regulator of the unfolded protein response. Mol Int. 2007;7(6):313-324.

28. Franco R, Cidlowski JA. Apoptosis and glutathione: beyond an antioxidant. Cell Death Differ. 2009;16(10):1303-1314.

29. Rapoport N, Marin A, Luo Y, Prestwich GD, Muniruzzaman MD. Intracellular uptake and trafficking of Pluronic micelles in drug-sensitive and MDR cells: effect on the intracellular drug localization. J Pharm Sci. 2002;91(1):157-170.

30. Konopleva MY, Jordan CT. Leukemia stem cells and microenvironment: biology and therapeutic targeting. J Clin Oncol. 2011;29(5):591-599.

31. Markovic J, Mora NJ, Broseta AM, Gimeno A, de-la-Concepcion N, Vina J, Pallardo FV. The depletion of nuclear glutathione impairs cell proliferation in 3t3 fibroblasts. PLoS One. 2009;4(7):e6413.

32. Gotoh T, Oyadomari S, Mori K, Mori M. Nitric oxide-induced apoptosis in RAW 264.7 macrophages is mediated by endoplasmic reticulum stress pathway involving ATF6 and CHOP. J Biol Chem. 2002;277(14):12343-12350.

33. Townsend DM, Manevich Y, He L, Xiong Y, Bowers RR, Jr., Hutchens S, Tew KD. Nitrosative stress-induced s-glutathionylation of protein disulfide isomerase leads to activation of the unfolded protein response. Cancer Res. 2009;69(19):7626-7634.

34. Li X, Zhang K, Li Z. Unfolded protein response in cancer: the physician's perspective. J Hematol Oncol. 2011;4:8.

35. de Luca A, Moroni N, Serafino A, Primavera A, Pastore A, Pedersen JZ, Petruzzelli R, Farrace MG, Pierimarchi P, Moroni G, Federici G, Sinibaldi Vallebona P, Lo Bello M. Treatment of doxorubicin-resistant MCF7/Dx cells with nitric oxide causes histone glutathionylation and reversal of drug resistance. Biochem J. 2011;440(2):175-183.

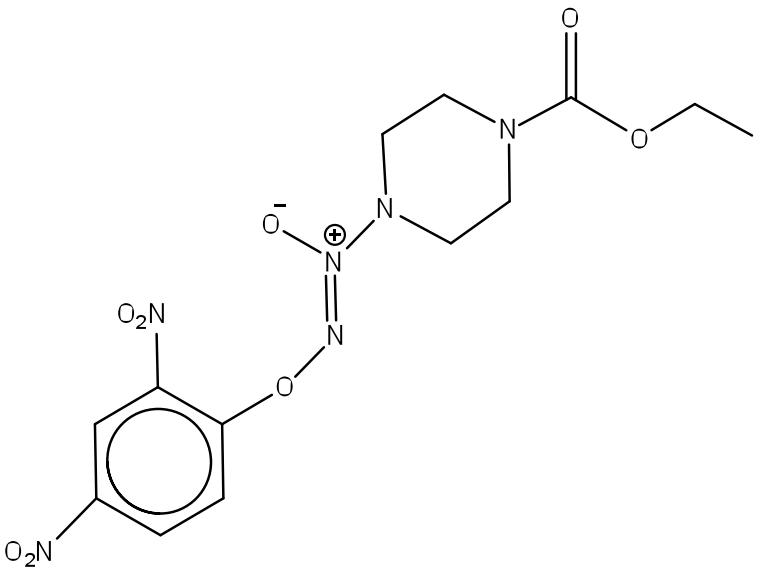

Fig. 3.1: Structure of JS-K

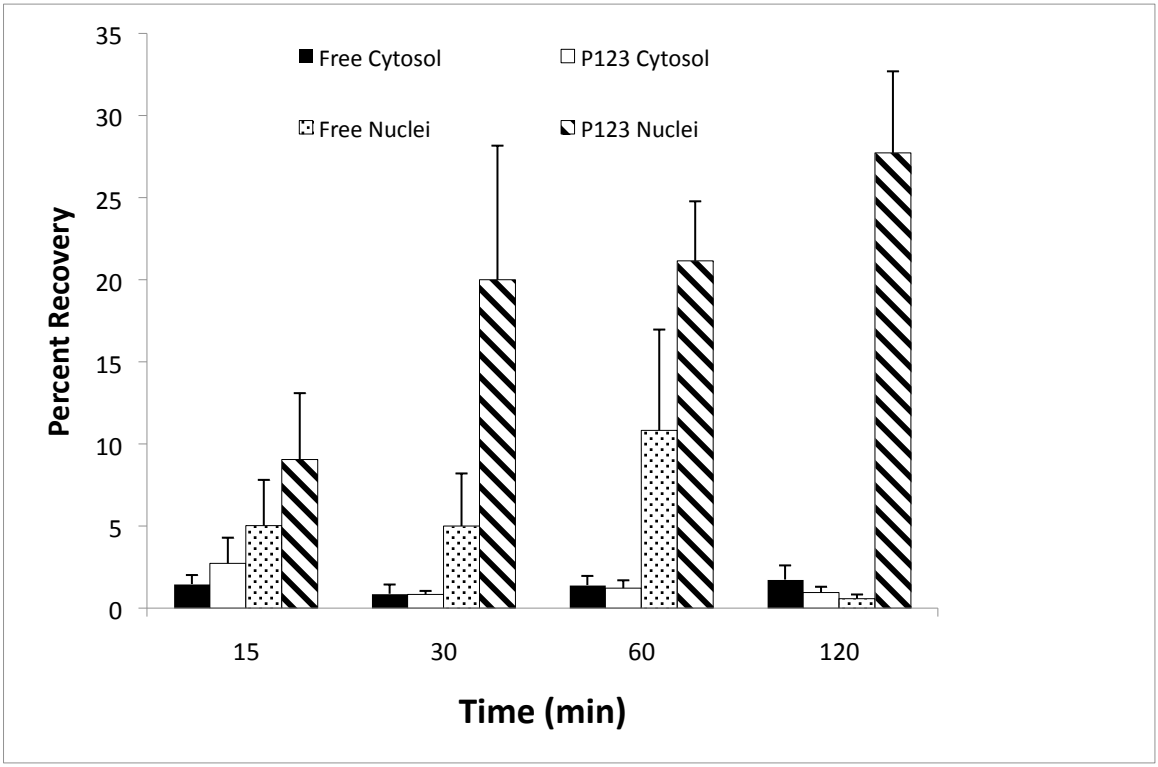

Fig. 3.2: Percent recovery of JS-K from cytoplasmic and nuclear fractions when cells were incubated in PBS: Values are expressed as percent of initial JS-K added. Cytosolic recovery of JS-K is low as compared to nuclear recovery. At any time point, JS-K recovery from the nucleus was higher when the drug was formulated in P123 Pluronic® micelles. Free Nuclei = JS-K recovery from nuclei with PBS/DMSO formulation. P123 Nuclei = JS-K recovery from nuclei with P123 formulation. Free Cytosol = JS-K recovery from cytosol with PBS/DMSO formulation. P123 Cytosol = JS-K recovery from cytosol with P123 formulation. The plot shows averages and standard errors of the mean of at least two separate experiments for each time point.

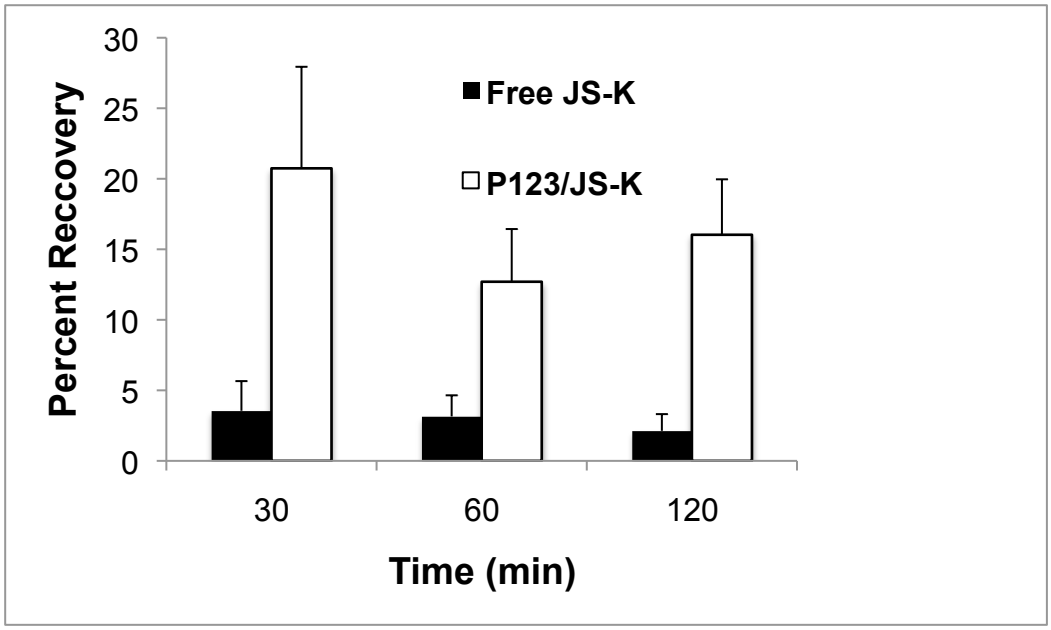

Fig. 3.3: Percent recovery of JS-K from the nuclear fraction when cells were incubated in PBS/10% FBS. Values are expressed as percent of initial JS-K added. At any time point, JS-K recovery from the nucleus was higher when the drug was formulated in P123 Pluronic® micelles. The plot shows averages and standard errors of the mean of at least two separate experiments for each time point. A 15 min. time point was not tested.

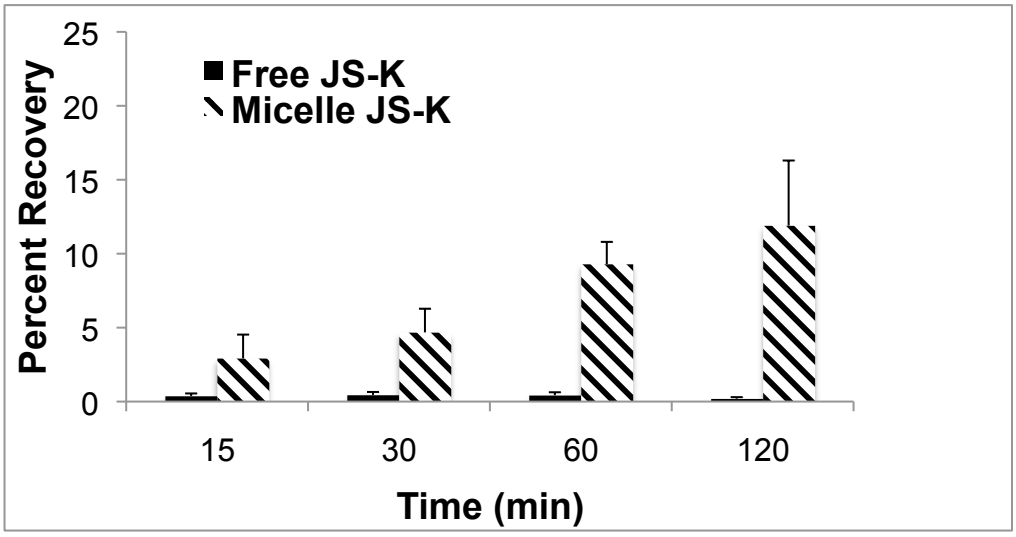

Fig. 3.4: Percent recovery of JS-K from the nuclear fraction when cells were incubated in RPMI/10% FBS: Values are expressed as percent of initial JS-K added. At any time point, JS-K recovery from the nucleus was higher when the drug was formulated in P123 Pluronic® micelles. The plot shows averages and standard errors of the mean of three separate experiments for each time point.

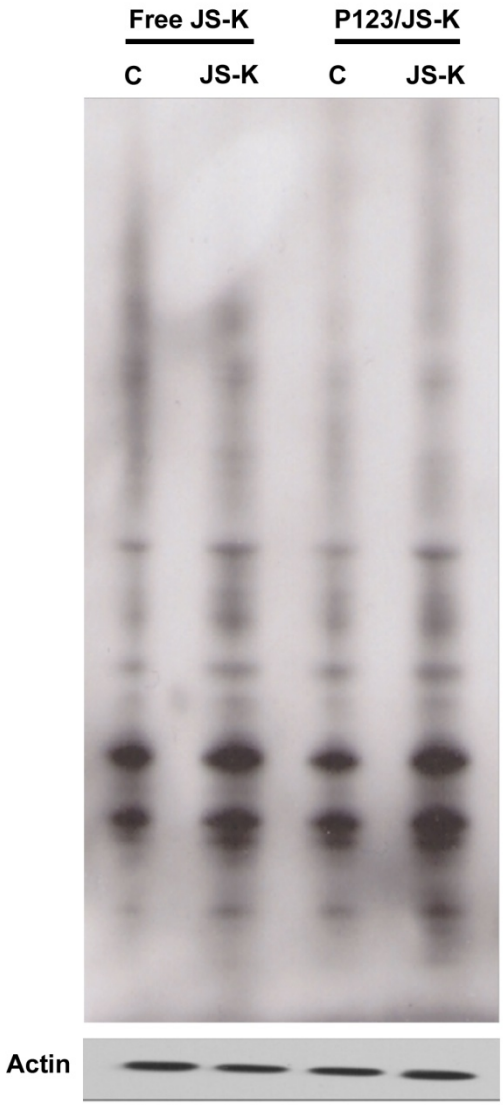

Fig. 3.5: *S*-glutathionylation of cytosolic proteins by JS-K: HL-60 cells were treated with 5 μM JS-K and incubated for 30 minutes. Evaluation of *S*-glutahionylation of cytosolic proteins was conducted as detailed in the text. JS-K in either formulation causes minimal *S*-glutathionylation of cytosolic proteins. 30μg of protein was loaded into each lane of the gel. Lane 1: DMSO control; Lane 2: HL-60 cells treated with free JS-K; Lane 3: P123 control; Lane 4: HL-60 cells treated with P123/JS-K. Actin was used as the loading control. The blot shown is representative of 4 separate experiments.

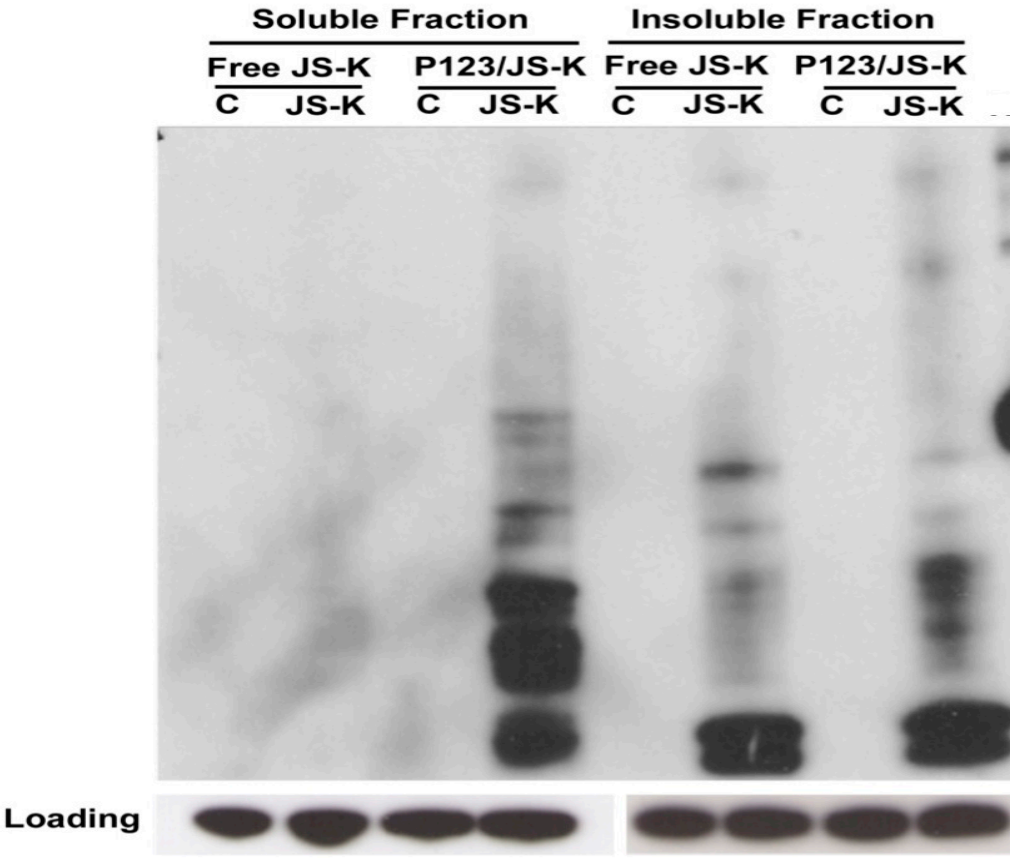

Fig. 3.6: *S*-glutathionylation of nuclear proteins by JS-K. HL-60 cells were treated with 5 μM JS-K and incubated for 30 minutes. Evaluation of *S*-glutahionylation of nuclear proteins was conducted as detailed in the text. JS-K caused *S*-glutathionylation of nuclear proteins. The effect is more pronounced with P123/JS-K. Among the nuclear proteins, soluble nuclear proteins are *S*-glutathionylated to a greater extent than insoluble nuclear proteins. 30μg of protein was loaded into each lane of the gel. Lane 1: No treatment control for soluble nuclear proteins; Lane 2: *S*-glutahionylation of soluble nuclear proteins caused by free JS-K; Lane 3: P123 control for soluble nuclear proteins; Lane 4: *S*-glutahionylation of soluble nuclear proteins caused by P123/JS-K; Lane 5: No treatment control for insoluble nuclear proteins; Lane 6: *S*-glutahionylation of insoluble nuclear proteins caused by free JS-K; Lane 7: P123 control for insoluble nuclear proteins; Lane 8: *S*-glutahionylation of insoluble nuclear proteins caused by P123. PCNA was used as the loading control for soluble nuclear proteins and Histone 3 protein was used as the loading control for insoluble nuclear proteins. The blot shown is representative of 4 separate experiments.

CHAPTER 4

MULTIPLE STRESS RESPONSES INDUCED BY THE NITRIC OXIDE-RELEASING PRODRUG JS-K

4.1 Abstract

Cancer cell killing is challenging as most clinically approved chemotherapeutics show nonselective effects by killing normal cells as well (1-3). Also, most chemotherapeutics act through specific mechanisms (3), which is prone to development of resistance by cancer cells (4). The rapidly acquired mutations in cancer cells make them resistant to the single effect/stress produced. In the present chapter, we studied two major stress mechanisms produced by JS-K or P123/JS-K in HL-60 human AML cells. Oxidative stress and endoplasmic reticulum stress contribute to the apoptotic effects produced by the drug. We also tested the effect of the drug on normal hematopoietic cells (HSCs). JS-K or P123/JS-K did not evoke such a stress response in HSCs. This effect was also not triggered by the positive control used in the study. We conclude that JS-K or P123/JS-K enhanced intracellular reactive oxygen species/reactive nitrogen species thus causing oxidative stress. It also evoked endoplasmic reticulum stress-mediated cell death in leukemia cells.

4.2 Introduction

The hallmarks of malignancies include uncontrolled cell proliferation, evasion of growth suppression and apoptosis, induction of angiogenesis, invasion and metastasis (5). Chemotherapeutics act on cancer cells in a diverse fashion. Generally, they act by damaging DNA (genotoxic), topoisomerase inhibition, mitotic inhibition or by interfering with key metabolic pathways. The overall strategy behind most chemotherapeutics is to generate some sort of cell stress in the cancer cells and drive them to apoptosis (6). The type of stress response generated and the extent of damage determines how effective the chemotherapeutic will be. This is because the cancer cell population is heterogeneous and distinct populations of sensitive and resistant cancer cells are present. Also, cancer cells can evoke repair mechanisms or efflux responses to the chemotherapeutics that limit their actions (7).

Cancer cells are different from normal cells because of the above-stated hallmarks. The deregulated growth signals and altered metabolism supports the tumor microenvironment. Additionally, the property of stemness of cancer cells makes their complete eradication very hard. Therefore, it is necessary to target the tumor, the tumor microenvironment, the associated metabolic pathways and the associated cell death pathways in order to eradicate it completely (8-12).

4.2.1 Endoplasmic reticulum stress

The endoplasmic reticulum (ER) is involved in a plethora of biological functions. ER is the site for biosynthesis of protein, steroids, cholesterol and other lipids. It is also the site for protein folding and assembly (13). It is also involved in posttranslational modifications such as glycosylation and disulfide bond formation (14). ER provides a

cellular store for calcium (15). Proteins translocated to the ER must be folded properly before translocating to the Golgi. Unfolded and misfolded proteins stay in the ER for refolding or degradation through ubiquitination. Accumulation of such unfolded or misfolded proteins or perturbations to any of the ER functions threatens ER integrity and cell survival (16). Such a condition is called ER stress. The adaptive response triggered as a result of ER stress is called the unfolded protein response (UPR). The ER therefore coordinates stress pathways maintaining the crosstalk between the cell's intracellular and extracellular environment (17). ER stress has been implicated in several conditions, including diabetes (18), (19), cancer (13, 20-29), neurodegenerative disorders (30), (31), cardiovascular disorders (32) and other environmental insults and pathophysiological conditions such as hypoxia (33), calcium imbalance (13, 34), oxidative stress (13) and viral infections (35). The UPR re-establishes ER homeostasis by either shutting down general protein translation or by increasing protein folding through upregulation of components of the ER folding machinery and ER quality control, like the ER-associated degradation (ERAD) pathway. However, during severe ER stress that cannot be controlled by adaptive response, the UPR switches from a prosurvival to a prodeath response (36).

4.2.1.1 Steps of UPR during ER stress

During the UPR, three ER stress sensors are triggered. PERK (pancreatic ER kinase), Ire1 (inositol requiring enzyme) and ATF6 (activating transcription factor) are present on the ER membrane (15). During the unstressed conditions, BiP/GRP78 (GRP78 from now onwards) is bound to these three ER stress sensors. GRP78 (glucose regulated protein) is an ER chaperone that is involved in the proper folding of proteins. During ER stress, due

to high demand of protein folding, GRP78 dissociates from the ER stress sensors and binds to the abnormal proteins. With GRP78 dissociation, the sensors are activated. While PERK and Ire1 are dimerized and autophosphorylated, ATF6 is transported to the Golgi and activated by two step cleavage by Site-1 and Site-2 proteases (37). These three sensors then act in a coordinated fashion to relieve the ER stress. In the first phase, general protein load is reduced by translational attenuation through phosphorylation of eIF-2α by PERK. In the second phase, induction of ER chaperones is observed that enhances the folding capacity of the ER. GRP78 is one such chaperone. The third phase is the ER associated degradation (ERAD), which involves degradation of unfolded or misfolded proteins accumulated in the ER through the ubiquitin-proteasome system in the cytosol. If all these adaptive responses fail and the ER homeostasis is not restored, then prosurvival UPR shifts to proapoptotic UPR to remove damaged cells. CHOP is the common proapoptotic protein activated by all three branches of UPR (15), (38), (39), (40). These phases are represented in Fig. 4.1.

4.2.1.2 Conditions leading to and resulting from ER stress

4.2.1.2.1 Misfolded/Unfolded protein accumulation

The cellular system is constantly challenged by environmental stresses that result in protein misfolding. Such a condition can arise inside the ER or outside the ER including the cytosol and nucleus (41). Such protein misfolding can result in pathological conditions.

ER stress has been suggested as an early marker in neurodegeneration (42). Neurodegenerative disorders such as Alzheimers disease, Parkinsons disease and Huntington's disease result from the accumulation of aggregated and misfolded proteins

(43). The misfolded proteins accumulated in ER transmit a toxic response in the form of disruption of synaptic function affecting neuronal function, calcium imbalance, free radical release causing redox imbalance, disruption in protein degradation pathway or programmed cell death as the eventual step. Such conditions arise due to deposition of misfolded proteins as inclusion bodies that enable interaction with cellular targets causing toxic response (44).

Diabetes is a condition resulting from disturbed insulin regulation. In the β cell, ER serves important functions in the assembly and processing of insulin. During hyperglycemia, the transcription and translation of pro-insulin is increased, leading to accumulation of misfolded pro-insulin in the ER lumen thus causing ER stress (45), (46).

Several cardiac disorders such as cardiac hypertrophy, cardiac failure, atherosclerosis and ischemic heart diseases are associated with ER stress. In this section, only atherosclerosis will be discussed as only this condition results from protein synthesis overload. Macrophages and smooth muscle cells cause atherosclerosis development. During the initial phase of atherosclerosis, high levels of secretory proteins are produced by macrophages and smooth muscle resulting in ER overload and thus ER stress (32), (47).

Cancer cells are highly proliferating cells and as a result have a high protein turnover. Such a demand for protein synthesis puts a load on the ER resulting in ER stress (48). ER stress response is triggered in the cancer cells as an adaptive response to cope with the external stress and high protein demand. It is prosurvival initially and in some solid tumors, it has been found to aid tumor progression (36). It can therefore be considered a

target for therapeutic intervention. Therapies aimed at enhancing ER stress can switch prosurvival ER stress to proapoptotic ER stress (36), (28).

4.2.1.2.2 Calcium imbalance

The ER is involved in Ca signaling. Ca fluxes can evoke the UPR and contribute to the cell survival or cell death depending on the extent of ER stress. Ca release from the ER has been linked with the proapoptotic response. Increased Ca release has been observed with Bcl2-deficient cells or proapoptotic Bcl2 members rich cells (49), (50), (51). The mechanism of ER stress response generated by Ca imbalance is related to sarco/endoplasmic reticulum calcium ATPase (SERCA) inhibition. This transmembrane protein pumps Ca ion into the ER, maintaining the gradient. Due to SERCA inhibition, Ca homeostasis is affected and UPR response triggered (52). In addition to tumors, ER stress caused by Ca imbalance is significant in cardiac pathologies. Recent evidence has suggested over expression of SERCA in failing hearts since heart failure is linked to Ca imbalance (32).

4.2.1.2.3 Redox imbalance

Redox imbalance has been linked to ER stress. Generally, tumors support a hypoxic environment and thus redox imbalance is observed. Oxidative stress is linked with the ER stress that either precedes it or follows it. ER is the site of protein folding which is an energy intensive process requiring molecular oxygen (53). Also, ER is involved in disulfide bond formation requiring an oxidizing environment (48). Hyperglycemia is also associated with generation of reactive oxygen species that enhances ER stress (45).

4.2.1.2.4 Metabolic imbalance

In solid tumors, poor vascularization leads to metabolic disorders because of acidosis and glucose starvation resulting in ER stress by activating glucose stress response through induction of glucose regulated protein 78 or GRP78 which is part of the UPR and thus ER stress (54). Apoptosis induced under metabolic stress is regulated by the Bcl2 family of proteins (55). Bim and PUMA, the proapoptotic Bcl2 family proteins, are expressed under ER stress caused by metabolic stress (56). Induction is caused by glucose imbalance that affects protein glycosylation and thus protein misfolding (57).

4.2.2 Oxidative stress

Leukemic cells in general contain elevated levels of ROS (58). Elevated ROS levels are associated with oxidative damage leading to cell death due to genomic instability, lipid peroxidation and DNA damage (59). This could be enhanced by chemotherapeutics that increase ROS levels. Several FDA approved antileukemic chemotherapeutics utilize this strategy of generating/enhancing oxidative stress to cause cancer cell death (60). ROS or oxidative stress has been shown to play a part in cancer initiation and progression and in cancer cell death as well. Like ER stress, the extent of oxidative stress determines cell survival or cell death. It has been shown that a reducing environment promotes cell survival and an oxidizing environment promotes differentiation or cell killing (61). Therefore, oxidative stress has been considered as a strategy to induce cancer cell death at the stem cell level that might be effective on its own or combined with other stresses (3).

4.3 Materials and Methods

4.3.1 Materials

JS-K was synthesized as previously described (62). JS-K was synthesized at Richman Laboratories (Lower Gwynedd, PA) under conditions of Good Manufacturing Practice (cGMP). Tunicamycin was purchased from Sigma Aldrich (St. Louis, MO). Thapsigargin was purchased from Calbiochem (Billerica, MA). Pluronic® polymers were obtained from BASF (Florham Park, NJ). Radio immuno precipitation assay (RIPA) cell lysis and extraction buffer was purchased from Thermo Fisher Scientific (Rockford, IL). The following reagents and antibodies were purchased from the indicated suppliers: Anti-BiP/ GRP78 from BD Biosciences (San Jose, CA), Anti-CHOP from Cell Signaling Technology (Beverly, MA) or from Santa Cruz Biotechnology, Inc (Dallas, TX), Anti-pJNK and anti-JNK were from Santa Cruz as well. 5-(and-6)-chloromethyl-2', 7'-dichlorodihydrofluorescein diacetate (CM-H2DCFDA) was purchased from Invitrogen, Molecular Probes (Eugene, OR). All other antibodies or chemicals and reagents were from Sigma Aldrich (St Louis, MO) unless otherwise indicated.

4.3.2 Cell culture

Human myeloid leukemia HL-60 cells (ATCC, Manassas, VA) were cultured in RPMI-1640 supplemented with 10% fetal bovine serum (FBS), penicillin/streptomycin and mycozap. Cells were cultured at 37°C in a 5% CO_2 humidified atmosphere. Normal human CD34+ hematopoietic cells (HSC) were purchased from All Cells (Alameda, CA).

4.3.3 Preparation of JS-K loaded P123 micelles, free JS-K, Tunicamycin and Thapsigargin

11.25% of P123 micelle stock solution was prepared in HPLC grade water (Fisher Scientific, Waltham, MA). The solution was further diluted to 2.25% in phosphate buffered saline (PBS) (pH 6.5). 1mM P123/JS-K was prepared by heating 3.34 mL of 2.25% P123 at 50°C and adding 70µL of 50 mM JS-K. The weight loading of drug in P123 micelle is 1.7%. Further dilution was made in PBS (pH 6.5). For free JS-K, 5 mM JS-K stock was prepared in DMSO out of 50 mM JS-K stock in DMSO. Further dilutions were made in PBS. Tunicamycin (5mg/mL) and Thapsigargin (1mg/mL) stocks were not diluted. Final concentration was achieved in the cell culture.

4.3.4 Western blot

Cells were treated with free JS-K (5 µM) formulated in DMSO or micelle JS-K (5 µM) formulated in 2.25% P123 for 4-12 h as indicated. The cells were also treated with Tunicamycin (25µg/mL) or Thapsigargin (3 µM) (as a positive control for ER stress) and a P123 and no drug control was established at 0 hour. After treatment, the cells were collected and washed with PBS. Following centrifugation, RIPA lysis buffer (25mM Tris HCl (pH 7.6), 150 mM NaCl, 1% NP-40, 1% sodium deoxycholate, 0.1% SDS) supplemented with phenylmethylsulfonyl fluoride (PMSF) and protease and phosphatase inhibitors were added to the pellet. The lysates were sonicated (50% intensity for 15 seconds), centrifuged and the supernatant was collected and protein concentration measured using the Bradford reagent (ThermoScientific) or BCA protein assay reagent (Pierce Biotechnology). Loading buffer and reducing agent (DTT, Invitrogen) were added to the samples and electrophoresed in a 10% polyacrylamide gel (Biorad). Proteins

were transferred to polyvinylidene difluoride (PVDF) membranes at 110 V for 95 min. (Biorad). The blots were blocked for 1.5 h in 2.5% nonfat dry milk diluted in tris-buffered saline containing 0.2% tween (TBST) and washed with TBST (3X, 7 min. each). The membrane was then incubated with primary antibody (anti-CHOP or anti-GRP-78 or anti-actin) in 2.5% nonfat dry milk/TBST overnight. Membranes were washed (3X, 7 min. each) and incubated with horseradish peroxidase-conjugated secondary antibody in 2.5% nonfat dry milk in TBST for 2 h. The membrane was washed again in TBST thrice for 7 min. each and transferred proteins were detected with ECL substrate (GE Healthcare, Piscataway, NJ).

4.3.5 Intracellular reactive oxygen/reactive nitrogen species

Quantification of intracellular levels of reactive oxygen/nitrogen species (ROS/RNS) was performed using the ROS/RNS-sensitive fluorophore 5-(and-6)-chloromethyl-2', 7'-dichlorodihydrofluorescein diacetate or CM-H2DCFDA. Cells growing on 24 well plates ($1x10^6$ cells/well) were loaded with 5 μM CM-H2DCFDA in PBS at 37°C and 5% CO2 for 30 min. (63), (64). The PBS-containing probe was removed by washing the cells with PBS and the cells were re-incubated in RPMI media only and treated with 5 μM JS-K or 5μM P123/JS-K or 5μM P123 or H_2O_2 (positive control) or not treated for the indicated time periods. The treated or nontreated cells were then collected and fluorescence was measured at 488 nm excitation and 530 nm emission using a BD FACSCanto flow cytometer equipped with FACSDiva software. All experiments were performed at least three times.

4.4 Results

4.4.1 JS-K and P123/JS-K enhances ER stress response in HL-60 cells

We have previously shown that JS-K and P123/JS-K cause glutathionylation of nuclear proteins in HL60 cells (Chapter 3). Glutathionylation can result in deleterious post-translational modifications and cause accumulation of enough misfolded proteins to exceed the folding capacity of the ER. This response can result in activation of the UPR leading to ER stress (65). Several researchers have shown that due to high protein turnover in the tumor cells, the ER stress is already activated in cancer cells. A chemotherapeutic should be able to enhance the ER stress so as to shift the prosurvival signal to a proapoptotic response (66).

4.4.1.1 GRP78/Bip expression

Treatment of HL-60 cells with JS-K or P123/JS-K enhanced the expression of GRP-78 from a 0 hour no treatment control. The expression of GRP78/BiP peaked at 6 h for both JS-K and P123/JS-K and showed a declining trend towards 8 h (Fig. 4.2). Densitometry analysis revealed that the effect produced by P123/JS-K was slightly lower than JS-K (results not shown). This could be attributed to the effect produced due to the use of Pluronics®. GRP-78 expression was also tested on normal human hematopoietic CD34+ cells (Fig. 4.3). None of the groups (treated or untreated or control) showed GRP78 expression.

4.4.1.2 CHOP/GADD153 expression

Basal levels of CHOP/GADD153 protein were low when a no treatment control was established in the HL-60 cells (Fig. 4.2). Treatment with both JS-K and P123/JS-K or the

positive control Tunicamycin enhanced the expression of this proapototic protein indicating the shift from a prosurvival response to a proapoptotic response. We did not see any expression of CHOP in HSC cells by neither the treatment group nor the positive control group (Fig. 4.3).

4.4.1.3 Effects on the levels of intracellular ROS

The fluorescent dye CM-H2DCFDA rapidly oxidizes to the fluorescent product dichlorofluorescein (DCF) in the presence of reactive oxygen or reactive nitrogen species. The intensity of fluorescence can therefore be regarded as proportional to the amount of intracellular reactive species generated. HL-60 cells were treated with JS-K or P123/JS-K or hydrogen peroxide (H_2O_2) as a positive control. We also prepared a combination of P123/JS-K and H_2O_2 to see the effect of the drug if oxidizing conditions already prevail inside the cells. The study was carried out over a period of 2 h (Fig. 4.4). JS-K caused a sustained increase in the release of ROS/RNS similar to the positive control H_2O_2. ROS/RNS levels did not change with P123/JS-K treatment for 2 h but the levels were higher as compared to no treatment control. This could be attributed again to the Pluronic effect as the treatment with Pluronics actually reduced the levels of ROS/RNS. Interestingly, treating the cells with H_2O_2 prior to the treatment with P123/JS-K increased the overall level of ROS/RNS generation. The levels of ROS/RNS were higher than the H_2O_2 control or P123/JS-K treatment indicating a potentially additive effect or an effect produced by priming the cell with the oxidizing agent prior to the actual treatment. The fold change as compared to no treatment is shown in Fig. 4.4. One way ANOVA was ran on the data using Tukey post hoc analysis. The results were considered statistically significant for $P<0.05$.

4.5 Discussion

The aim of the present study was to investigate different stress responses produced by the prospective chemotherapeutic drug JS-K. We also investigated potential differences that might arise due to Pluronic micelle formulation of the drug. JS-K is a nitric oxide releasing drug. The different biological metabolites formed as a result of JS-K degradation (apart from NO) include 2,4-dinitrophenyl-S-glutathione (SG-DNP) and 1-carboethoxypiperazine (67). Subsequently, glutathione can dissociate from the dinitrophenyl ring separating glutathione from the aryl ring. Protein S-glutathionylation is a phenomenon of mixed disulphide formation between glutathione and cysteinyl residues (68). However, under basal conditions, the reaction rate is slow and lacks any physiological relevance (68). The process is reversible under reducing conditions whereas it is permanent under oxidizing/stressed condition (69).

We previously studied the cellular distribution of JS-K and P123/JS-K. As expected, P123/JS-K was more stable and localized to a greater extent than the free drug, which decomposed rapidly. The drug principally distributed to the nucleus. As the distribution study performed was a quantitative analysis based on actual drug quantification, it was concluded from the study that drug degrades in the cytosol if its not protected by a micelle shell. Secondly, it was also concluded that micelles aid in nuclear localization of the drug. The higher degradation of the drug in the cytosol could be attributed to the higher reducing environment in the cytosol (high GSH) as compared to the nucleus (70). This led to corollary that the drug degraded in the cytosol or in the nucleus generates NO or SG-DNP or also leads to protein glutathionylation. NO release can have several implications, including RNS in the form of radicals or nitrosylation of proteins (71). The

reduction of glutathione concentration also contributes to a more oxidizing environment leading to oxidative stress (10). With such conclusions and plausible ramifications, we next sought to investigate the process of protein glutathionylation in the cell. In the study carried out, JS-K glutathionylated nuclear proteins principally. Again, the extent of nuclear protein glutathionylation was higher in P123/JS-K treated HL-60 cells than the drug alone. Protein glutathionylation can produce certain unwanted posttranslational modifications leading to accumulation of glutathionylated proteins. Such a condition can result in ER stress (48). Also, the oxidative stress and changes in the redox environment of the cell can cause ER stress and contribute to the cell death cascade (72), (73).

The ER is a critical subcellular compartment involved in execution of apoptosis (72), (40), (66). It is involved in protein synthesis and protein folding as well as calcium storage. All the proteins translocated to ER are subjected to posttranslational modifications. Only correctly folded proteins are exported out of the ER. Unfolded or misfolded proteins are retained inside the ER and are subjected to either refolding or degradation (74). Accumulation of such unfolded or misfolded proteins inside the ER generates the UPR to increase the folding capacity of the ER. This situation is particularly relevant in the cancer cell as the cancer cells require high protein turnover, compromising the ER capacity (48). Consequently, basal level UPR response is always present in cancer cells (66). Such a response is prosurvival initially, but if stress is enhanced beyond the ER capacity, apoptosis ensues. GRP-78/BiP is an ER chaperone that is involved in the protein folding mechanism. This chaperone keeps the transcription factors PERK, ATF6 and Ire-1 in an inactivated state till the induction of UPR. During UPR, GRP-78 dissociates from these transcription factors (75). All the three transcription

factors then work in a concerted fashion to relieve the stress either by increasing the ER capacity (through reducing the overall protein load by degrading the misfolded proteins or by enhancing the folding capacity of the ER) or by activating the apoptosis cascade. Several studies have been carried out to integrate the programmed cell death with ER stress. All the conditions that cause perturbations of ER functions or that stress the functional capacity of the ER can lead to ER stress. These include, protein synthesis or folding at a rate higher than ER's capacity, calcium imbalance, oxidative stress or redox changes in the cell (73). Therefore, all the conditions can be integrated with the apoptotic cascade. The common apoptotic downstream target of the UPR branch is CHOP (C/EBP-homologous protein) also known as GADD153 (growth arrest and DNA damage-inducible protein-153). Prolonged CHOP expression has been linked to activation of apoptotic mechanisms involving activation of death receptors, outer mitochondrial membrane polarization, JNK phosphorylation and Bcl2 proteins interaction (73). We did not get any CHOP or GRP-78 induction by JS-K in normal CD34+ cells (HSC-containing cells). However, we did not see any expression of ER stress markers with Tunicamycin (the positive control) either. This implies that either the CD34+ cells are resistant to the induction of ER stress or it implies that both the drugs are selective in killing cancer cells, thus sparing normal stem cells.

With GRP-78 expression, it became clear that JS-K is enhancing ER stress in the cells. Prolonged CHOP expression suggested triggering of the apoptotic response. Further downstream, we investigated only the CHOP and oxidative stress pathway of ER stress-induced cell death. Although oxidative stress or redox imbalance causes ER stress, it has been suggested that with prolonged ER stress, the lumen of the ER gets hyperoxidized

with release of H_2O_2 in the cytoplasm, leading to cell death. In this pathway, ERO1α oxidase is involved which leads to either hyperoxidizing conditions in the cytosol or induction of NADPH oxidase subunit Nox2, resulting in generation of ROS and leading to oxidative stress (via CHOP-ERO1α-IP3R1-CaMKII pathway) (13). The common effector for both pathways is JNK activation which has been linked to oxidative stress and cell death (76). JS-K being a NO releaser and glutathione quencher is expected to cause redox imbalance leading to oxidative stress. Therefore, in our set of studies, we investigated the effect on ROS/RNS levels after JS-K or P123/JS-K treatment. As expected, a 2-4 fold increase in ROS/RNS level was observed as compared to controls after HL-60 cells were treated with JS-K or P123/JS-K. There was a sustained increase in ROS/RNS levels from 30 min. to 2 h after the cells were treated with JS-K. The levels of ROS/RNS levels did not increase drastically when cells were treated with P123/JS-K. This could be explained by results obtained from prior experiments. JS-K alone is sensitive to GSH present in the cells. Therefore, with time, drug degradation increased and therefore levels of ROS/RNS also increased. In contrast, P123/JS-K is stabilized in the micelle core and does not degrade as readily. Also, the drug translocates to the nucleus with time to a greater extent than free JS-K. The dye is intracellular and does not diffuse in the nucleus (77). Therefore, whatever degradation occurs inside the cytosol is reflected in the form of increased ROS/RNS as compared to the basal level. The reduced signal of P123 and P123/JS-K at 120 min. could be explained by considering the change in membrane permeability brought about by P123 (or Pluronic micelles) (78) causing dye leakage out of the cell and thus reduced response.

We also wanted to see the effect of cell priming with a known oxidizing agent. We primed the cells with H_2O_2 for 15 min. and treated the cells with P123/JS-K. The ROS/RNS levels were higher as compared to H_2O_2 or P123/JS-K alone. This means JS-K generates more ROS/RNS in the presence of an oxidizing agent.

Following the above results, we then sought to integrate the ER stress response to the oxidative stress. Some studies have shown that ER stress leads to ROS production. Studies have suggested links between oxidative and ER stress. Malhotra et al. proposed two mechanisms of ROS generation (or oxidative stress) during UPR evocation. First, ROS is produced as a byproduct of mitochondrial oxidative phosphorylation during the binding of misfolded proteins to ER chaperone such as GRP-78. Second, ROS is generated during electron transfer from thiols to molecular oxygen generating hydrogen peroxide during disulfide bond formation. The authors showed that antioxidants attenuated ER stress and oxidative stress that inhibited apoptosis (79). A common effector in both pathways may be JNK protein (73). Although molecular pathways linking ER stress with oxidative stress have not been elucidated in detail, some studies have suggested JNK protein phosphorylation could be linked with oxidative stress and ER stress induced cell death (80, 81). The whole proposed mechanism is presented in the Fig. 4.5. Cancer cells have high levels of ROS and are under oxidative stress, which is essential for tumor progression (9). We could not observe consistent phosphorylation of JNK with JS-K treatment of HL-60 cells. However, the release of ROS/RNS with JS-K treatment indicate involvement of oxidative stress in producing its effect. If oxidative stress is linked to ER stress, this could be confirmed by studying the expression of Ero1α

as this chaperone is involved in apoptosis induced by pJNK due to oxidative stress caused by ER stress (72), (73). All the pJNK results have been reported in the Appendix A.

4.6 Conclusions

In this study, we showed that the NO releasing prodrug JS-K induces a differential stress response in HL-60 cells and/or primary AML cells. The stress response produced is affected by the Pluronic micelle formulation of JS-K. JS-K and P123/JS-K activates the endoplasmic reticulum stress response. We showed increased expression of ER stress specific markers GRP-78 and CHOP protein by JS-K treatment in HL-60 cells. The major reasons for induction of ER stress could be attributed to accumulation of misfolded glutathionylated proteins and possibly due to redox imbalance of the tumor cell caused by the release of RNS/ROS by JS-K. We showed that intracellular ROS/RNS levels increased after JS-K treatment. The levels increased steadily for the free drug over a period of 2 h whereas they remained constant with P123/JS-K treatment. Free drug is likely more prone to attack by cellular thiols such as GSH and likely releases NO more quickly as compared to P123/JS-K. Reduction in the glutathione levels could create a more oxidizing environment and disturb the redox balance of the cell (82). We conclude that one of the mechanism of antileukemic activity of JS-K may involve induction of multiple stresses.

4.7 References

1. Maeda H, Bharate GY, Daruwalla J. Polymeric drugs for efficient tumor-targeted drug delivery based on EPR-effect. Eur J Pharm Biopharm. 2009;71(3):409-419.

2. Steven van Zutphen JR. Targeting platinum anti-tumour drugs: Overview of strategies employed to reduce systemic toxicity. Coord Chem Rev. 2005;249(24):2845-2853.

3. Jordan CT. The leukemic stem cell. Best Pract Res Clin Haematol. 2007;20(1):13-18.

4. Fodale V, Pierobon M, Liotta L, Petricoin E. Mechanism of cell adaptation: when and how do cancer cells develop chemoresistance? Cancer J. 2011;17(2):89-95.

5. Hanahan D, Weinberg RA. Hallmarks of cancer: the next generation. Cell. 2011;144(5):646-674.

6. Herr I, Debatin KM. Cellular stress response and apoptosis in cancer therapy. Blood. 2001;98(9):2603-2614.

7. Ouyang L, Shi Z, Zhao S, Wang FT, Zhou TT, Liu B, Bao JK. Programmed cell death pathways in cancer: a review of apoptosis, autophagy and programmed necrosis. Cell Prolif. 2012;45(6):487-498.

8. Long JS, Ryan KM. New frontiers in promoting tumour cell death: targeting apoptosis, necroptosis and autophagy. Oncogene. 2012;31(49):5045-5060.

9. Wilson WR, Hay MP. Targeting hypoxia in cancer therapy. Nat Rev Cancer. 2011;11(6):393-410.

10. Fulda S, Galluzzi L, Kroemer G. Targeting mitochondria for cancer therapy. Nat Rev Drug Discov. 2010;9(6):447-464.

11. Russo M, Mupo A, Spagnuolo C, Russo GL. Exploring death receptor pathways as selective targets in cancer therapy. Biochem Pharmacol. 2010;80(5):674-682.

12. Sounni NE, Noel A. Targeting the tumor microenvironment for cancer therapy. Clin Chem. 2013;59(1):85-93.

13. Li X, Zhang K, Li Z. Unfolded protein response in cancer: the physician's perspective. J Hematol Oncol. 2011;4:8.

14. Szegezdi E, Logue SE, Gorman AM, Samali A. Mediators of endoplasmic reticulum stress-induced apoptosis. EMBO Rep. 2006;7(9):880-885.

15. Gotoh T, Mori M. Nitric oxide and endoplasmic reticulum stress. Arterioscler Thromb Vasc Biol. 2006;26(7):1439-1446.

16. Gardner BM, Pincus D, Gotthardt K, Gallagher CM, Walter P. Endoplasmic reticulum stress sensing in the unfolded protein response. Cold Spring Harb Perspect Biol. 2013;5(3):a013169.

17. Shore GC, Papa FR, Oakes SA. Signaling cell death from the endoplasmic reticulum stress response. Curr Opin Cell Biol. 2011;23(2):143-149.

18. Kitamura M. The unfolded protein response triggered by environmental factors. Semin Immunopathol. 2013; 35(3):259-275.

19. Iwawaki T, Oikawa D. The role of the unfolded protein response in diabetes mellitus. Semin Immunopathol. 2013;35(3):333-350.

20. Al-Rawashdeh FY, Scriven P, Cameron IC, Vergani PV, Wyld L. Unfolded protein response activation contributes to chemoresistance in hepatocellular carcinoma. Eur J Gastroenterol Hepatol. 2010;22(9):1099-1105.

21. Anshu A, Thomas S, Agarwal P, Ibarra-Rivera TR, Pirrung MC, Schonthal AH. Novel proteasome-inhibitory syrbactin analogs inducing endoplasmic reticulum stress and apoptosis in hematological tumor cell lines. Biochem Pharmacol. 2011;82(6):600-609.

22. Boelens J, Lust S, Offner F, Bracke ME, Vanhoecke BW. Review. The endoplasmic reticulum: a target for new anticancer drugs. In Vivo. 2007;21(2):215-226.

23. Fribley A, Zeng Q, Wang CY. Proteasome inhibitor PS-341 induces apoptosis through induction of endoplasmic reticulum stress-reactive oxygen species in head and neck squamous cell carcinoma cells. Mol Cell Biol. 2004;24(22):9695-9704.

24. Hill DS, Martin S, Armstrong JL, Flockhart R, Tonison JJ, Simpson DG, Birch-Machin MA, Redfern CP, Lovat PE. Combining the endoplasmic reticulum stress-inducing agents bortezomib and fenretinide as a novel therapeutic strategy for metastatic melanoma. Clin Cancer Res. 2009;15(4):1192-1198.

25. Kahali S, Sarcar B, Fang B, Williams ES, Koomen JM, Tofilon PJ, Chinnaiyan P. Activation of the unfolded protein response contributes toward the antitumor activity of vorinostat. Neoplasia. 2010;12(1):80-86.

26. Lee E, Nichols P, Spicer D, Groshen S, Yu MC, Lee AS. GRP78 as a novel predictor of responsiveness to chemotherapy in breast cancer. Cancer Res. 2006;66(16):7849-7853.

27. Mandic A, Hansson J, Linder S, Shoshan MC. Cisplatin induces endoplasmic reticulum stress and nucleus-independent apoptotic signaling. J Biol Chem. 2003;278(11):9100-9106.

28. Martinon F. Targeting endoplasmic reticulum signaling pathways in cancer. Acta Oncol. 2012;51(7):822-830.

29. Wang G, Yang ZQ, Zhang K. Endoplasmic reticulum stress response in cancer: molecular mechanism and therapeutic potential. Am J Transl Res. 2010;2(1):65-74.

30. Hoozemans JJ, Scheper W. Endoplasmic reticulum: the unfolded protein response is tangled in neurodegeneration. The International J Biochem Cell Biol. 2012;44(8):1295-1298.

31. Bernales S, Soto MM, McCullagh E. Unfolded protein stress in the endoplasmic reticulum and mitochondria: a role in neurodegeneration. Front Aging Neurosci. 2012;4:5.

32. Minamino T, Kitakaze M. ER stress in cardiovascular disease. J Mol Cell Cardiol. 2010;48(6):1105-1110.

33. Chhunchha B, Fatma N, Kubo E, Rai P, Singh SP, Singh DP. Curcumin abates hypoxia-induced oxidative stress based-ER stress-mediated cell death in mouse hippocampal cells (HT22) by controlling Prdx6 and NF-kappaB regulation. Am J Physiol Cell Physiol. 2013;304(7):C636-655.

34. Orrenius S, Zhivotovsky B, Nicotera P. Regulation of cell death: the calcium-apoptosis link. Nature Reviews Mol Cell Biol. 2003;4(7):552-565.

35. Joubert PE, Werneke SW, de la Calle C, Guivel-Benhassine F, Giodini A, Peduto L, Levine B, Schwartz O, Lenschow DJ, Albert ML. Chikungunya virus-induced autophagy delays caspase-dependent cell death. J of Exp Med. 2012;209(5):1029-1047.

36. Kim I, Xu W, Reed JC. Cell death and endoplasmic reticulum stress: disease relevance and therapeutic opportunities. Nat Rev Drug Discov. 2008;7(12):1013-1030.

37. Ozcan L, Tabas I. Role of endoplasmic reticulum stress in metabolic disease and other disorders. Annu Rev Med. 2012;63:317-328.

38. Healy SJ, Gorman AM, Mousavi-Shafaei P, Gupta S, Samali A. Targeting the endoplasmic reticulum-stress response as an anticancer strategy. Eur J Pharmacol. 2009;625(1-3):234-246.

39. Merksamer PI, Papa FR. The UPR and cell fate at a glance. J Cell Sci. 2010;123(Pt 7):1003-1006.

40. Pae HO, Jeong SO, Jeong GS, Kim KM, Kim HS, Kim SA, Kim YC, Kang SD, Kim BN, Chung HT. Curcumin induces pro-apoptotic endoplasmic reticulum stress in human leukemia HL-60 cells. Biochem Biophys Res Commun. 2007;353(4):1040-1045.

41. Rao RV, Bredesen DE. Misfolded proteins, endoplasmic reticulum stress and neurodegeneration. Curr Opin Cell Biol. 2004;16(6):653-662.

42. Hoozemans JJ, van Haastert ES, Nijholt DA, Rozemuller AJ, Scheper W. Activation of the unfolded protein response is an early event in Alzheimer's and Parkinson's disease. Neurodegener Dis. 2012;10(1-4):212-215.

43. Hoozemans JJ, van Haastert ES, Eikelenboom P, de Vos RA, Rozemuller JM, Scheper W. Activation of the unfolded protein response in Parkinson's disease. Biochem Biophys Res Commun. 2007;354(3):707-711.

44. Haapasalo A, Viswanathan J, Bertram L, Soininen H, Tanzi RE, Hiltunen M. Emerging role of Alzheimer's disease-associated ubiquilin-1 in protein aggregation. Biochem Soc Trans. 2010;38(Pt 1):150-155.

45. Fonseca SG, Gromada J, Urano F. Endoplasmic reticulum stress and pancreatic beta-cell death. Trends Endocrinol Metab. 2011;22(7):266-274.

46. Papa FR. Endoplasmic reticulum stress, pancreatic beta-cell degeneration, and diabetes. Cold Spring Harb Perspect Med. 2012;2(9):a007666.

47. Minamino T, Komuro I, Kitakaze M. Endoplasmic reticulum stress as a therapeutic target in cardiovascular disease. Circ Res. 2010;107(9):1071-1082.

48. Townsend DM, Manevich Y, He L, Xiong Y, Bowers RR, Jr., Hutchens S, Tew KD. Nitrosative stress-induced s-glutathionylation of protein disulfide isomerase leads to activation of the unfolded protein response. Cancer Res. 2009;69(19):7626-7634.

49. Breckenridge DG, Germain M, Mathai JP, Nguyen M, Shore GC. Regulation of apoptosis by endoplasmic reticulum pathways. Oncogene. 2003;22(53):8608-8618.

50. Pinton P, Rizzuto R. Bcl-2 and Ca2+ homeostasis in the endoplasmic reticulum. Cell Death Differ. 2006;13(8):1409-1418.

51. Hetz CA. ER stress signaling and the BCL-2 family of proteins: from adaptation to irreversible cellular damage. Antioxid Redox Signal. 2007;9(12):2345-2355.

52. Schonthal AH. Endoplasmic reticulum stress and autophagy as targets for cancer therapy. Cancer Lett. 2009;275(2):163-169.

53. Chakravarthi S, Jessop CE, Bulleid NJ. The role of glutathione in disulphide bond formation and endoplasmic-reticulum-generated oxidative stress. EMBO Rep. 2006;7(3):271-275.

54. Reddy RK, Mao C, Baumeister P, Austin RC, Kaufman RJ, Lee AS. Endoplasmic reticulum chaperone protein GRP78 protects cells from apoptosis induced by topoisomerase inhibitors: role of ATP binding site in suppression of caspase-7 activation. J Biol Chem. 2003;278(23):20915-20924.

55. Altman BJ, Rathmell JC. Metabolic stress in autophagy and cell death pathways. Cold Spring Harb Perspect Biol. 2012;4(9):a008763.

56. Puthalakath H, O'Reilly LA, Gunn P, Lee L, Kelly PN, Huntington ND, Hughes PD, Michalak EM, McKimm-Breschkin J, Motoyama N, Gotoh T, Akira S, Bouillet P, Strasser A. ER stress triggers apoptosis by activating BH3-only protein Bim. Cell. 2007;129(7):1337-1349.

57. Kaufman RJ, Back SH, Song B, Han J, Hassler J. The unfolded protein response is required to maintain the integrity of the endoplasmic reticulum, prevent oxidative stress and preserve differentiation in beta-cells. Diabetes, Obes Metab. 2010;12 Suppl 2:99-107.

58. Irwin ME, Rivera-Del Valle N, Chandra J. Redox control of leukemia: from molecular mechanisms to therapeutic opportunities. Antioxid Redox Signal. 2013;18(11):1349-1383.

59. Trachootham D, Lu W, Ogasawara MA, Nilsa RD, Huang P. Redox regulation of cell survival. Antioxid Redox Signal. 2008;10(8):1343-1374.

60. Ahmed Abdal Dayem H-YC, Jung-Hyun Kim and Ssang-Goo Cho. Role of Oxidative Stress in Stem, Cancer, and Cancer Stem Cells. Cancers. 2010;2:859-884.

61. Konopleva MY, Jordan CT. Leukemia stem cells and microenvironment: biology and therapeutic targeting. J Clin Oncol. 2011;29(5):591-599.

62. Udupi V, Yu M, Malaviya S, Saavedra JE, Shami PJ. JS-K, a nitric oxide prodrug, induces cytochrome c release and caspase activation in HL-60 myeloid leukemia cells. Leuk Res. 2006;30(10):1279-1283.

63. Maciag AE, Chakrapani H, Saavedra JE, Morris NL, Holland RJ, Kosak KM, Shami PJ, Anderson LM, Keefer LK. The nitric oxide prodrug JS-K is effective against non-small-cell lung cancer cells in vitro and in vivo: involvement of reactive oxygen species. J Pharmacol Exp Ther. 2011;336(2):313-320.

64. Eruslanov E, Kusmartsev S. Identification of ROS using oxidized DCFDA and flow-cytometry. Methods Mol Biol. 2010;594:57-72.

65. Zhang K, Kaufman RJ. From endoplasmic-reticulum stress to the inflammatory response. Nature. 2008;454(7203):455-462.

66. Schonthal AH. Pharmacological targeting of endoplasmic reticulum stress signaling in cancer. Biochem Pharmacol. 2013;85(5):653-666.

67. Chakrapani H, Kalathur RC, Maciag AE, Citro ML, Ji X, Keefer LK, Saavedra JE. Synthesis, mechanistic studies, and anti-proliferative activity of glutathione/glutathione S-transferase-activated nitric oxide prodrugs. Bioorg Med Chem. 2008;16(22):9764-9771.

68. Dalle-Donne I, Rossi R, Giustarini D, Colombo R, Milzani A. S-glutathionylation in protein redox regulation. Free Radic Biol Med. 2007;43(6):883-898.

69. Beer SM, Taylor ER, Brown SE, Dahm CC, Costa NJ, Runswick MJ, Murphy MP. Glutaredoxin 2 catalyzes the reversible oxidation and glutathionylation of mitochondrial membrane thiol proteins: implications for mitochondrial redox regulation and antioxidant defense. J Biol Chem. 2004;279(46):47939-47951.

70. Franco R, Cidlowski JA. Apoptosis and glutathione: beyond an antioxidant. Cell Death Differ. 2009;16(10):1303-1314.

71. Leon L, Jeannin JF, Bettaieb A. Post-translational modifications induced by nitric oxide (NO): implication in cancer cells apoptosis. Nitric Oxide. 2008;19(2):77-83.

72. Rao RV, Ellerby HM, Bredesen DE. Coupling endoplasmic reticulum stress to the cell death program. Cell Death Differ. 2004;11(4):372-380.

73. Tabas I, Ron D. Integrating the mechanisms of apoptosis induced by endoplasmic reticulum stress. Nat Cell Biol. 2011;13(3):184-190.

74. Schroder M, Kaufman RJ. ER stress and the unfolded protein response. Mutat Res. 2005;569(1-2):29-63.

75. Hampton RY. ER stress response: getting the UPR hand on misfolded proteins. Curr Biol. 2000;10(14):R518-521.

76. Verma G, Datta M. The critical role of JNK in the ER-mitochondrial crosstalk during apoptotic cell death. J Cell Physiol. 2012;227(5):1791-1795.

77. Grisham MB. Methods to detect hydrogen peroxide in living cells: Possibilities and pitfalls. Comp Biochem Physiol A Mol Integr Physiol. 2013;165(4):429-438.

78. Rapoport NY, Herron JN, Pitt WG, Pitina L. Micellar delivery of doxorubicin and its paramagnetic analog, ruboxyl, to HL-60 cells: effect of micelle structure and ultrasound on the intracellular drug uptake. J Control Release 1999;58(2):153-162.

79. Malhotra JD, Miao H, Zhang K, Wolfson A, Pennathur S, Pipe SW, Kaufman RJ. Antioxidants reduce endoplasmic reticulum stress and improve protein secretion. Proc Natl Acad Sci U S A. 2008;105(47):18525-18530.

80. Panieri E, Gogvadze V, Norberg E, Venkatesh R, Orrenius S, Zhivotovsky B. Reactive oxygen species generated in different compartments induce cell death, survival, or senescence. Free Radic Biol Med. 2013;57:176-187.

81. Logue SE, Cleary P, Saveljeva S, Samali A. New directions in ER stress-induced cell death. Apoptosis. 2013;18(5):537-546.

82. DeBerardinis RJ. Good neighbours in the tumour stroma reduce oxidative stress. Nat Cell Biol. 2012;14(3):235-236.

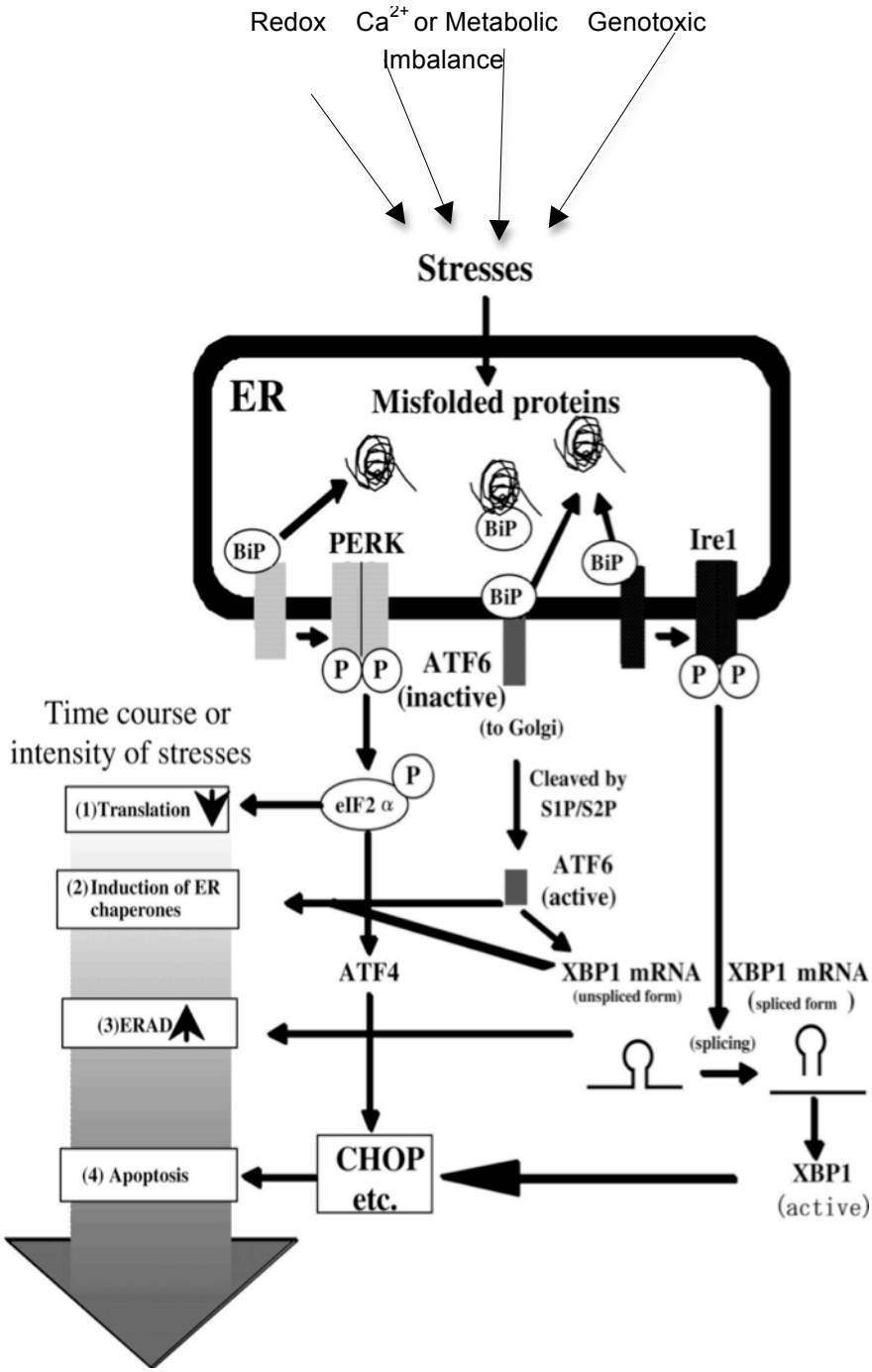

Fig. 4.1: Phases and conditions of ER stress. Adapted and modified from Gotoh T and Mori M. Arterioscler Thromb Vasc Biol 2006, 26, 1439-1446.

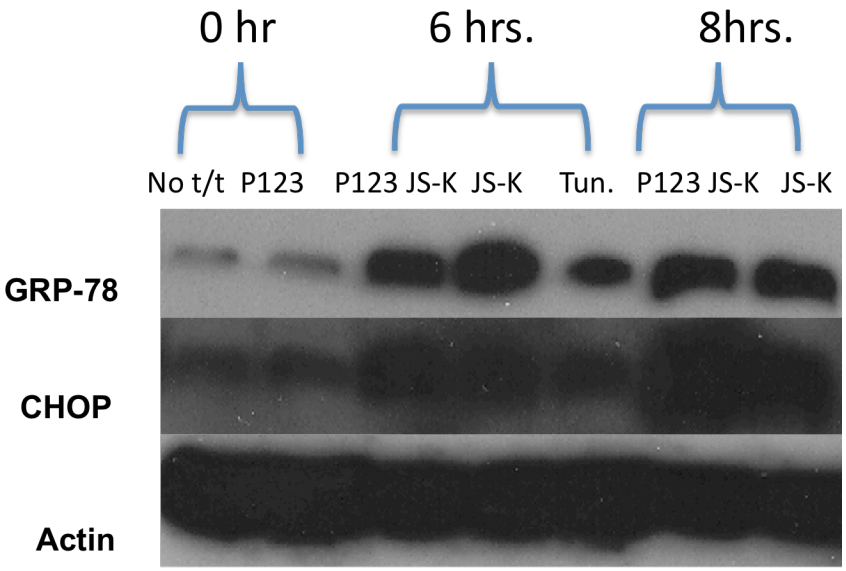

Fig. 4.2: Activation ER stress by JS-K. HL-60 cells were treated with the indicated drugs for the indicated period of time. Induction of GRP-78 or CHOP was compared to no treatment. No t/t: no treatment; Tun.: Tunicamycin

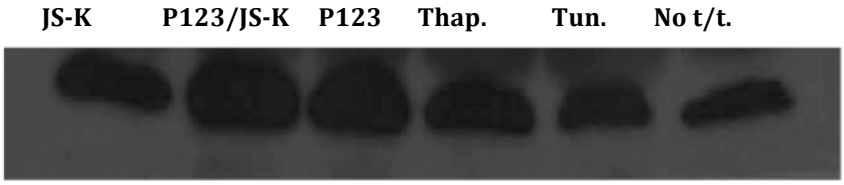

Fig. 4.3: Actin band seen on HSC cells. ER stress was not found to be activated in treated or nontreated cells. Therefore no bands observed. Thap: Thanpsigargin; Tun.: Tunicamycin; No t/t: No treatment

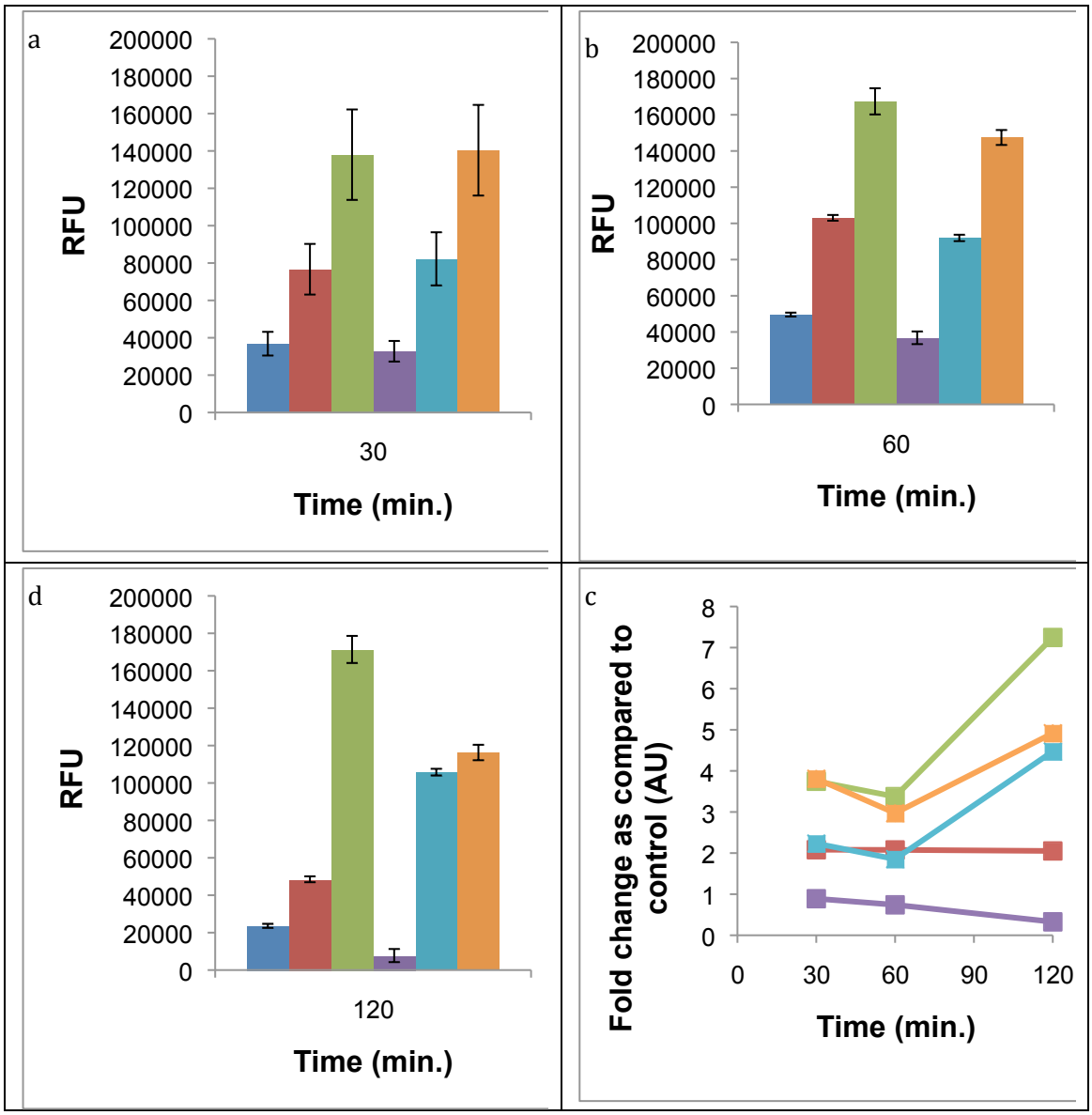

Fig. 4.4: Intracellular ROS levels after treatment with JS-K, P123/JS-K, P123, H2O2 or H2O2+P123/JS-K at 30, 60 and 120 min. Each point is a representative of the average and SEM of three independent experiments performed in triplicates. $P<0.05$ for all formulations except P123 control at 30 and 60 min. when compared to no treatment. Color code: ☐ No treatment; ☐ P123/JS-K; ☐ Free JS-K; ☐ P123 only; ☐ H2O2 only; ☐ H2O2+P123/JS-K

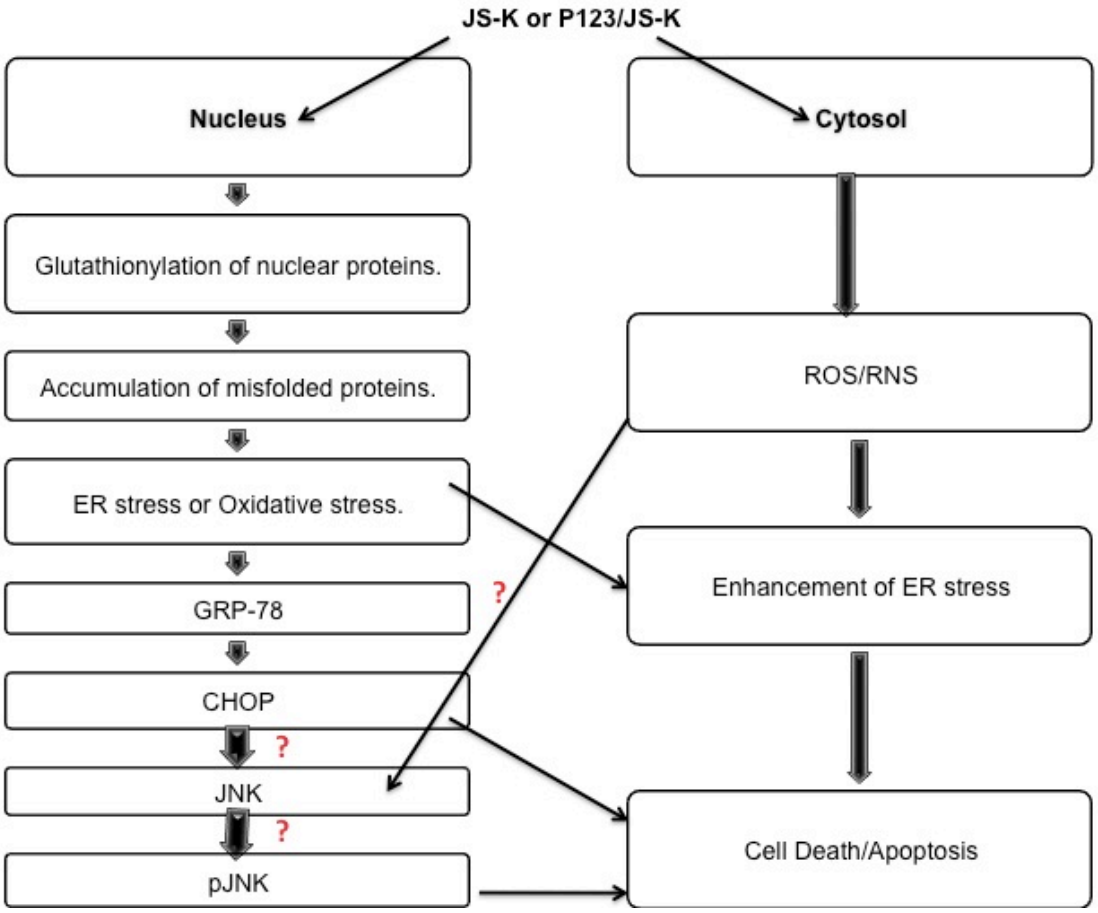

Figure 4.5: Proposed mechanism of stress response induced by JS-K

CHAPTER 5

DEVELOPMENT AND VALIDATION OF A METHOD TO MEASURE LEVELS OF THE NITRIC OXIDE-PRODUCING PRODRUG JS-K USING ULTRA PERFORMANCE LIQUID CHROMATOGRAPHY

5.1 Abstract

O^2-(2,4-dinitrophenyl) 1-[(4-ethoxycarbonyl)piperazin-1-yl]diazen-1-ium-1,2-diolate or JS-K is an anticancer lead compound of the arylated diazeniumdiolate class. JS-K is active against acute myeloid leukemia in *in vitro* and *in vivo* models. In this paper, we describe a sensitive and reproducible Ultra Performance Liquid Chromatography (UPLC) method JS-K measurement. We established linearity, accuracy, precision and specificity. We also developed a method to resolve, identify and quantify JS-K from its two major metabolites (2,4-dinitrophenol and S-(2,4-dinitrophenyl)-glutathione). We also compared two different extraction procedures and established the extraction efficiency of both. We compared a single step protein precipitation method/direct method with a two-step solid phase extraction procedure in blood and organic solvents. The recovery of JS-K demonstrated the extraction efficiency of both methods. The solid phase extraction procedure was more efficient as compared to the single step protein precipitation method. We also established the efficiency of solid phase extraction to determine if any drug loss

occurred during the extraction procedure. Insignificant loss of JS-K occurred with the final method developed. This method could be used for measurement of JS-K in clinical samples in the future. Also, this method lays the foundation for future studies in metabonomics and metabolomics.

5.2 Introduction

Acute myeloid leukemia (AML) is a clonal, hematological malignancy characterized by proliferation and accumulation of myeloid blast cells in the bone marrow. It is the most common type of adult acute leukemia with a median age at diagnosis of 67 years (1). Current treatment regimens for AML rely primarily on cytarabine and anthracyclines (2). There is a need for new agents that effectively target leukemia cells and leukemic stem cells (3).

Nitric oxide (NO) and NO donors have shown promise in producing cytotoxicity in cancer cells (4-7). O^2-(2,4-dinitrophenyl) 1-[(4-ethoxycarbonyl)piperazin-1-yl]diazen-1-ium-1,2-diolate or JS-K is a NO-donor that belongs to the arylated diazeniumdiolate class. This prodrug releases 2 molecules of NO upon nucleophilic attack by thiols. Mechanistically, JS-K releases NO upon attack by glutathione (GSH) (8), the most abundant cellular thiol (9). The reaction is catalyzed by glutathione-S-transferases (GST). This class of enzymes is overexpressed in several malignancies (10). Apart from the cytotoxic effects produced by NO release, JS-K's cytolethality has also been speculated to involve arylation of key cellular proteins resulting in posttranslational modification leading to cell death (11). JS-K induces cytochrome-*c* release from mitochondria and activates caspase 3, 9 and 8 (12). In addition to AML, *in vivo* murine models have shown that JS-K is effective against prostate cancer (8), hepatoma (13), multiple myeloma (14),

non-small cell lung cancer (15) and glioma (16). JS-K also possesses anti-angiogenic activity both *in vitro* and *in vivo* (17). JS-K is selective in its toxicity towards malignant cells. It did not affect the growth of normal human peripheral blood mononuclear cells (14) and normal mammary epithelial cells (18). Thus, JS-K is a promising clinical candidate for cancer therapy.

Advances in analytical instrumentation have led to the development of Ultra Performance Liquid Chromatography (UPLC). In contrast to High Performance Liquid Chromatography (HPLC), this chromatographic system ensures sensitive quantification with reduced analysis time. This is because the stationary phase of UPLC utilizes 2µm particles. Small particle size drastically improves resolution per unit time (19).

As JS-K is a clinical lead, it was important to develop a protocol for its qualitative and quantitative analysis. We have developed a UPLC method to measure JS-K and its two major metabolites 2,4 dinitrophenol (2,4-DNP) and S-(2,4-dinitrophenyl)-glutathione (GS-2,4-DNP) (Fig. 5.1). The method developed could be used for quantification of the drug or its metabolites and to track its biodistribution. It involves a two-step approach for JS-K quantification comprised of protein precipitation followed by solid phase extraction (SPE). Quantification was performed via UPLC. The method developed is sensitive to detect intact drug and its metabolites. It also offers high throughput adaptability enabling JS-K detection in patient samples once it enters clinical trials.

5.3 Methods

5.3.1 Chemicals and reagents

JS-K was obtained from 2 different sources. One stock of JS-K (NCI JS-K) was synthesized at the National Cancer Institute by Dr. Joseph Saavedra as previously

described (20). For the purposes of this study, we treated this stock as an "unknown purity" compound. The other stock (Richman JS-K) was obtained from a scale-up batch produced at Richman Laboratories (Lower Gwynedd, PA) under conditions of Good Manufacturing Practice (cGMP). This JS-K was certified as 100% pure and therefore was used as a "standard" for quality control (QC) for the purposes of this study. In some experiments, JS-K was solubilized in micelles using Pluronic® P123 (Lot # WPYG535B) obtained from BASF (Florham Park, NJ). Solvents used for UPLC analysis were of HPLC-grade (Fisher Scientific, Waltham, MA). All other chemicals were from Sigma (St. Louis, MO) unless otherwise stated.

5.3.2 Instrumentation and chromatographic conditions

Solid phase extraction (SPE) C18 columns, 1g/8mL from Grace Davison Discovery Sciences (Deerfield, IL) were used for SPE of samples. Samples were analyzed on a Waters Acquity UPLC, Binary Solvent Manager (BSM) (Waters, Millford, MA) using Acquity UPLC BEH C18 columns (2.1 x 50 mm, 1.7 μm particle size) connected to a Waters Acquity UPLC PDA detector powered by Empower 2 software. For sample elution, we used an isocratic mobile phase (A and B), consisting of 10% acetonitrile (ACN) in 0.02M ammonium formate (pH~3) (A) and 100% ACN (B). It was used at a ratio of 70% A and 30% B for 4 min. This was followed by gradient wash for an additional 2 min. Flow rate was kept constant at 0.6mL/min for 6 min. The mobile phase was filtered through a 0.45 μm Teflon coated membrane filter (Millipore, Bilerica, MA). During chromatographic separation JS-K, 2,4-DNP and GS-2,4-DNP were monitored by absorbance at 300 nm.

5.3.3 Drug and sample preparation

5.3.3.1 JS-K preparation

50 mM JS-K stocks were prepared in DMSO. Free JS-K was formulated by diluting stock to 1/10 in DMSO. Subsequent dilutions were made in phosphate buffered saline (PBS) (pH~6.5) or DMSO as indicated. For JS-K preparation in P123 micelles (P123/JS-K), 50 mM JS-K was diluted in 2.25% P123 to a final concentration of 1 mM P123/JS-K. Subsequent dilutions were made in PBS if required.

5.3.3.2 Sample preparation

To obtain 2,4-DNP and GS-2,4-DNP calibration curves, three 0.2 mM final preparations were made in DMSO in duplicate. For JS-K method validation, NCI JS-K or Richman JS-K solutions were prepared at 5 different concentrations (5, 50, 100, 150 and 200 μM). The JS-K peak was obtained at 300 nm; the 2,4-DNP peak was obtained at 280 nm; and the GS-2,4-DNP peak was obtained at 340 nm. For method validation, United States Pharmacopeia (USP) parameters were applied.

5.3.4 Solid phase extraction efficiency

We developed a solid phase extraction (SPE) procedure for the analysis of JS-K and its metabolites in *in vivo* samples. We established the efficiency of SPE by comparing recovery of JS-K from samples using SPE (two step extraction or TSE) to samples using a single step extraction (SSE) or protein precipitation (PP). The efficiency of SPE was established in JS-K samples prepared in relevant solvent or in mouse blood samples spiked with JS-K and then extracted using either a SSE via protein precipitation with

ACN/formate or a TSE via protein precipitation followed by SPE. For both techniques, JS-K standards were used. Both protocols are detailed as follows:

5.3.4.1 Non-blood sample analysis

3 mL of 10 μM or 100 μM JS-K or P123/JS-K were prepared from their respective stocks in 40% ACN/60% 0.02 M formate in water (pH~3). This preparation was divided into 2 halves. The first half was directly analyzed by UPLC. This was used as a baseline to calculate the loss of JS-K, if any, from SPE. The other half of the preparation was diluted with 0.02 M formate in water to reduce the final ACN percentage to 20% with a final volume of 3 mL. This dilution was used because in exploratory experiments we found that sample application with a high percentage of ACN (above 25%) led to loss of drug and its metabolites during washing steps. This 3 mL was then applied to SPE columns previously activated with methanol (MeOH) followed by 40% ACN/60% formate. The flowthrough was discarded. The columns were then washed with a weak solvent (2% ACN/98% 0.02M formate). The wash was discarded as well. Finally, columns were eluted with 100% MeOH twice. The eluates were collected and aliquoted for UPLC run. For the calculations, necessary adjustments were made based on the final amount of sample used in a particular experiment.

5.3.4.2 Blood sample analysis

Mouse blood was collected in polypropylene tubes containing 0.3 mL 4% citrate (pH~5) using a protocol approved by the University of Utah Institutional Animal Care and Use Committee. Samples were spiked with 1 mM P123/JS-K or 5 mM JS-K to obtain a final JS-K concentration of 0.5 mM. Area under the curve (AUC) was obtained

for these two preparations after extraction in 40% ACN/60% 0.02 M formate (total count). This total count was subsequently treated as actual JS-K added and the SPE treated and nontreated sample recovery was calculated relative to total count. The tubes were then placed for 2 min. at room temperature before centrifugation at 2500 rpm for 10 min. The supernatant (SN) was extracted and divided equally into two sets for SSE or TSE. For SSE, the sample set was spin filtered and the eluate was collected. The spin filtration was performed in order to avoid development of any backpressure of the UPLC BEH column leading to system overpressure. The spin-filtered samples were ran on the UPLC directly. For the TSE, the sample sets were diluted with 0.02 M formate to reduce ACN percentage to 20% and extracted with SPE as detailed above. Necessary dilutions/adjustments were made for calculation purposes.

5.3.5 JS-K method validation parameters

5.3.5.1 Accuracy and linearity

Accuracy is defined as "closeness of test results obtained by that procedure to the true value" (21). We analyzed the accuracy of the JS-K method by calculating the percentage recovery of JS-K samples of "unknown purity" (NCI JS-K) from JS-K standards of "known purity" (Richman JS-K). We evaluated percent recovery across a range of five different concentrations, namely 5, 50, 100, 150 and 200μM. We also conducted the analysis at two different injection volumes, namely 1 and 5 μL. In addition, we also analyzed accuracy by showing curve linearity and near superimposability of measurements obtained with NCI JS-K samples over Richman JS-K standards. The curve was obtained by plotting the peak AUC against the theoretical amount injected.

5.3.5.2 Precision

Precision of JS-K curve was analyzed in terms of repeatability and ruggedness (intermediate precision). We analyzed repeatability by running 5 different JS-K concentrations, each concentration in triplicate. Each set was injected twice at 2 different injection volumes. The standards and the samples were prepared in DMSO. Standard deviation (SD), relative standard deviation (RSD) and percentage of relative standard deviation (or coefficient of variation) was analyzed for each set of concentrations. Intermediate precision was analyzed by analyzing standards and samples on two different days with two sets of standards and samples prepared each day. The analyst, instrument and method were the same on both days. Samples and standards were prepared as detailed above. For statistical analysis, SD and RSD between two sets were calculated.

5.3.5.3 Specificity

Specificity of the JS-K peak was analyzed by injecting standards prepared in DMSO or standards prepared in P123 Pluronic® (P123/JS-K). Similar concentrations were prepared for each set (5, 50, 100, 150 and 200 μM) in DMSO in triplicate and evaluated at injection volumes of 1 and 5 μL in replicates. The AUC obtained at two different injection volumes was plotted against the amount injected and the linearity of the curve was established to show specificity of the method.

5.4 Results and Discussion

5.4.1 Recovery of JS-K and its metabolites

Fig. 5.1 shows the structure of JS-K and its metabolites. We have developed a sensitive UPLC method to detect JS-K and its major metabolites in a single run. The

method is highly efficient and short enough to run multiple samples in 1 day. Fig. 5.2 shows the recovery and resolution of JS-K and its metabolites peaks from a single run.

5.4.2 Solid phase extraction (SPE)

In order to develop the best and most sensitive method for analysis of JS-K and its metabolites, we compared two different extraction procedures. The single-step extraction (SSE) or protein precipitation (PP) method was compared to the two-step extraction (TSE) that involves PP followed by SPE. The SPE method was developed in order to analyze biological samples with high accuracy because drug detection can be limited by proteins or other blood components such as phospholipids (22). Consequently, the SPE method aims at getting rid of interfering blood components in order to enhance recovery of metabolites and the main analyte efficiently.

We first determined the amount of JS-K or P123/JS-K lost during SPE. From the same pool, we analyzed one sample using direct extraction and the other one using SPE. Table 5.1 shows the percentage of JS-K lost with the use of SPE. As shown, negligible amounts of drug were lost with either formulation, suggesting the method works efficiently.

Next, we analyzed a biological sample spiked with JS-K. The sample was extracted as summarized in the methods section using either SSE or TSE. Drug recovery was calculated based on the total amount of drug added and the amount measured. Results are shown in Table 5.2. One can conclude from these data that JS-K or P123/JS-K recovery from biological samples is significantly higher if the samples are processed with SPE.

5.4.3 Calibration curves

We then prepared calibration curves for 2,4-DNP and GS-2,4-DNP (Figs. 5.3 and 5.4) as explained in the methods section. Both curves were linear with the following equations (5.1 and 5.2) for 2,4-DNP and GS-2,4-DNP, respectively:

$$580958x - 44245 \text{ with } R^2 = 0.996 \qquad (5.1)$$

$$895306x - 25328 \text{ with } R^2 = 0.999 \qquad (5.2)$$

Both curves have a correlation coefficient close to 1, showing the sensitivity of the method. The linearity obtained for metabolites is important for this study because during the clinical development of JS-K, metabolite detection will prove useful.

5.4.4 JS-K method validation

5.4.4.1 Accuracy and linearity

The accuracy of JS-K measurements (calculated as percent recovery) was analyzed as explained in the methods section. As seen in Table 5.3, the percentage recovery is close to 100% for most of the samples. To further validate accuracy, we also compared the linearity of the JS-K standards from Richman (Richman JS-K) with JS-K samples from the NCI (NCI JS-K). The linearity of the two curves was established in terms of the slope of the lines. As seen in Figs. 5.5 and 5.6, the slopes of the obtained curves are:

Fig. 5.5: injection volume of 1µL

$$\textbf{Richman JS-K: } y = 3E+06x + 3096.8;\ R^2 = 0.999 \qquad (5.3)$$

$$\textbf{NCI JS-K: } 3E+06x + 4091.7;\ R^2 = 0.999 \qquad (5.4)$$

Fig. 5.6: injection volume of 5µL

Richman JS-K: $y = 3E+06x +21060$; $R^2 = 0.998$ (5.5)

NCI JS-K: $3E+06x +19031$; $R^2 = 0.999$ (5.6)

As is evident from both the figures and equations, the standard deviations are small and the correlation coefficients are close to one. Both standards and samples share similar slopes.

The curves generated led to JS-K detection over a linear range of 0.001921 µg - 0.07684 µg for 1µL injections and over a range of 0.01 µg - 0.384 µg for 5µL injections. Based on the linearity curve, the lower limit of detection (LLOD) and lower and lower limit of quantitation (LLOQ) is therefore below 1.921ng or 5 picomoles.

5.4.4.2 Precision

Precision was calculated both in terms of intraday repeatability and interday reproducibility of the peaks. Table 5.4 shows intraday repeatability results calculated for Richman and NCI samples. As seen in the table, RSD values are small at high concentrations and deviations are evident at lower JS-K concentrations in both sets. This is typical for most assays as the variability in measurement of peak height or AUC is greater at such low concentrations. The interday precision or ruggedness results are shown in Table 5.5. Again, high RSD values are seen at lower concentrations. It is interesting to note that injection volume did not make much difference in the standard deviations or RSD obtained, reflecting the fact that standard deviation is a result of sample preparation and not that of the imprecision by the instrument.

5.4.4.3 Specificity

Specificity of the method was established by comparing free JS-K standards with JS-K in P123 micelles as explained in the material and method section. At injection volumes of 1 or 5 µL, both standards were superimposable with JS-K in P123 indicating that addition of diluant/excipient did not cause changes in analyte detection. The curves are shown in Figs. 5.7 and 5.8.

5.5 Discussion

In this study, a method was developed and validated for the measurement of JS-K and its major metabolites (2,4-DNP and GS-2,4 DNP). The method was validated using a sensitive and rapid analysis provided by UPLC equipped with a UV detector. We compared two different extraction procedures that can be useful in the analysis of other agents than JS-K. Multiple studies have reported drug detection from biologics using HPLC or other analytical techniques with or without mass spectrometry analysis. For such studies, generally sample preparation is done using protein precipitation (23), (24), (25). The method is easy but lacks sensitivity and is time consuming. This method also requires larger sample volumes. Moreover, not all the proteins are precipitated by this method, which could lead to HPLC column clogging resulting in higher maintenance cost. Due to less sensitive resolution, longer sample runs are required on HPLC resulting in utilization of extensive mobile phase leading to higher costs and requiring more time. Advances in liquid chromatography with the introduction of UPLC have improved the performance for analysis substantially. High flow rate is obtained due to high operating pressure that cannot be achieved with HPLC (19).

Method validation was performed using lab-prepared JS-K (NCI) and standards from JS-K produced under cGMP conditions. We obtained good peak resolution and separation between JS-K and its metabolites. Unlike other bioanalytical assays, we did not establish the LOQ or LOD via signal/noise ratio as the noise detected was far below quantitation. We therefore established the range of LOQ based on the linearity curve. The accuracy and precision values calculated were in good agreement. The standard deviation or RSD calculated was slightly higher than expected in some concentrations. However, differences observed were between triplicates of the same sample/standard and not within the replicates. This indicates that the method developed is sensitive in peak detection and AUC calculation and the variability or deviations observed were due to user-based sample preparation differences. This also indicates that the same user preparation showed differences.

5.6 Conclusions

JS-K is an anticancer agent in preclinical development. We have developed a sensitive method to measure JS-K and its metabolites. The method has several potential applications. The method developed can therefore be used to perform bio-distribution, pharmacokinetic and toxicokinetic studies in animal models, which can guide dosing in humans. Also, this method can be combined with even more sensitive analytical techniques such as mass spectrometry (MS) and be applied for pharmacokinetic and elimination studies in patient samples. In the future, the method could be used for metabonomic studies. Metabonomic analysis is a comparatively new field and has wide applications such as toxicity analysis (26, 27), metabotyping, disease models (28, 29) and

"functional genomics" (30). Our method can serve as the basis for future pharmacokinetic studies of JS-K as an anticancer agent.

5.7 Acknowledgements

This work was supported by grant RO1 CA129611 from the National Cancer Institute.

5.8 Disclosures

Paul Shami is Scientific Founder, Chief Medical Officer and Chairman of the Board of Directors of JSK Therapeutics Inc.

5.10 References

1. O'Donnell MR, Abboud CN, Altman J, Appelbaum FR, Arber DA, Attar E, Borate U, Coutre SE, Damon LE, Goorha S, Lancet J, Maness LJ, Marcucci G, Millenson MM, Moore JO, Ravandi F, Shami PJ, Smith BD, Stone RM, Strickland SA, Tallman MS, Wang ES, Naganuma M, Gregory KM. Acute myeloid leukemia. J Natl Compr Canc Netw. 2012;10(8):984-1021.

2. Robak T, Wierzbowska A. Current and emerging therapies for acute myeloid leukemia. Clin Ther. 2009;31 Pt 2:2349-2370.

3. Jordan CT. The leukemic stem cell. Best Pract Res Clin Haematol. 2007;20(1):13-18.

4. Konovalova NP, Goncharova SA, Volkova LM, Rajewskaya TA, Eremenko LT, Korolev AM. Nitric oxide donor increases the efficiency of cytostatic therapy and retards the development of drug resistance. Nitric Oxide. 2003;8(1):59-64.

5. de Luca A, Moroni N, Serafino A, Primavera A, Pastore A, Pedersen JZ, Petruzzelli R, Farrace MG, Pierimarchi P, Moroni G, Federici G, Sinibaldi Vallebona P, Lo Bello M. Treatment of doxorubicin-resistant MCF7/Dx cells with nitric oxide causes histone glutathionylation and reversal of drug resistance. Biochem J. 2011;440(2):175-183.

6. Huerta S, Chilka S, Bonavida B. Nitric oxide donors: novel cancer therapeutics (review). Int J Oncol. 2008;33(5):909-927.

7. Sullivan R, Graham CH. Chemosensitization of cancer by nitric oxide. Curr Pharm Des. 2008;14(11):1113-1123.

8. Shami PJ, Saavedra JE, Wang LY, Bonifant CL, Diwan BA, Singh SV, Gu Y, Fox SD, Buzard GS, Citro ML, Waterhouse DJ, Davies KM, Ji X, Keefer LK. JS-K, a glutathione/glutathione S-transferase-activated nitric oxide donor of the diazeniumdiolate class with potent antineoplastic activity. Mol Cancer Ther. 2003;2(4):409-417.

9. Chu G. Cellular responses to cisplatin. The roles of DNA-binding proteins and DNA repair. J Biol Chem. 1994;269(2):787-790.

10. Sau A, Pellizzari Tregno F, Valentino F, Federici G, Caccuri AM. Glutathione transferases and development of new principles to overcome drug resistance. Arch Biochem Biophys. 2010;500(2):116-122.

11. Shami PJ, Saavedra JE, Bonifant CL, Chu J, Udupi V, Malaviya S, Carr BI, Kar S, Wang M, Jia L, Ji X, Keefer LK. Antitumor activity of JS-K [O2-(2,4-dinitrophenyl) 1-[(4-ethoxycarbonyl)piperazin-1-yl]diazen-1-ium-1,2-diolate] and related O2-aryl diazeniumdiolates in vitro and in vivo. J Med Chem. 2006;49(14):4356-4366.

12. Udupi V, Yu M, Malaviya S, Saavedra JE, Shami PJ. JS-K, a nitric oxide prodrug, induces cytochrome c release and caspase activation in HL-60 myeloid leukemia cells. Leuk Res. 2006;30(10):1279-1283.

13. Ren Z, Kar S, Wang Z, Wang M, Saavedra JE, Carr BI. JS-K, a novel non-ionic diazeniumdiolate derivative, inhibits Hep 3B hepatoma cell growth and induces c-Jun phosphorylation via multiple MAP kinase pathways. J Cell Physiol. 2003;197(3):426-434.

14. Kiziltepe T, Hideshima T, Ishitsuka K, Ocio EM, Raje N, Catley L, Li CQ, Trudel LJ, Yasui H, Vallet S, Kutok JL, Chauhan D, Mitsiades CS, Saavedra JE, Wogan GN, Keefer LK, Shami PJ, Anderson KC. JS-K, a GST-activated nitric oxide generator, induces DNA double-strand breaks, activates DNA damage response pathways, and induces apoptosis in vitro and in vivo in human multiple myeloma cells. Blood. 2007;110(2):709-718.

15. Maciag AE, Chakrapani H, Saavedra JE, Morris NL, Holland RJ, Kosak KM, Shami PJ, Anderson LM, Keefer LK. The nitric oxide prodrug JS-K is effective against non-small-cell lung cancer cells in vitro and in vivo: involvement of reactive oxygen species. J Pharmacol Exp Ther. 2011;336(2):313-320.

16. Weyerbrock A, Osterberg N, Psarras N, Baumer B, Kogias E, Werres A, Bette S, Saavedra JE, Keefer LK, Papazoglou A. JS-K, a glutathione S-transferase-activated nitric oxide donor with antineoplastic activity in malignant gliomas. Neurosurgery. 2012;70(2):497-510.

17. Kiziltepe T, Anderson KC, Kutok JL, Jia L, Boucher KM, Saavedra JE, Keefer LK, Shami PJ. JS-K has potent anti-angiogenic activity in vitro and inhibits tumour angiogenesis in a multiple myeloma model in vivo. J Pharm Pharmacol. 2010;62(1):145-151.

18. McMurtry V, Saavedra JE, Nieves-Alicea R, Simeone AM, Keefer LK, Tari AM. JS-K, a nitric oxide-releasing prodrug, induces breast cancer cell death while sparing normal mammary epithelial cells. Int J Oncol. 2011;38(4):963-971.

19. Wang J, Li H, Jin C, Qu Y, Xiao X. Development and validation of a UPLC method for quality control of rhubarb-based medicine: fast simultaneous

determination of five anthraquinone derivatives. J Pharm Biomed Anal. 2008;47(4-5):765-770.

20. Saavedra JE, Srinivasan A, Bonifant CL, Chu J, Shanklin AP, Flippen-Anderson JL, Rice WG, Turpin JA, Davies KM, Keefer LK. The secondary amine/nitric oxide complex ion R(2)N[N(O)NO](-) as nucleophile and leaving group in S9N)Ar reactions. J Org Chem. 2001;66(9):3090-3098.

21. Validation of Compendial Procedures. In. First Supplement United States Pharmacopeia. Rockville, MD; 2009. p. 3988 <1225> 3990.

22. Tulipani S, Llorach R, Urpi-Sarda M, Andres-Lacueva C. Comparative analysis of sample preparation methods to handle the complexity of the blood fluid metabolome: when less is more. Anal Chem. 2013;85(1):341-348.

23. Pokrajac M, Miljkovic B, Simic D, Brzakovic B, Galetin A. Comparative pharmacokinetics and bioavailability of two cotrimoxazole preparations. Die Pharmazie. 1998;53(7):470-472.

24. Sala F, Marangon E, Bagnati R, Livi V, Cereda R, D'Incalci M, Zucchetti M. Development and validation of a high-performance liquid chromatography-tandem mass spectrometry method for the determination of the novel proteasome inhibitor CEP-18770 in human plasma and its application in a clinical pharmacokinetic study. J Mass Spectrom. 2010;45(11):1299-1305.

25. Zhao M, Hartke C, Jimeno A, Li J, He P, Zabelina Y, Hidalgo M, Baker SD. Specific method for determination of gefitinib in human plasma, mouse plasma and tissues using high performance liquid chromatography coupled to tandem mass spectrometry. J Chromatogr B Analyt Technol Biomed Life Sci. 2005;819(1):73-80.

26. Lu X, Tian Y, Zhao Q, Jin T, Xiao S, Fan X. Integrated metabonomics analysis of the size-response relationship of silica nanoparticles-induced toxicity in mice. Nanotechnology. 2011;22(5):055101.

27. Lv H, Liu L, Zhang Y, Song T, Lu J, Chen X. Ingenuity pathways analysis of urine metabonomics phenotypes toxicity of gentamicin in multiple organs. Mol Biosyst. 2010;6(10):2056-2067.

28. Nicholson JK, Holmes E, Kinross JM, Darzi AW, Takats Z, Lindon JC. Metabolic phenotyping in clinical and surgical environments. Nature. 2012;491(7424):384-392.

29. Gika H, Theodoridis G. Sample preparation prior to the LC-MS-based metabolomics/metabonomics of blood-derived samples. Bioanalysis. 2011;3(14):1647-1661.

30. Jiang W, Qiu Y, Ni Y, Su M, Jia W, Du X. An automated data analysis pipeline for GC-TOF-MS metabonomics studies. J Proteome Res. 2010;9(11):5974-5981.

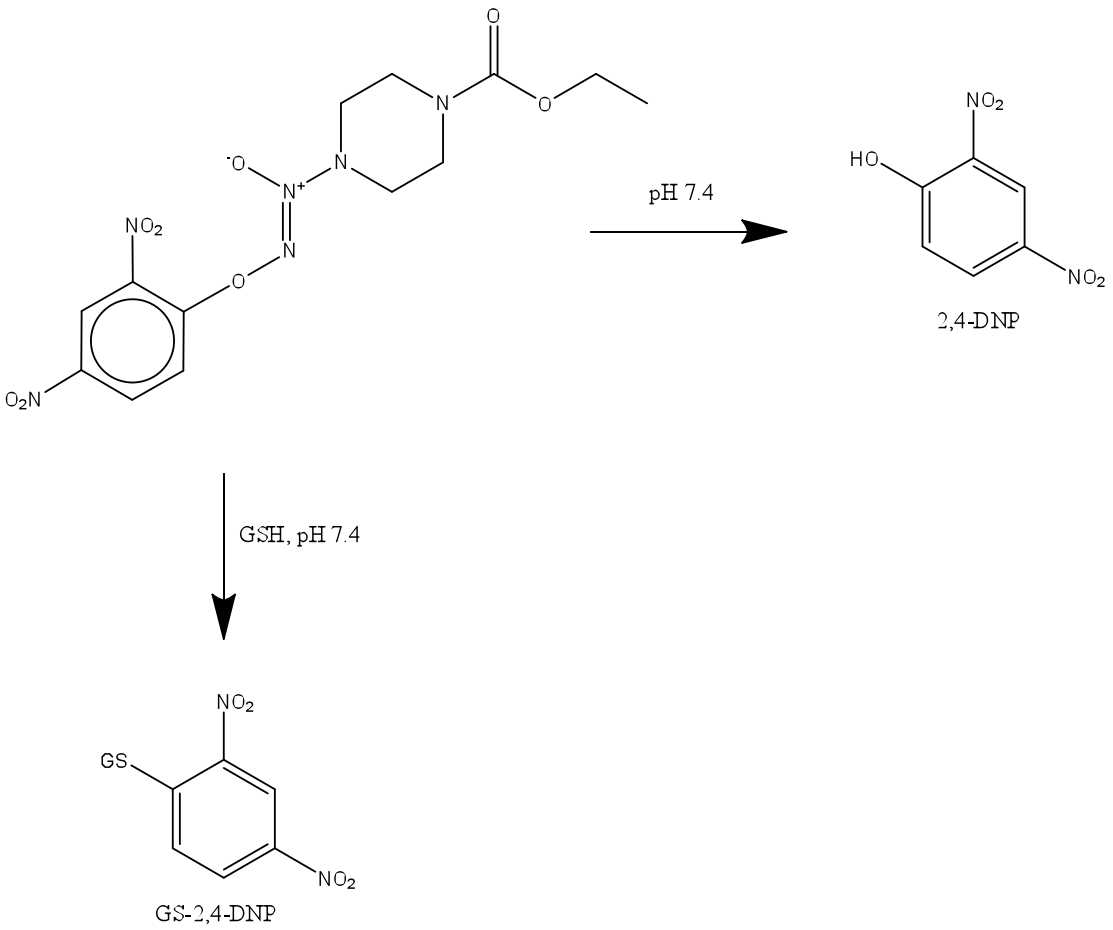

Fig. 5.1: Structure and metabolism of JS-K

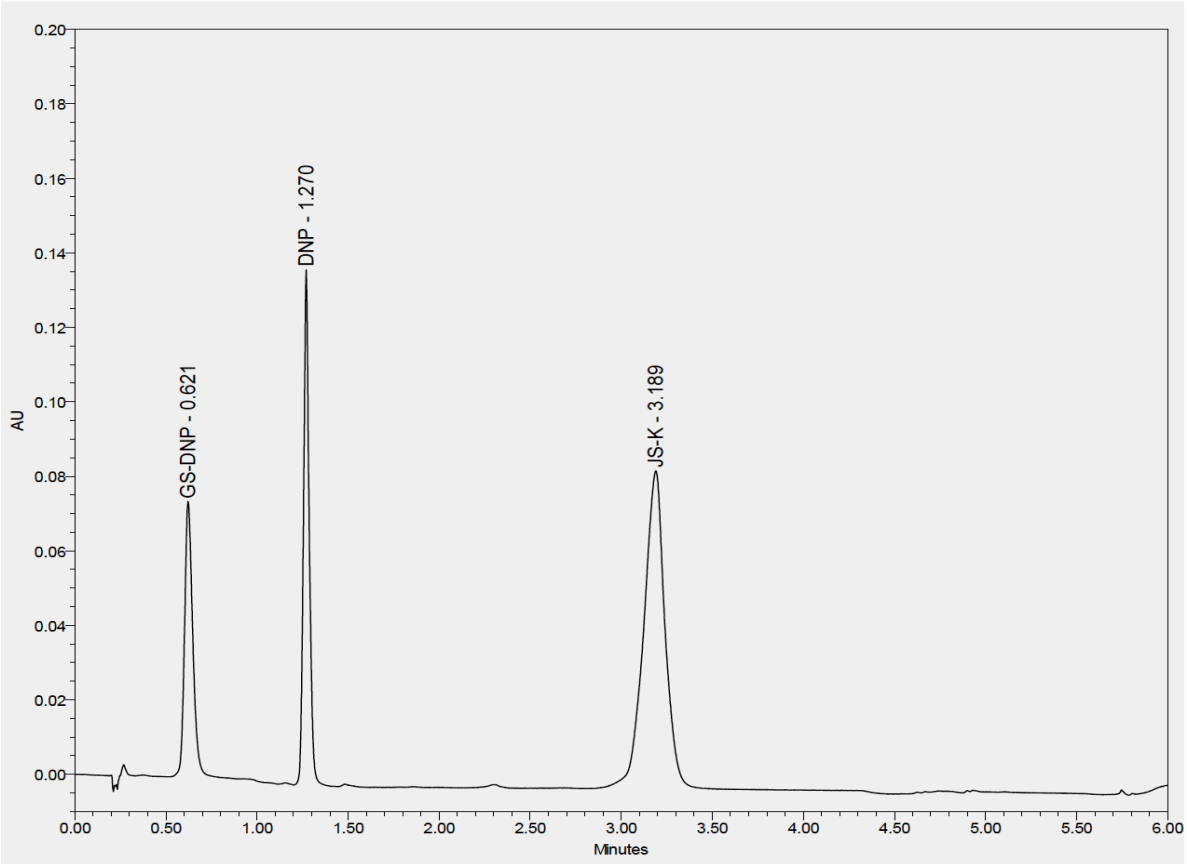

Fig. 5.2: Chromatogram of JS-K and its metabolites. JS-K; 2,4-DNP and GS-2,4-DNP (0.1 mM) were ran together as a single sample. The chromatogram shows clear and distinct peaks in a single 6-min. run.

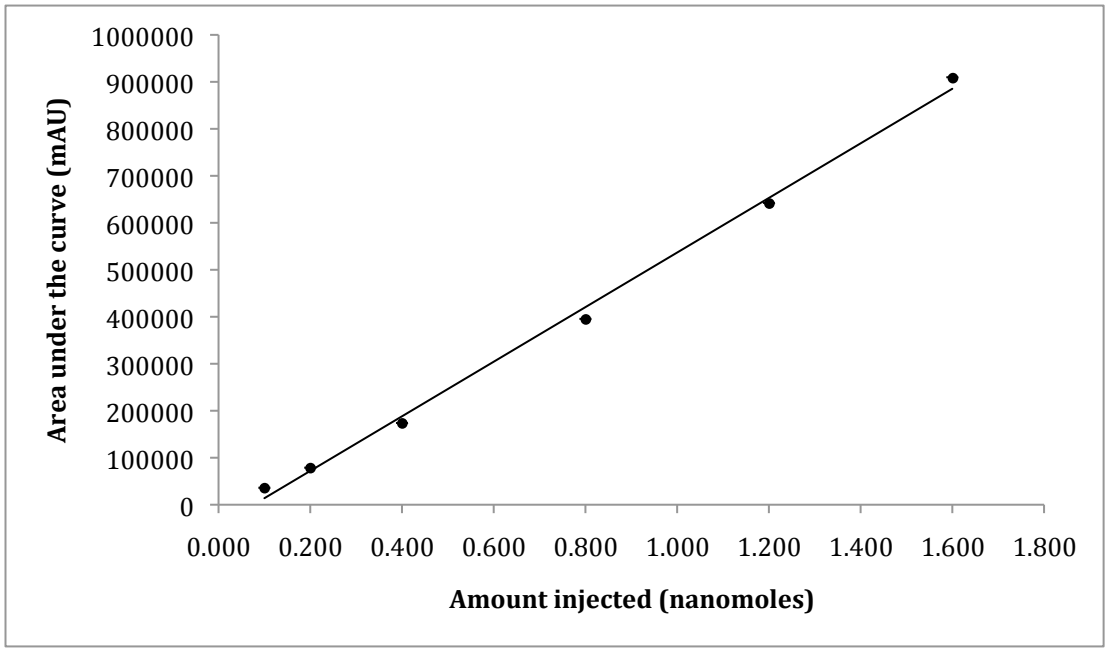

Fig. 5.3: 2,4-DNP standard curve using UV absorbance at 300 nm. Three 0.2 mM 2,4-DNP samples were prepared in duplicate and run at 6 different injection volumes (0.5, 1, 2, 4, 6 and 8 μL). A linear curve was obtained. Each point is an average and SEM of 6 unique readings. As seen, error bars are small with a tight fit. The slope of the line and the R^2 value obtained are y = 580958x – 44245, R^2 = 0.99657.

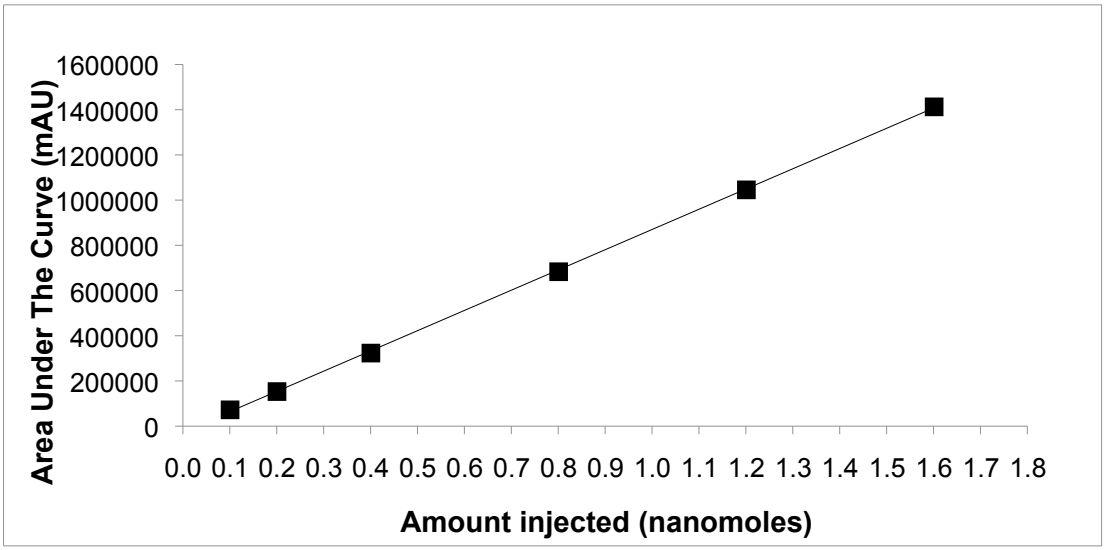

Fig. 5.4: GS-2,4-DNP standard curve using UV absorbance at 300 nm. Three 0.2 mM GS-2,4-DNP samples were prepared in duplicate and ran at 6 different injection volumes (0.5, 1, 2, 4, 6 and 8 µL). A linear curve was obtained. Each point is an average and SEM of 6 unique readings. As seen, error bars are small with a tight fit. The slope of the line and the R^2 value obtained are y = 895306x – 25328, $R^2 = 0.99983$.

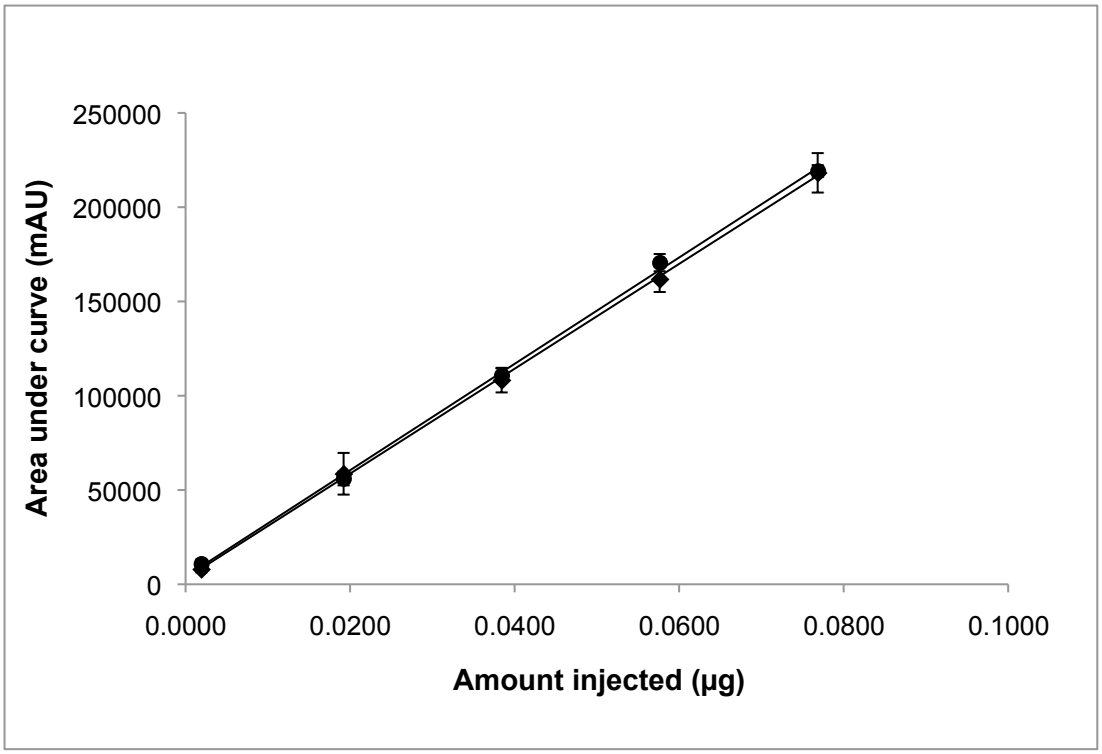

Fig. 5.5: Linearity of Richman JS-K compared to NCI JS-K samples at 5, 50, 100, 150 and 200 µM at 1 µL injection volume. Each concentration was made in triplicate and run in duplicate using UPLC. The injection volume was 1 µL. Each point on the curve is the average of peak area (n=6) with their standard deviations. For curve information, see text. Legend: ♦ = Richman JS-K; • = NCI JS-K.

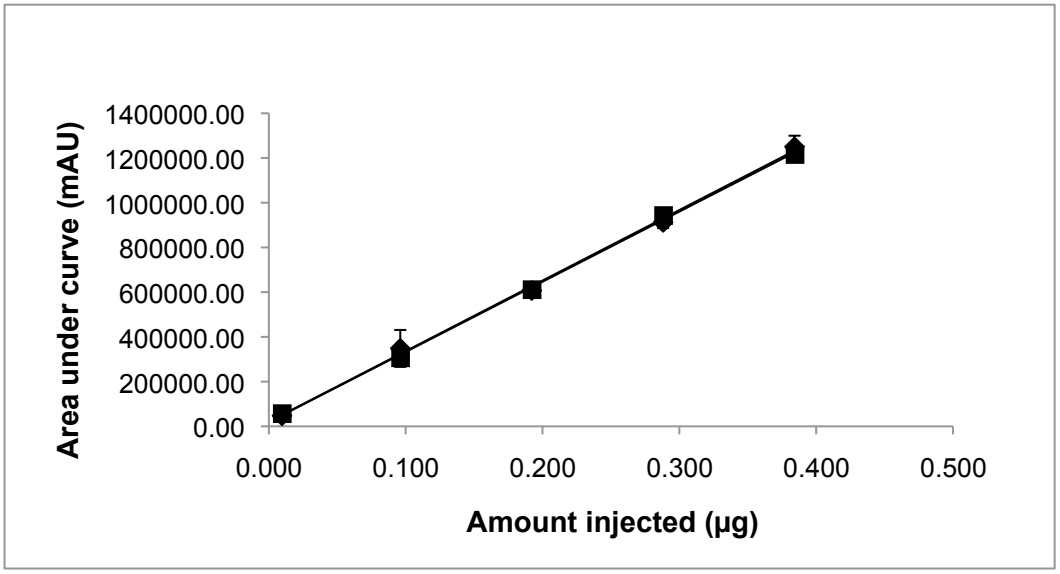

Fig. 5.6**:** Linearity of JS-K standards compared to JS-K samples at 5, 50, 100, 150 and 200 µM at 5 µL injection volume. For each concentration three replicates were made and each replicate was run in duplicate using UPLC. The injection volume was 5 µL. Each point on the curve is the average of peak area (n=6) with their standard deviations. For curve information, see text. Legend: ♦ = Richman JS-K; ■ = NCI JS-K.

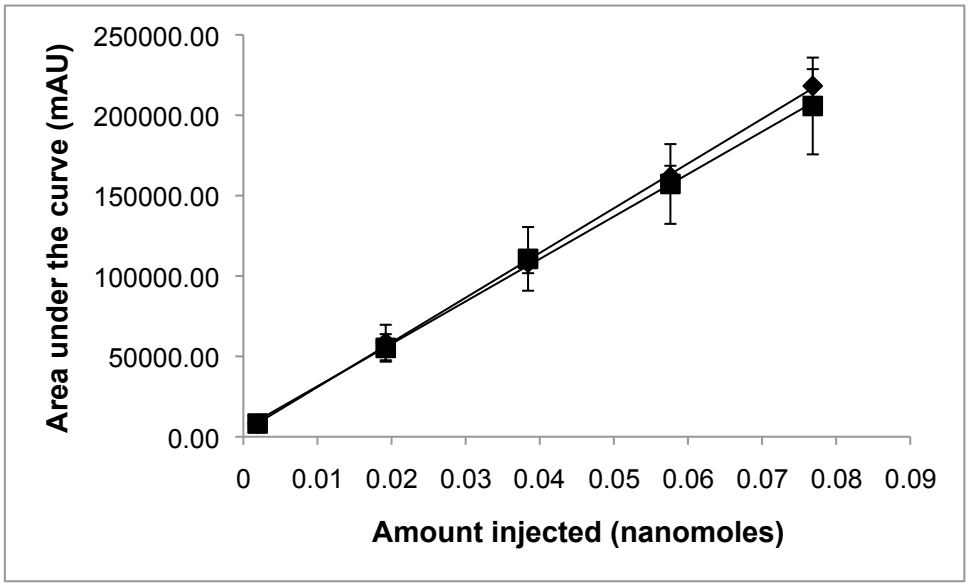

Fig. 5.7: Specificity of JS-K at 1 µL injection. JS-K standards at 5, 50, 100, 150 and 200 µL were run in triplicate. Each set was injected twice. Similarly JS-K samples were prepared at 5, 50, 100, 150 and 200 µL in P123 diluant in triplicate. Again each set was injected twice. Area under the curve obtained for each set was plotted against the nanomoles injected. Each point on the curve is the average and SEM of six readings. Legend: ♦ = Richman JS-K; ■= NCI JS-K.

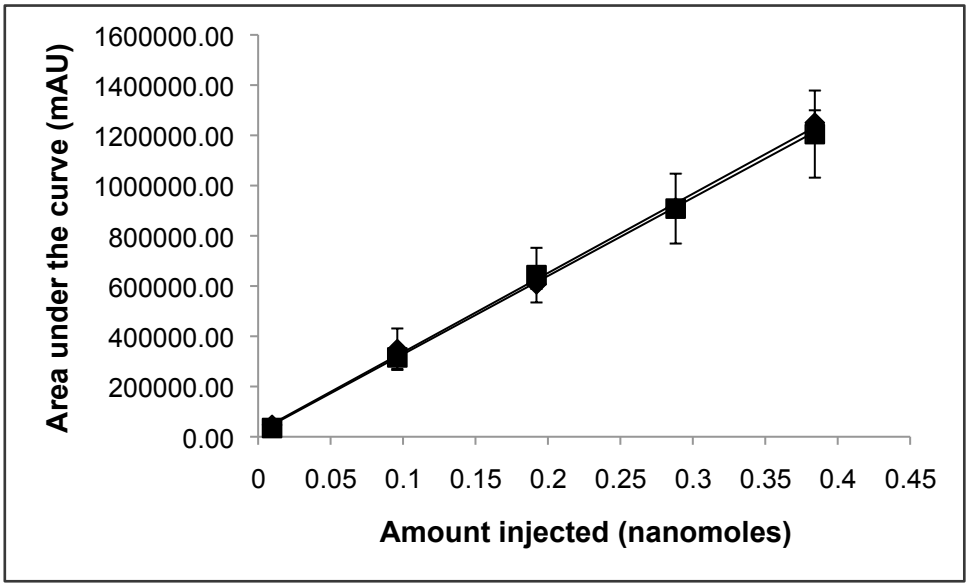

Fig. 5.8: Specificity of JS-K at 5 µL injection: JS-K standards at 5, 50, 100, 150 and 200 µL were run in triplicates. Each set was injected twice. Similarly, JS-K samples were prepared at 5, 50, 100, 150 and 200 µL in P123 diluant in triplicates. Each set was injected twice. Area under the curve obtained for each set was plotted against the nanomoles injected. Each point on the curve is the average and SEM of six readings. Legend: ♦ = Richman JS-K; ■ = NCI JS-K.

Table 5.1 – Drug loss with solid phase extraction (SPE)

Concentration (μM)	**% JS-K lost in SPE***	**% P123/JS-K lost in SPE***
10	-2.263 ± 1.05	-3.331 ± 4.14
100	-0.544 ± 3.3	-3.817 ± 5.72

*Percentage drug loss was calculated based on the total initial amount of JS-K or P123/JS-K added. Reported is the average and SEM of 3 separate experiments.

Table 5.2 – Comparison of solid phase extraction (SPE) and direct extraction method efficiency

Method	**% JS-K loss** *	**% P123/JS-K loss** *
SPE	5.712±5.80	0.335±5.418
Direct	33.778±3.69	39.424±4.316

*Drug recovery from mouse blood was calculated based on the total initial amount of JS-K or P123/JS-K added. Reported is the average and SEM of 3 separate experiments.

Table 5.3 – Intraday accuracy of JS-K measurements

Concentration of JS-K (µM)	**Injection Volume (µL)**	**Amount injected (µg)**	**Average peak area (mAU)** ± SD***	**Accuracy (% Recovery)[§]**
5	1	0.002	10965 ± 2254	137
50	1	0.019	56126 ± 3669	96
100	1	0.038	110855 ± 3642	102
150	1	0.058	170597 ± 4567	105
200	1	0.077	219143 ± 3190	100
5	5	0.010	58270 ± 11329	123
50	5	0.096	307904 ± 24230	88
100	5	0.192	612312 ± 20099	101
150	5	0.288	943774 ± 22920	103
200	5	0.384	1216464 ± 29646	97

**Three standards or samples were prepared for each concentration and injected in duplicate. [*]SD: Standard Deviation. [§]Accuracy calculated in terms of percentage recovery.

Table 5.4 – Intraday precision for Richman JS-K samples and NCI JS-K samples

Formul--ation	JS-K (µM)	Injection Volume (µL)	Peak Area (mAU) (Average, n=6)**	SD*	CV* (%)	RSD*
Richma--n Standar ds of JS-K formula -ted in DMSO	5	1	8051	1705	21.18	0.21
	50	1	58626	11057	18.86	0.19
	100	1	108282	6522	6.02	0.06
	150	1	161794	6779	4.19	0.04
	200	1	218218	10464	4.8	0.05
	5	5	47174	16315	34.59	0.35
	50	5	348560	82553	23.68	0.24
	100	5	607231	18590	3.06	0.03
	150	5	912099	25360	2.78	0.03
	200	5	1250103	49650	3.97	0.04
NCI samples of JS-K formula ted in DMSO	5	1	10964	2254	20.55	0.20
	50	1	56125	3669	6.54	0.06
	100	1	110855	3641	3.28	0.03
	150	1	170597	4567	2.67	0.02
	200	1	21914	3190	1.45	0.01
	5	5	58270	11330	19.44	0.19
	50	5	307904	24230	7.87	0.08
	100	5	612312	20099	3.29	0.03
	150	5	943774	22920	2.43	0.02
	200	5	1216464	29646	2.44	0.02

**Three standards or samples were prepared for each concentration and injected in duplicate. SD*: Standard Deviation; CV*: Coefficient of Variation; RSD*: Relative Standard Deviation.

Table 5.5 – Intermediate precision for Richman JS-K samples (formulated in DMSO) prepared and analyzed on two different days

JS-K (µM)	**Injection Volume (µL)**	**Average Peak Area (mAU)****	**SD***	**RSD***
5	1	9191	2871	0.31
50	1	57309	8023	0.14
100	1	116636	9965	0.09
150	1	173972	13608	0.08
200	1	240587	29086	0.12
5	5	49978	18839	0.38
50	5	343490	72768	0.21
100	5	649859	42502	0.07
150	5	988835	50218	0.05
200	5	1367869	171209	0.13

**Three standards or samples were prepared for each concentration and injected in duplicate. SD*: Standard Deviation; RSD*: Relative Standard Deviation.

CHAPTER 6

SUMMARY OF RESEARCH, CRITIQUES AND SUGGESTED FUTURE WORK

In this final chapter, each scientific chapter has been summarized succinctly to highlight the major hypothesis, findings and the goal achieved. Also, each chapter has been critically analyzed and based on those criticism, future work has been summarized.

6.1 Chapter 2- Development and Characterization of a Pluronic® P123 Formulation for the Nitric Oxide-generating Agent JS-K

6.1.1 Hypothesis and motivation

JS-K, an arylated diazeniumdiolate (ADZD), is a nitric oxide (NO)-releasing prodrug. NO donors have shown promising anticancer effects (1-10). Past studies with JS-K showed encouraging results (11-14). However, the instability of the drug in the presence of nucleophiles limits its applicability. Due to the above stated reasons, polymeric Pluronics® were screened in order to develop a formulation that would allow the clinical development of JS-K. The choice of using Pluronics® as compared to other polymeric systems were their ease of availability, cost effectiveness and comparative nontoxicity. Several Pluronics® have been approved by FDA and regarded as "Generally Recognized as Safe" (GRAS) (15). To start with our studies, we characterized the Pluronic® P123 formulation of JS-K, and then tested it *in vivo*.

After the development of the P123/JS-K formulation, the first step was to analyze the overall utility of the formulation. Since JS-K rapidly degraded in the presence of GSH, we hypothesized that Pluronic micelles stabilized JS-K. We also hypothesized that Pluronic did not impart major toxicity on their own. Finally, we hypothesized that the formulation P123/JS-K will be effective *in vivo.*

6.1.2 Summary of research

After the initial comparison of four different poloxamers based on the drug loading, drug retention and formulation toxicity in HL-60 and U-937 myeloid leukemia cells, we performed the major stability analysis of JS-K and P123/JS-K. The stability was tested using, RPMI media with 10% fetal bovine serum, normal human blood and plasma, and 4mM GSH. All the experiments showed that P123/JS-K was more stable than free JS-K. We then analyzed the protein binding of the free and Pluronic formulation, of JS-K. After the stability and the protein binding studies of the formulation, we characterized the poloxamer before starting the *in vivo* part. We measured the size (blank and formulation) of the Pluronic® micelles using dynamic light scattering. The size of the formulation was slightly smaller than the blank micelles. This could be because of the stabilization of both the drug and the unimers inside the micelle core. The micelles formed are very dynamic in nature and JS-K incorporation inside the core of the micelles stabilized the structure, thus reducing the size. The shape of the formulation was found to be spherical as obtained from transmission electron microscopy (TEM). The zeta potential measurement of the formulation was also carried out in distilled water. We also performed the critical micelle concentration (CMC) measurement and analyzed the specific gravity, cloud point and viscosity of the Pluronic. All the values were well within the range as reported by the

manufacturer. The *in vivo* tumor regression study was carried out on NOD/SCID *IL2Rg*^{null} mice. The mice were treated with 4 µmol/kg JS-K or 4 or 5 µmol/kg P123/JS-K or P123 only or were not treated at all. The treatment was performed every other day and was continued until the tumor size was greater than 10% of the body weight or when the mice became moribund. Interestingly, nearly 50% of the tumor regression was observed when treated mice (JS-K or P123/JS-K) were compared to untreated mice (no treatment or control treatment). Not much difference was observed between the free drug and the formulation initially, but a statistically significant difference was seen on the last day of the treatment. We expect the difference to go higher past that but we could not continue the treatment due to ethical reasons. The *in vivo* study clearly indicates that JS-K is an effective chemotherapeutic for the treatment of AML. The Pluronic formulation works as effectively as free drug with no observed major toxicity of the Pluronic by itself.

6.1.3 Critical analysis and suggested future work

This chapter of dissertation discussed the formulation prepared for JS-K. The major goals achieved with the formulation design were: a) stability of JS-K and b) increased solubility of the drug. The major assumption in the use of Pluronic was the polymer obtained from BASF was pure and ready to use. cGMP or medical grade Pluronic® P123 is not available commercially but it could be made to produce by cGMP labs. At this point, the major goal was to confirm if the prepared formulation will work and is shown to be effective in *in vitro* and *in vivo* studies. In regards to Pluronic characterization, studies were performed based on physical parameters like specific gravity, cloud point, viscosity, critical micelle concentration, size and shape. All the parameters tested conformed with the previously reported values available in the literature or from the

manufacturer. We also performed some qualitative/quantitative studies based on the peak area by measuring the refractive index of the polymer on HPLC.

6.1.3.1 Negative zeta potential

While poloxamer P123 is a neutral polymer, the zeta potential analyzed was negative. The study performed by a different lab also showed negative zeta potential and our value is close to theirs (16). One of the possible explanations for such a value calculated by different labs could be the purity of the Pluronic available commercially. Therefore, it is suggested that in the future, Pluronic purity should be analyzed via chromatography.

6.1.3.2 *In vivo* tumor model

The tumor cell implantation in NOD/SCID *IL2Rγ*^{null} mice to study tumor regression is an old model and does not mimic the actual clinical disease. As the drug is expected to enter the clinic study, a model that more closely reproduces the disease needs to be established. Broadly two models could be generated:

6.1.3.2.1 Implantation of bioluminescent leukemia cells in irradiated NOD/SCID IL2Rγ^{null} *mice.* Leukemia is a hematological malignancy. The older xenograft mouse models require the subcutaneous implantation of the leukemia cells, which does not reflect that actual disease involving the bone marrow (17). Therefore, a suitable model would be a systemic leukemia model with bioluminescent leukemia cells. This will have two major advantages. First, disease evolution will be close to the actual disease in humans with involvement of hematopoietic organs. Second, with the use of bioluminescent leukemia cells, tumor tracking will be reliable and quicker.

6.1.3.2.2 Leukemia stem cell mouse model. It has been found that chemotherapy resistant AML stem cells home in the endosteal region of the bone marrow (18). Since our focus is to establish specificity of P123/JS-K at the cancer stem cell level, it would be appropriate to generate an AML stem cell model in NOD/SCID *IL2Rγ*^{null} mice.

6.2 Chapter 3 – Cellular Distribution Studies of the Nitric Oxide-generating Antineoplastic Prodrug JS-K, Formulated in Pluronic® P123 Micelles

6.2.1 Hypothesis and motivation behind the study

Polymeric micelles have been found to affect cellular penetration and cellular distribution (19). The polymers could have acidic functional groups, basic functional groups or be neutral polymers. Depending on the polymer type, drug release from the polymer could be acidic release, basic release or by simple diffusion (20). As it has been reported in the literature that micelles affect cellular penetration and the cellular distribution of the drug, focusing on such a result, we were motivated to analyze the variable distribution of our drug and formulation system. Rapaport et al. reported the nuclear penetration of their Pluronic/drug system. The drug used in the study was also hydrophobic like JS-K and the Pluronic system they used was P105 (21). Keeping this result in mind, we carried out our studies. Also, past studies have shown that JS-K stability is compromised in complex media such as RPMI with or without FBS as these media have free cysteine groups that could release NO from JS-K. This encouraged us to study if the stability of JS-K affected the cellular distribution of the drug. This experimental set up was also instrumental in answering a corollary observation, namely if the type of formulation affected the stability and thus the distribution. From the

mechanistic point, we wanted to address the post-translational modifications produced by the drug and the formulation. PABA-NO, an arylated diazeniumdiolate (ADZD), has shown extensive glutathionylation in human leukemia HL-60 cells (22). JS-K is also an ADZD and therefore, JS-K is also expected to glutathionylate proteins to different extents. The cellular distribution study was also important from future studies point of view. With cellular distribution study carried out, it was easier to hypothesize and analyze the cell death mechanism of JS-K.

The polymeric formulation stabilized JS-K appreciably as explained in the previous chapter. The next step was to study the cellular distribution of the drug. The cellular distribution of the drug could be affected by the type of formulation and type of media used for incubation. We hypothesized that cell distribution will be different for the free JS-K and P123/JS-K. Also, the incubation media used for the cells and the drugs will affect their stability and thus the distribution. We further hypothesized that the distribution will affect the glutathionylation response induced by JS-K or P123/JS-K. Such a differential effect produced affects posttranslational modifications produced by the drug or the formulation in the proteins of various cell compartments finally affecting cell death. Posttranslational modifications such as glutathionylation are critical in cell survival (23). Such modifications induced are dependent on the type of the protein involved in the posttranslational modification and the cellular function carried out by that protein. This might work in favor or against the cell survival process. Also glutathionylation posttranslational modification has been particularly associated with cellular stress conditions such as oxidative stress and endoplasmic reticulum stress. Both the stress condition can result in the cell death response (24-33).

6.2.2 Summary of research

This study was carried out with two clear objectives. The first objective was to analyze the differential distribution of the free drug compared to micelle formulated P123/JS-K. This is because micelles have been shown to affect the intracellular distribution and localization of several drugs. Also, with JS-K stability determined by the type of incubating solutions, we wanted to confirm if that affects the cellular distribution of the two formulations. The second objective was to explore the mechanistic effect of the free drug and the formulation and thus the effect produced due to the polymer used. This study was important in order to carry out future mechanistic studies of JS-K and the formulation P123/JS-K.

In this study, the initial exploratory experiments were carried out to confirm the free drug or P123/JS-K uptake by human leukemia HL-60 cells. These initials experiments were positive and therefore, we moved to the next step of the differential distribution of the drug when incubated in different media. This study was carried out by treating HL-60 cells with either JS-K or P123/JS-K when incubated in PBS that does not contain any proteins or amino acids that might lead to drug degradation. The incubated cells were then fractionated into cytosolic and nuclear isolates after indicated time points. The intact drug recovered from each compartment was calculated as percentage recovery of the actual amount of the drug added. We found that at each time point P123/JS-K recovery was higher than free JS-K. Also, nuclear drug recovery was higher than the cytosolic drug recovery. With this study, we were confident that the drug translocates primarily to nucleus. We then moved forward with more complex media where the HL-60 cells were incubated in RPMI/10% FBS media or PBS/10% FBS media. As postulated, the drug

recovery was lower as the drug degraded. RPMI/10% FBS media is the most complex media as it contains free cysteines and serum. PBS/10% FBS on the other hand, was a system with intermediate complexity. While it is not as gentle as PBS, it is not as harsh as RPMI/10% FBS. The studies also revealed that regardless of the incubating media, P123/JS-K recovery was higher than free JS-K from the nucleus.

The glutathionylation studies carried out confirmed the nuclear entry of the drug as the nuclear proteins were glutathionylated to a higher extent as compared to the cytosolic proteins. Again, glutathionylation induced by P123/JS-K was higher than the free JS-K, again indicating polymeric micelles modulate drug's function.

6.2.3 Critical analysis and suggested future work

6.2.3.1 High concentration of drug used

In the study carried out, we used 50 μM of JS-K or 50 μM of P123/JS-K that was added to HL-60 cells and fractionated at different time points. While the IC_{50} of free JS-K is 0.5 μM, it could be argued that 100X times higher concentration should not have been used for the distribution study. The prime reason to start with such a high concentration was due to the limitation of the assay and sensitivity of the instrument. We used HPLC to quantify whole JS-K. We tried a lower concentration of the drug, but detection was an issue. Later, we developed a method on UPLC. When we used 5 μM JS-K or P123/JS-K, again we could not detect intact drug. Therefore, high concentration of the drug was used for cell uptake experiments. Another critique of the study was the degradation of the drug to its metabolites. We can justify the use of high concentration, as our aim was to detect the whole intact drug as it distributes. We were not analyzing any pharmacological effect produced by the drug, therefore we did not worry about the concentration or the

metabolites produced. Also, there are several clinically available drugs that have very low IC_{50} but are used at high concentrations when exploring pharmacological effects produced *in vitro* (34).

6.2.3.2 Pluronic® uptake not quantified

P123/JS-K showed higher nuclear distribution and higher nuclear protein glutathionylation. The polymeric micelles affected the cell translocation. We analyzed the distribution of JS-K or P123/JS-K; in both the studies, whole JS-K was quantified and the effect of polymer was inferred from the higher recovery of P123/JS-K. We still need to determine whether the drug is still inside the micelle core when it is taken up by the cell. Also, how soon does the drug come out of the micelle core? Also, are the micelles differentially distributed? The corrolary question could be whether P123 (micelles or unimers) is taken up by cells. Additionally, we have shown differential protein binding between JS-K and P123/JS-K. This raises the possibility of interaction between P123 unimers (or micelles) with albumin in addition to existing interaction between JS-K or P123/JS-K and albumin. If such a complex interaction is taking place, then this could affect the local concentration of JS-K. All these possibilities will require labeling of the Pluronic micelles with a dye and then tracking them via fluorescence. Also, in order to determine how soon JS-K is released from the micelle core or if P123/JS-K as a whole distributes in the nuclei, we will have to prepare labeled Pluronics® and then quantify both JS-K and Pluronics®.

6.2.3.3 Types of proteins glutathionylated not identified

In this study, the aim was to analyze global glutathionylation of cytosolic and nuclear proteins. With the confirmed result that both JS-K and P123/JS-K cause glutathionylation of the cytosolic and the nuclear proteins, the next step should be to analyze the types of nuclear (soluble and insoluble nuclear proteins) and cytosolic proteins glutathionylated by running the relevant markers and generating hypothesis for the possible proteins that could be glutathionylated.

6.3 Chapter 4- Multiple Stress Response Induced by the Nitric Oxide-releasing Prodrug JS-K.

6.3.1 Hypothesis and motivation behind the work

Nitric oxide has been associated with pro-apoptotic and anti-apoptotic effects. As explained in detail in the chapter, the delivery and site of NO release determines the type of the effect produced. Initial studies have confirmed that NO released due to JS-K or other ADZD has been associated with their pro-apoptotic effects. This motivated us to further explore the possible mechanisms that might be involved in producing such effects. There are several effects produced by JS-K as shown by past studies. There are certain effects that are tumor type specific and some are due to properties of JS-K. The major effects produced by JS-K could be attributed possibly to a) release of NO, b) ability to undergo nucleophilic substitution reaction with GSH, c) catalysis by GST enzyme system, d) specificity towards cancer cells due to targeting of pathways elevated in cancer, e) posttranslational modifications induced due to S-nitrosylation, S-glutathionylation and arylation, f) oxidative stress or nitrosative stress (redox imbalance) caused by consumption of GSH or release of NO, g) endoplasmic reticulum stress caused

by accumulation of proteins as a result of S-glutathionylation or S-nitrosylation or due to oxidative stress. Therefore, apoptotic effects produced by JS-K could be attributed to either one or all the possible mechanisms stated above. In order to achieve complete remission from cancer, the drug should produce multiple effects so that even if one possible target gains resistance, a chemotherapeutic should be able to work effectively in killing tumor cells. An effective chemotherapeutic should be able to modulate the intrinsic and the extrinsic components of cell survival. While the intrinsic component includes targeting of multiple stress responses such as the survival pathways and the self-renewal pathways (of cancer stem cells), the extrinsic components is comprised of the tumor microenvironment, adhesion factors and angiogenic factors (35). In addition to these factors, it is also important for the chemotherapeutic to not cause any nonspecific toxicity to normal cells or noncancer cells. As stated in the introduction chapter, JS-K was found to be nontoxic in normal peripheral blood mononuclear cells, normal mammary cells, normal renal cells, normal murine hematopoietic stem cells and normal human CD34+ hematopoietic cells.

With past studies indicating that JS-K possessed a broad mechanism of action, we based our hypothesis to carry out this project. We hypothesized that JS-K caused ER stress due to glutathionylation, nitrosylation, arylation, oxidative stress or nitrosative stress. We hypothesized that JS-K activated several components of intrinsic pathways of cell survival by producing multiple stress responses, thus acting through a broad mechanism of action.

6.3.2 Summary of research

In this chapter, we presented our results showing that both JS-K and P123/JS-K caused ER stress and oxidative stress. We showed that when HL-60 cells were treated with 5 μM of JS-K or P123/JS-K for 4-8 hours, the unfolded protein response (UPR) sensitive chaperone GRP-78 was activated. GRP-78 is also considered a sensor of ER stress as this chaperone is involved in the refolding of misfolded proteins. This chaperone splits from the other ER stress markers- PERK, ATF6 and IRE1 and gets involved in the refolding of the misfolded proteins. CHOP, a gene and DNA damaging protein (GADD 153), is considered the effector of ER stress. We also found that by treating HL-60 cells with 5 μM JS-K or P123/JS-K for 6-8 hours, CHOP activation was seen with Western blots. With positive results obtained in both experiments, we concluded that JS-K or P123/JS-K activated ER stress response. We then continued our studies to analyze the oxidative stress response. When HL-60 cells were treated with 5 μM JS-K or P123/JS-K, Western blot showed activation of JNK protein in some experiments and negligible activation in others. JNK protein activation (or JNK protein phosphorylation) is generally linked to oxidative stress response. To confirm if JS-K actually caused any sort of oxidative stress response or nitrosative response, we treated the cells with JS-K or P123/JS-K for 30, 60 or 120 minutes and later treated them with a reactive oxygen/reactive nitrogen species sensitive fluorescent dye for 30 minutes. The results showed that free JS-K had highest intracellular ROS/RNS which did not change significantly after 30 minutes of treatment. This could be due to the immediate release of NO from the free JS-K that was not sheltered in the micelle core. P123/JS-K on the other hand showed comparatively low levels of intracellular ROS/RNS. Again this could be

due to sheltering of the drug inside the micelle core thus stabilizing the drug for a period of time. When the cells were treated with both positive control (H_2O_2, a ROS generator) and P123/JS-K, the ROS/RNS levels were higher than the individual ROS levels of only H_2O_2 treated cells or only P123/JS-K treated cells, suggesting that ROS/RNS levels could be increased if the cells are pretreated with a ROS generator. Interestingly, P123 only treated cells, showed lower levels of ROS/RNS when compared to nontreated cells. Even though the results were not statistically significant, this suggests that either P123 reduced levels of ROS/RNS acting as a quencher or did not produce any effect at all. This also explains the reason for reduced levels of ROS/RNS detected for P123/JS-K cells. We next carried out our studies on AML patient cells. These cells were isolated from two relapsed AML patients and we carried out our ER stress-related studies. We obtained positive results in one set of patient cells and negative results in the other set. Several reasons could explain this observation. To start with, we had archived samples collected several years prior to the experiments and thus may have been altered during storage. The second could be differences in the phenotype of each individual leukemia as AML is a heterogenous disease. With further study, this could lead to a personalized medicine strategy. Another explanation could be the inherent ER stress response variability. It has been shown that in patient cell isolates where ER stress response was seen in the nontreated cells, such patients had increased survival chances as compared to patients with negative ER stress markers to start with (36). This may be because leukemias with baseline elevated levels of ER stress markers could be pushed beyond their threshold level switching the cancer cell survival response to cell death response. In the next set of studies, we tried to analyze JS-K's effect on normal human CD34+ hematopoietic cells, a

population of cells that is rich in normal hematopoietic stem cells (HSC). The HSC were treated with JS-K or P123/JS-K and an MTT cell survival assay was carried out. Neither of the groups (treated or untreated) showed any difference. This result indicated that JS-K did not show any nonspecific toxicity towards the normal HSC. We then carried out our study to explore if JS-K activated ER stress response in normal HSC. The cells were treated with either JS-K or P123/JS-K or P123 only or positive control of ER stress response tunicamycin or not treated at all. Western blot analysis was then carried out on the treated or nontreated cells. Interestingly, none of the groups showed any activation. This could imply that none of the drugs were active on HSC or triggered the ER stress response. This could also imply that the treatment time was not enough as HSC are generally nonresponsive to any kind of stress response generated. More work is required in that area.

6.3.3 Critical analysis and suggested future work

In Chapter 4 of this dissertation, mechanistic effects of JS-K were studied in detail and an attempt was made to explore the broad pharmacological effects produced by the drug. The hypotheses for the proposed experiments were based on previous studies performed on JS-K and ADZD. In general, the confirmatory experiments to validate the hypothesis were performed and the conclusions were made based on the results obtained.

Several hypotheses could be proposed to a particular result obtained and therefore, specific experiments should be performed for the proposed hypothesis as explained later. Also, in the studies performed, although we used positive controls, we did not use negative control in any study. This is due to the fact that the mechanism explored could be activated by several pathways. Our intent was to establish the activation of the

mechanism in general. With more specific future studies, appropriate negative controls should be included. Also, other AML cell lines with different phenotypes (example U937 cells) should also be tested.

6.3.3.1 Accumulation of S-glutathionylated or S-nitrosylated proteins lead to ER stress

When the ER stress experiments were started, S-glutathionylation and S-nitrosylation caused by JS-K was considered a prime reason for causing accumulation of unfolded or misfolded proteins leading to ER overload thus causing ER stress. While global S-glutathionylation has been showed in a set of experiments as explained in Chapter 3, we did not study the S-nitrosylation response produced by JS-K or P123/JS-K. Specific proteins glutathionylated or S-nitrosylated should be analyzed and their effect on ER stress activation should be studied.

6.3.3.2 Link up of oxidative stress and ER stress

A very broad assumption could be made linking up ER stress with oxidative stress. While in the literature, there are several studies that link up both the stresses (37-41), in our case, confirmatory experiments should be performed. Induction of ERO1 (ER oxidoreductase enzyme) has been correlated with ER stress caused by oxidative stress. This further leads to activation of JNK protein and finally results in apoptosis.

6.3.3.3 Inconclusive JNK activation

JNK activation should be confirmed with follow-up experiments testing for the activation of ERO1. Also, HL-60 cells could be pretreated with JNK inhibitors and then treated with JS-K followed by either an MTT experiment (to show if JNK involved in

cell death), an ER stress experiment (by testing for GRP-78 and CHOP to show if JNK is involved in ER stress) or a ROS/RNS generation experiment (to show if JNK is involved in oxidative stress).

6.3.3.4 Consumption of GSH related to oxidative stress

Another hypothesis proposed in the study was induction of oxidative stress in HL-60 cells due to consumption of GSH. Again, confirmatory experiments should be performed. Although GSH consumption studies have been done in past (14, 42), in the study proposed, a link would be established between GSH (anti-oxidant), oxidative stress and ER stress. For the study, GSH levels should be monitored before and after JS-K and P123/JS-K treatment in HL-60 cells. This should be followed by another experiment where HL-60 cells are pretreated with the GSH precurson N-acetyl-cysteine. The cells should be then treated with JS-K or P123/JS-K. After appropriated time, reactive oxygen/nitrogen species generation should be tested. This should be followed by ER stress activation experiments. This will confirm if glutathionylation caused by JS-K or P123/JS-K treatment led to accumulation of misfolded proteins thus leading to ER stress. This will also show any possible link between oxidative stress and ER stress.

6.3.3.5 Effect on HSC

The effect on HSC should be analyzed in more detail by carrying out experiments at extended hours as HSC may not be responsive to stress conditions due to their inherent dormancy.

6.3.4 Additional suggested future work

6.3.4.1 Effect on leukemic stem cell (LSC)

In order to investigate the complete intrinsic pathway activated by JS-K, its effect on LSC should be analyzed. These can be challenging experiments because of the small number of LSCs in any given isolate and because of the heterogeneity of the phenotype of LSCs.

6.3.4.2 Combination studies

Combination studies with clinically used ER stress generating drugs should be performed. One such drug is Bortezomib used for the treatment of multiple myeloma and mantle cell lymphoma. This drug is a proteasome inhibitor and causes both oxidative and ER stress generating cell death.

6.3.4.3 Cell senescence experiments

It is possible that JS-K caused cell death through other pathways than programmed cell death. A number of studies have shown that the drugs causing oxidative stress cause cell death due to senescence. Confirmatory studies with JS-K should be performed.

6.3.4.4 Personalized medicine

JS-K specificity for one patient type suggests JS-K might be helpful in personalized medicine. The genes upregulated and down regulated by JS-K should be explored to use JS-K for a particular patient population.

6.3.4.5 Cell survival pathways

Nuclear factor kappa B (NF-kB) has been shown to be upregulated in leukemia and LSC and provide survival factors to leukemic cells and LSC (35, 43).

6.4 Chapter 5- Development and Validation of a Method to Measure Levels of the NO-producing Prodrug JS-K Using Ultra Performance Liquid Chromatography (UPLC)

6.4.1 Motivation behind the work

In this chapter, a rapid and robust quantitative method was developed to analyze JS-K and its metabolites (2,4-dintrophenol and S-(2,4-dinitrophenyl)-Glutathione). The method was developed using Ultra Performance Liquid Chromatography (UPLC). This method holds importance as P123/JS-K is a clinical candidate. Therefore, this method could be used for the clinical study of pharmacokinetic parameters such as elimination, half-life, metabolite generation and tissue distribution. Also, the method could be used for dosage designing and future metabolomic and metabonomic studies. This is the fist assay developed for the simultaneous measurement of JS-K and its metabolites. The detection of metabolites is important as JS-K degrades to its metabolites rapidly. Information about metabolites could help in studies related to toxicity, elimination and drug tracking. Because of JS-K's reactivity, the method used to extract JS-K from plasma and tissues is extremely important.

6.4.2 Summary of research

In this chapter, method development and validation of JS-K were discussed. For all the validation studies carried out, United States Pharmacopoeia (USP) parameters were

followed. The chromatogram of JS-K and its metabolites was obtained in a single run with all the three peaks separated from each other. A total run time of 6 minutes was developed. An isocratic followed by isogradient solvent system was utilized. We compared two extraction systems that lead to maximum drug recovery. We compared direct protein precipitation (PP) method with solid phase extraction (SPE) followed by protein precipitation method.

JS-K spiked blood samples or JS-K prepared in solvent systems was used to calculate the percentage recovery using either extraction procedure. The results indicated that SPE followed by PP showed higher extraction of JS-K. After the extraction procedure development and method development, we validated the whole method. Validation was conducted by determining the linearity, specificity, accuracy, robustness and precision of the developed method. For the validation studies, we considered the lab prepared JS-K as "samples" and cGMP prepared JS-K as "standards".

6.4.3 Suggested future work

6.4.3.1 Pharmacokinetic (PK) study

This is one of the major and the direct application of the developed method. During the PhD, I have performed several PK experiments but the drug could not be recovered, even in the shortest time interval of 2 minutes. Also, those experiments were performed on HPLC, which is less sensitive as compared to UPLC. Therefore, it was important to develop a sensitive method with an efficient extraction procedure. While we did not perform a full PK analysis with the new method developed on UPLC, method development studies were carried out on mouse organs treated with JS-K for 2 minutes. The results obtained from UPLC were then validated by running the same samples on the

mass spectrometer and similar results were obtained. Full PK analysis will therefore be possible in future studies.

6.4.3.2 Metabonomic study

The method developed could be used for future metabolomic and metabonomic analysis by coupling UPLC to a mass spectrometer. This could be helpful in toxicity analysis, metabolic profiling and personalized medicine.

6.5 References

1. Burgaud JL, Riffaud JP, Del Soldato P. Nitric-oxide releasing molecules: a new class of drugs with several major indications. Curr Pharm Des. 2002;8(3):201-213.

2. Chegaev K RC, Lazzarato L, Rolando B, Guglielmo S, Campia I, Fruttero R, Bosia A, Gasco A. Nitric Oxide Donor Doxorubicins Accumulate into Doxorubicin-Resistant Human Colon Cancer Cells Inducing Cytotoxicity. ACS Med Chem Lett. 2011.

3. Donia M, Maksimovic-Ivanic D, Mijatovic S, Mojic M, Miljkovic D, Timotijevic G, Fagone P, Caponnetto S, Al-Abed Y, McCubrey J, Stosic-Grujicic S, Nicoletti F. In vitro and in vivo anticancer action of Saquinavir-NO, a novel nitric oxide-derivative of the protease inhibitor saquinavir, on hormone resistant prostate cancer cells. Cell Cycle. 2011;10(3):492-499.

4. Huerta S, Chilka S, Bonavida B. Nitric oxide donors: novel cancer therapeutics (review). Int J Oncol. 2008;33(5):909-927.

5. Jia L, Wu CC, Guo W, Young X. Antiangiogenic effects of S-nitrosocaptopril crystals as a nitric oxide donor. Eur J Pharmacol. 2000;391(1-2):137-144.

6. Keefer LK. Nitric oxide (NO)- and nitroxyl (HNO)-generating diazeniumdiolates (NONOates): emerging commercial opportunities. Curr Top Med Chem. 2005;5(7):625-636.

7. Konovalova NP, Goncharova SA, Volkova LM, Rajewskaya TA, Eremenko LT, Korolev AM. Nitric oxide donor increases the efficiency of cytostatic therapy and retards the development of drug resistance. Nitric Oxide. 2003;8(1):59-64.

8. Qu W, Liu J, Dill AL, Saavedra JE, Keefer LK, Waalkes MP. V-PROLI/NO, a nitric oxide donor prodrug, protects liver cells from arsenic-induced toxicity. Cancer Sci. 2009;100(3):382-388.

9. Rigas B, Williams JL. NO-donating NSAIDs and cancer: an overview with a note on whether NO is required for their action. Nitric Oxide. 2008;19(2):199-204.

10. Stevens EV, Carpenter AW, Shin JH, Liu J, Der CJ, Schoenfisch MH. Nitric oxide-releasing silica nanoparticle inhibition of ovarian cancer cell growth. Mol Pharm. 2010;7(3):775-785.

11. Shami PJ, Maciag AE, Eddington JK, Udupi V, Kosak KM, Saavedra JE, Keefer LK. JS-K, an arylating nitric oxide (NO) donor, has synergistic anti-leukemic activity with cytarabine (ARA-C). Leuk Res. 2009;33(11):1525-1529.

12. Shami PJ, Saavedra JE, Bonifant CL, Chu J, Udupi V, Malaviya S, Carr BI, Kar S, Wang M, Jia L, Ji X, Keefer LK. Antitumor activity of JS-K [O2-(2,4-dinitrophenyl) 1-[(4-ethoxycarbonyl)piperazin-1-yl]diazen-1-ium-1,2-diolate] and related O2-aryl diazeniumdiolates in vitro and in vivo. J Med Chem. 2006;49(14):4356-4366.

13. Shami PJ, Saavedra JE, Wang LY, Bonifant CL, Diwan BA, Singh SV, Gu Y, Fox SD, Buzard GS, Citro ML, Waterhouse DJ, Davies KM, Ji X, Keefer LK. JS-K, a glutathione/glutathione S-transferase-activated nitric oxide donor of the diazeniumdiolate class with potent antineoplastic activity. Mol Cancer Ther. 2003;2(4):409-417.

14. Udupi V, Yu M, Malaviya S, Saavedra JE, Shami PJ. JS-K, a nitric oxide prodrug, induces cytochrome c release and caspase activation in HL-60 myeloid leukemia cells. Leuk Res. 2006;30(10):1279-1283.

15. Yang M, Lai SK, Wang YY, Zhong W, Happe C, Zhang M, Fu J, Hanes J. Biodegradable nanoparticles composed entirely of safe materials that rapidly penetrate human mucus. Angew Chem Int Ed Engl. 2011;50(11):2597-2600.

16. Liu Z, Liu D, Wang L, Zhang J, Zhang N. Docetaxel-loaded pluronic p123 polymeric micelles: in vitro and in vivo evaluation. Int J Mol Sci. 2011;12(3):1684-1696.

17. Lee MW, Kim HJ, Yoo KH, Kim DS, Yang JM, Kim HR, Noh YH, Baek H, Kwon H, Son MH, Lee SH, Cheuh HW, Jung HL, Sung KW, Koo HH. Establishment of a bioluminescent imaging-based in vivo leukemia model by intra-bone marrow injection. Int J Oncol. 2012;41(6):2047-2056.

18. Saito Y, Uchida N, Tanaka S, Suzuki N, Tomizawa-Murasawa M, Sone A, Najima Y, Takagi S, Aoki Y, Wake A, Taniguchi S, Shultz LD, Ishikawa F. Induction of cell cycle entry eliminates human leukemia stem cells in a mouse model of AML. Nat Biotechnol. 2010;28(3):275-280.

19. Yoo HS, Park TG. Biodegradable polymeric micelles composed of doxorubicin conjugated PLGA-PEG block copolymer. J Control Release. 2001;70(1-2):63-70.

20. Lee JH, Jung HW, Kang IK, Lee HB. Cell behaviour on polymer surfaces with different functional groups. Biomaterials. 1994;15(9):705-711.

21. Rapoport N, Marin A, Luo Y, Prestwich GD, Muniruzzaman MD. Intracellular uptake and trafficking of Pluronic micelles in drug-sensitive and MDR cells: effect on the intracellular drug localization. J Pharm Sci. 2002;91(1):157-170.

22. Townsend DM, Findlay VJ, Fazilev F, Ogle M, Fraser J, Saavedra JE, Ji X, Keefer LK, Tew KD. A glutathione S-transferase pi-activated prodrug causes kinase activation concurrent with S-glutathionylation of proteins. Mol Pharmacol. 2006;69(2):501-508.

23. Dalle-Donne I, Rossi R, Giustarini D, Colombo R, Milzani A. S-glutathionylation in protein redox regulation. Free Radic Biol Med. 2007;43(6):883-898.

24. Castro L, Demicheli V, Tortora V, Radi R. Mitochondrial protein tyrosine nitration. Free Radic Res. 2011;45(1):37-52.

25. Cumming RC, Andon NL, Haynes PA, Park M, Fischer WH, Schubert D. Protein disulfide bond formation in the cytoplasm during oxidative stress. J Biol Chem. 2004;279(21):21749-21758.

26. Dalle-Donne I, Rossi R, Giustarini D, Colombo R, Milzani A. S-glutathionylation in protein redox regulation. Free Radic Biol Med. 2007;43(6):883-898.

27. Ghezzi P. Regulation of protein function by glutathionylation. Free Radic Res. 2005;39(6):573-580.

28. He S, Liao TT, Chen YT, Kuo HM, Lin YL. Glutathione-S-transferase enhances proliferation-migration and protects against shikonin-induced cell death in breast cancer cells. Kaohsiung J Med Sci. 2011;27(11):477-484.

29. Hess DT, Matsumoto A, Kim SO, Marshall HE, Stamler JS. Protein S-nitrosylation: purview and parameters. Nat Rev Mol Cell Biol. 2005;6(2):150-166.

30. Hess DT, Stamler JS. Regulation by S-nitrosylation of protein post-translational modification. J Biol Chem. 2012;287(7):4411-4418.

31. Leon L, Jeannin JF, Bettaieb A. Post-translational modifications induced by nitric oxide (NO): implication in cancer cells apoptosis. Nitric Oxide. 2008;19(2):77-83.

32. Townsend DM. S-glutathionylation: indicator of cell stress and regulator of the unfolded protein response. Mol Interv. 2007;7(6):313-324.

33. West MB, Hill BG, Xuan YT, Bhatnagar A. Protein glutathiolation by nitric oxide: an intracellular mechanism regulating redox protein modification. FASEB J. 2006;20(10):1715-1717.

34. Yoo HS, Lee KH, Oh JE, Park TG. In vitro and in vivo anti-tumor activities of nanoparticles based on doxorubicin-PLGA conjugates. J Control Rel. 2000;68(3):419-431.

35. Konopleva MY, Jordan CT. Leukemia stem cells and microenvironment: biology and therapeutic targeting. J Clin Oncol. 2011;29(5):591-599.

36. Schardt JA, Weber D, Eyholzer M, Mueller BU, Pabst T. Activation of the unfolded protein response is associated with favorable prognosis in acute myeloid leukemia. Clin Cancer Res. 2009;15(11):3834-3841.

37. Fribley A, Zeng Q, Wang CY. Proteasome inhibitor PS-341 induces apoptosis through induction of endoplasmic reticulum stress-reactive oxygen species in head and neck squamous cell carcinoma cells. Mol Cell Biol. 2004;24(22):9695-9704.

38. Malhotra JD, Kaufman RJ. Endoplasmic reticulum stress and oxidative stress: a vicious cycle or a double-edged sword? Antioxid Redox Signal. 2007;9(12):2277-2293.

39. Nishitoh H, Matsuzawa A, Tobiume K, Saegusa K, Takeda K, Inoue K, Hori S, Kakizuka A, Ichijo H. ASK1 is essential for endoplasmic reticulum stress-induced neuronal cell death triggered by expanded polyglutamine repeats. Genes Dev. 2002;16(11):1345-1355.

40. Tabas I, Ron D. Integrating the mechanisms of apoptosis induced by endoplasmic reticulum stress. Nat Cell Biol. 2011;13(3):184-190.

41. Verma G, Datta M. The critical role of JNK in the ER-mitochondrial crosstalk during apoptotic cell death. J Cell Physiol. 2012;227(5):1791-1795.

42. Maciag AE, Chakrapani H, Saavedra JE, Morris NL, Holland RJ, Kosak KM, Shami PJ, Anderson LM, Keefer LK. The nitric oxide prodrug JS-K is effective against non-small-cell lung cancer cells in vitro and in vivo: involvement of reactive oxygen species. J Pharmacol Exp Ther. 2011;336(2):313-320.

43. Jordan CT. The leukemic stem cell. Best Pract Res Clin Haematol. 2007;20(1):13-18.

APPENDIX

ACTIVATION OF ENDOPLASMIC RETICULUM STRESS IN PRIMARY CELLS AND ACTIVATION OF JNK PROTEIN BY JS-K OR P123/JS-K− A POTENTIAL MISSING LINK BETWEEN ENDOPLASMIC RETICULUM STRESS AND OXIDATIVE STRESS

A.1 Introduction

Endoplasmic reticulum (ER) is involved in a plethora of biological and physiological functions (1-7). One important role played by ER is in protein disulphide bond formation. If during the process, protein disulphide bond formation goes awry, it not only leads to accumulation of misfolded proteins evoking the unfolded protein response (UPR) and causing ER stress, but also leads to oxidative stress due to the continuous reductive and oxidative cycles generating H_2O_2 (8). Oxidant levels in the cell are controlled by the intracellular anti-oxidants including glutathione (GSH). Oxidative stress can be enhanced if the anti-oxidants get depleted in the process as well (9). The classes of oxidoreductases (Er oxidoreductase) and isomerases (protein disulfide isomerase) enzyme systems are involved in the disulphide bond formation between the proteins. Any modification to the enzymes involved also induces conditions of ER stress and oxidative stress (10, 11). Several attempts have been made to link ER stress with oxidative stress. Even then, no confirmatory pathway has been elucidated that links both stresses (12). Malhotra and

Kaufman suggested four different reasons of oxidative stress caused by ER stress. They suggested two pathways of reactive oxygen species (ROS) generation during disulfide bond formation and two pathways independent of disulfide bond. The first case is the production of ROS as a byproduct during the transfer of electrons from thiol groups (in proteins) to molecular oxygen when the reaction is catalyzed by protein disulfide isomerase and ER oxidoreductase. In the second case, ROS production occurs due to depletion of GSH during improper disulfide bond formation. ROS production could also result independently of disulfide formation. This could happen either due to calcium leak into the cytosol or during mitochondrial oxidative phosphorylation (12). It has been shown that ER stress can follow (9) or precede (13) oxidative stress.

Jun N terminal kinase (JNK) protein belongs to the class of mitogen activated protein kinase (MAPK). This protein has been found to be involved in the apoptotic response by inactivation of the anti-apoptotic protein Bcl-2. Phosphorylation or activation of the JNK protein to p-JNK has been found to be brought about by the UPR transducer-Ire1 (14). During the ER stress, Ire1 has been found to interact with tumor necrosis factor type 2 receptor associated protein (TRAF2) to form a complex with mitogen activated kinase kinase kinase protein- apoptosis signal regulating kinase 1 (ASK1) which then activates JNK by phosphorylation of JNK protein (15). Oxidative stress has been linked with a similar molecular pathway. ROS has been found to activate pJNK through oxidation of thioredoxin which forms a complex with ASK1. Due to the disruption of the complex, free ASK1 activates JNK and other MAPK involved in the cell death (16). Therefore, JNK activation could be considered a common pathway that links oxidative stress and ER stress (12).

The supplementary chapter of the thesis is an attempt to explore and link the two stresses observed with JS-K treatment. Also, this chapter has been devoted to show some incomplete studies that hold potential if investigated fully in the future. As shown in Chapter 4, ER stress was triggered by JS-K or P123/JS-K treatment in HL-60 cells. We extended our study to patient AML cell isolates. We tested the stress response in primary cells obtained from relapsed AML patients. We found that out of the two AML patient samples tested, one showed activation of ER stress. In the other set of the study carried out, we tested a common link between ER stress and oxidative stress. Oxidative stress and ER stress can be linked due to the anti-oxidant systems involved. As JS-K causes oxidative stress and hypothetically depletes GSH, the process of ER stress and oxidative stress might be linked.

A.2 Materials and Methods

A.2.1 Materials

JS-K was synthesized as previously described (17). Pluronic® polymers were obtained from BASF (Florham Park, NJ). Radio immuno precipitation assay (RIPA) cell lysis and extraction buffer was purchased from Thermo Fisher Scientific (Rockford, IL). Anti-pJNK and anti-JNK antibodies were obtained from Santa Cruz Biotechnology, Inc (Dallas, TX). All other antibodies or chemicals and reagents were from Sigma Aldrich (St Louis, MO) unless otherwise indicated. Densitometric analysis were performed by a lab outside the University of Utah using Fluorochem 2000 software (ProteinSimple, CA).

A.2.2 Cell culture

Human myeloid leukemia HL-60 cells (ATCC, Manassas, VA) were cultured in RPMI-1640 supplemented with 10% fetal bovine serum (FBS), penicillin/streptomycin and mycozap. Cells were cultured at 37°C in a 5% CO_2 humidified atmosphere. Primary AML patient samples were obtained from two relapsed AML patients and were frozen under liquid nitrogen under a protocol approved by the University of Utah Institutional Review Board.

A.2.3 Western blot

HL-60 cells or AML patients samples were treated with free JS-K (5 **μ**M) formulated in DMSO or micelle JS-K (5 **μ**M) formulated in 2.25% P123 for 6-18 h for ER stress experiments on AML patient sample cells or for 4-6 h for pJNK experiments in HL-60 cells. The cells were also treated with JNK or pJNK positive control and a P123 and no drug control was established. After treatment, the cells were collected and washed with PBS. Following centrifugation, commercially available RIPA lysis buffer (25mM Tris HCl (pH 7.6), 150mM NaCl, 1% NP-40, 1% sodium deoxycholate, 0.1% SDS) supplemented with phenylmethylsulfonyl fluoride (PMSF) and protease inhibitor was added to the pellet. The lysates were sonicated (50% intensity for 15 seconds), centrifuged and the supernatant was collected and protein concentration measured using the BCA protein assay reagent (Pierce Biotechnology). Loading buffer and reducing agent (DTT, Invitrogen) were added to the samples and electrophoresed in a 10% polyacrylamide gel (Biorad). Proteins were transferred to polyvinylidene difluoride (PVDF) membranes at 110 V for 95 min. (Biorad) for ER stress experiments or at 30 V for 120 min. (Invitrogen) for pJNK experiments. The blots were blocked for 1 h in 2.5%

nonfat dry milk diluted in tris-buffered saline containing 0.2% tween (TBST) and washed with TBST (3X, 7 min. each). The membrane was then incubated with primary antibody (anti-GRP-78 or anti-CHOP or anti-JNK or anti-pJNK or anti-actin) in 2.5% nonfat dry milk/TBST overnight. Membranes were washed (3X, 7 min. each) and incubated with horseradish peroxidase-conjugated secondary antibody in 2.5% nonfat dry milk in TBST for 2 h. The membrane was washed again in TBST thrice for 7 min. each and transferred proteins were detected with ECL substrate (GE Healthcare, Piscataway, NJ).

A.3 Results and Discussion

This study was also carried out on 2 archived AML patient samples. We saw enhanced GRP-78 expression in 1 of the 2 patient samples (Fig. A1). We also showed prolonged CHOP expression by JS-K or P123/JS-K treatment in 1 of 2 AML patient samples (Fig. A1). Basal level GRP-78 and CHOP expression was also observed in the same sample. The expression in an AML patient sample has two implications. First, JS-K or P123/JS-K treatment could induce ER stress in some patients. In fact, we observed that even basal level of GRP-78 or CHOP expression was not observed in patient 2 sample. It has been suggested that basal level of ER stress protein expression is essential for enhancing the stress and driving them towards the apoptotic response. In one study carried out on patient samples, it was found that patient samples with basal level expression of ER stress proteins were associated with a better prognosis and survival (18). In the case of JS-K, further investigation with a larger number of patient samples is necessary in order to confirm our preliminary observations. One factor to take into account as well is the effect of prolonged storage on archived patient samples.

The kinase protein c-JNK (c-JUN-NH2-terminal kinase) was activated when the HL-60 cells were treated with JS-K or P123/JS-K (Fig. A.2). JNK activation leads to phosphorylation of the JNK protein, which then is involved in the apoptotic cascade. We obtained variable results with Western blots (Fig. A.3). Densitometric analysis showed some differences between the different treatment and control groups (Table A.1). However, results were variable and not uniformly reproducible. In some, JNK activation increased from 4 to 6 hours. Therefore, JNK activation could not be treated as the link connecting ER stress response with oxidative stress. To establish any link, more conclusive studies are required.

As explained in Chapter 4, the JNK study was carried out to explore a link, if any, between ER stress and oxidative stress. JNK activation has been previously shown by JS-K treatment in lung cancer (19), liver cancer (20) and multiple myeloma (21). However, all the studies showed JNK activation in response to MAPK or oxidative stress. This was the first time we tried to link the two pathways activated by JS-K. Although the results obtained with JNK activation are inconclusive at this point, more direct study such as activation of Ire-1 and Ero-1 could confirm if ER stress and oxidative stress are linked.

A.4 Conclusions

We showed increased expression of ER stress markers in 1 of 2 AML primary samples studied. The study discussed yielded inconclusive results about the involvement of JNK protein for mediating apoptotic response. It could not be ascertained from the study if JNK could be considered a link between ER stress and oxidative stress. Therefore, more investigation would be needed in order to determine whether JS-K produces apoptosis by producing oxidative stress followed by ER stress in AML.

A.5 References

1. English AR, Voeltz GK. Endoplasmic reticulum structure and interconnections with other organelles. Cold Spring Harb Perspect Biol. 2013;5(4):a013227.

2. Gardner BM, Pincus D, Gotthardt K, Gallagher CM, Walter P. Endoplasmic reticulum stress sensing in the unfolded protein response. Cold Spring Harb Perspect Biol. 2013;5(3):a013169.

3. Hoozemans JJ, Scheper W. Endoplasmic reticulum: the unfolded protein response is tangled in neurodegeneration. Int J Biochem Cell Biol. 2012;44(8):1295-1298.

4. Hosoi T, Ozawa K. Endoplasmic reticulum stress in disease: mechanisms and therapeutic opportunities. Clin Sci (Lond). 2010;118(1):19-29.

5. Kaufman RJ, Back SH, Song B, Han J, Hassler J. The unfolded protein response is required to maintain the integrity of the endoplasmic reticulum, prevent oxidative stress and preserve differentiation in beta-cells. Diabetes Obes Metab. 2010;12 Suppl 2:99-107.

6. Li X, Zhang K, Li Z. Unfolded protein response in cancer: the physician's perspective. J Hematol Oncol. 2011;4:8.

7. Minamino T, Komuro I, Kitakaze M. Endoplasmic reticulum stress as a therapeutic target in cardiovascular disease. Circ Res. 2010;107(9):1071-1082.

8. Wu RF, Ma Z, Liu Z, Terada LS. Nox4-derived H2O2 mediates endoplasmic reticulum signaling through local Ras activation. Mol Cell Biol. 2010;30(14):3553-3568.

9. Guo R, Ma H, Gao F, Zhong L, Ren J. Metallothionein alleviates oxidative stress-induced endoplasmic reticulum stress and myocardial dysfunction. J Mol Cell Cardiol. 2009;47(2):228-237.

10. Townsend DM, Manevich Y, He L, Xiong Y, Bowers RR, Jr., Hutchens S, Tew KD. Nitrosative stress-induced s-glutathionylation of protein disulfide isomerase leads to activation of the unfolded protein response. Cancer Res. 2009;69(19):7626-7634.

11. Szegezdi E, Logue SE, Gorman AM, Samali A. Mediators of endoplasmic reticulum stress-induced apoptosis. EMBO Rep. 2006;7(9):880-885.

12. Malhotra JD, Kaufman RJ. Endoplasmic reticulum stress and oxidative stress: a vicious cycle or a double-edged sword? Antioxid Redox Signal. 2007;9(12):2277-2293.

13. Malhotra JD, Miao H, Zhang K, Wolfson A, Pennathur S, Pipe SW, Kaufman RJ. Antioxidants reduce endoplasmic reticulum stress and improve protein secretion. Proc Natl Acad Sci U S A. 2008;105(47):18525-18530.

14. Chiu SC, Chen SP, Huang SY, Wang MJ, Lin SZ, Harn HJ, Pang CY. Induction of apoptosis coupled to endoplasmic reticulum stress in human prostate cancer cells by n-butylidenephthalide. PLoS One. 2012;7(3):e33742.

15. Nishitoh H, Matsuzawa A, Tobiume K, Saegusa K, Takeda K, Inoue K, Hori S, Kakizuka A, Ichijo H. ASK1 is essential for endoplasmic reticulum stress-induced neuronal cell death triggered by expanded polyglutamine repeats. Genes Dev. 2002;16(11):1345-1355.

16. Tobiume K, Saitoh M, Ichijo H. Activation of apoptosis signal-regulating kinase 1 by the stress-induced activating phosphorylation of pre-formed oligomer. J Cell Physiol. 2002;191(1):95-104.

17. Udupi V, Yu M, Malaviya S, Saavedra JE, Shami PJ. JS-K, a nitric oxide prodrug, induces cytochrome c release and caspase activation in HL-60 myeloid leukemia cells. Leuk Res. 2006;30(10):1279-1283.

18. Schardt JA, Weber D, Eyholzer M, Mueller BU, Pabst T. Activation of the unfolded protein response is associated with favorable prognosis in acute myeloid leukemia. Clin Cancer Res. 2009;15(11):3834-3841.

19. Maciag AE, Chakrapani H, Saavedra JE, Morris NL, Holland RJ, Kosak KM, Shami PJ, Anderson LM, Keefer LK. The nitric oxide prodrug JS-K is effective against non-small-cell lung cancer cells in vitro and in vivo: involvement of reactive oxygen species. J Pharmacol Exp Ther. 2011;336(2):313-320.

20. Ren Z, Kar S, Wang Z, Wang M, Saavedra JE, Carr BI. JS-K, a novel non-ionic diazeniumdiolate derivative, inhibits Hep 3B hepatoma cell growth and induces c-Jun phosphorylation via multiple MAP kinase pathways. J Cell Physiol. 2003;197(3):426-434.

21. Kiziltepe T, Hideshima T, Ishitsuka K, Ocio EM, Raje N, Catley L, Li CQ, Trudel LJ, Yasui H, Vallet S, Kutok JL, Chauhan D, Mitsiades CS, Saavedra JE, Wogan GN, Keefer LK, Shami PJ, Anderson KC. JS-K, a GST-activated nitric oxide generator, induces DNA double-strand breaks, activates DNA damage response

pathways, and induces apoptosis in vitro and in vivo in human multiple myeloma cells. Blood. 2007;110(2):709-718.

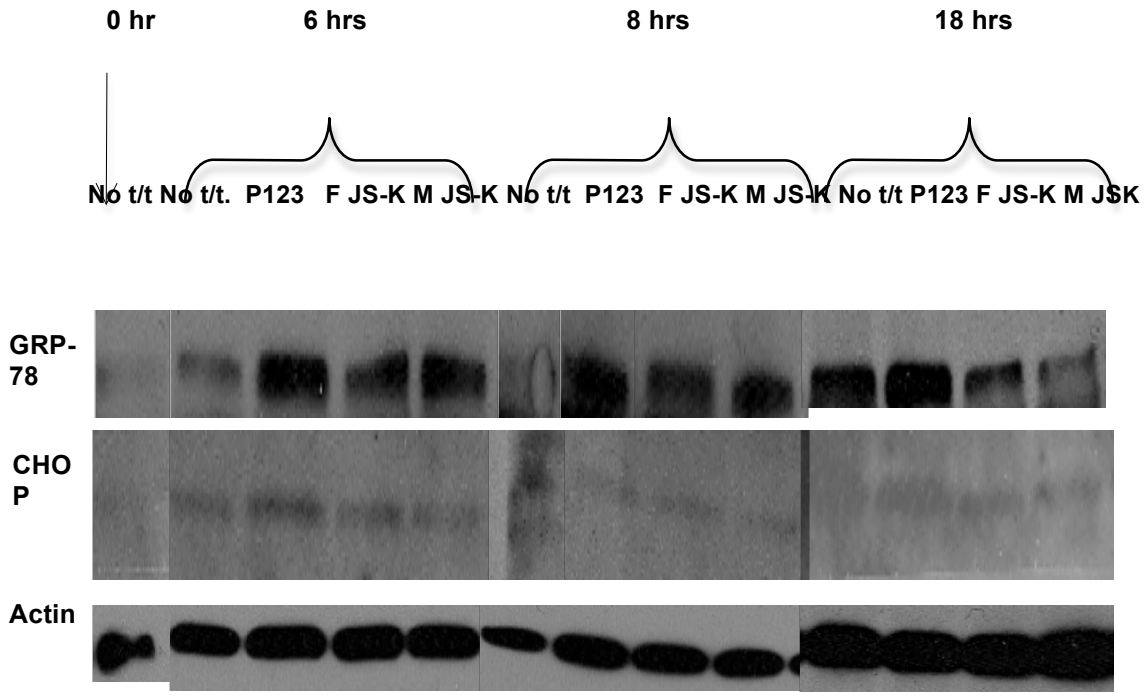

Fig. A.1: Activation ER stress by JS-K. Primary AML cells from patient 1 were treated with the indicated drugs for the indicated period of time. Induction of GRP-78 or CHOP was verified when compared to No treatment. No t/t: No treatment

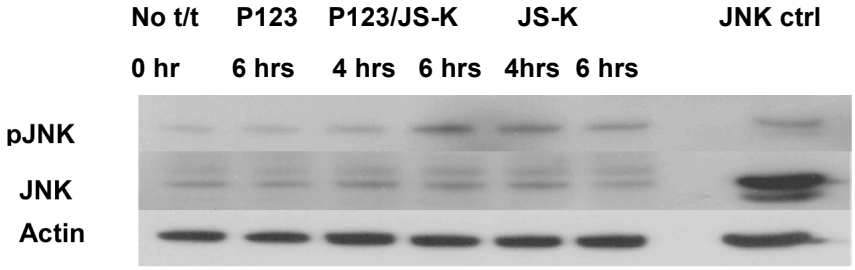

Fig. A.2: JNK protein phosphorylation after 4 hr or 6 hr treatment of HL-60 cells with JS-K or P123/JS-K. No t/t: no treatment; JNK ctrl: positive JNK control

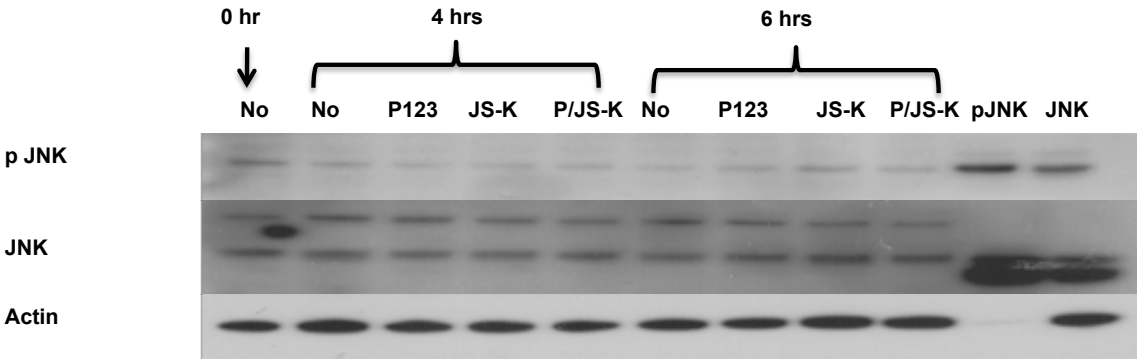

Fig A.3: JNK protein phosphorylation after 4 hr or 6 hr treatment of HL-60 cells with JS-K or P123/JS-K treatment. Not much difference was observed in no treatment and treatment. No: No treatment; P/JS-K: P123/JS-K; pJNK and JNK: positive controls

Table A.1: JNK, pJNK and actin levels in two separate experiments. Notice the difference in pJNK levels in the two experiments when treatment is compared to no treatment.

Time (hrs)/Exp#	Formulation	pJNK	JNK	JNK/pJNK	Actin
0/1	No Treatment	22984	71820	0.320022278	116964
4/1	No Treatment	23426	72960	0.321080044	121068
4/1	P123	23426	70680	0.331437465	116964
4/1	JSK	24310	71820	0.338485102	125856
4/1	P123/JS-K	26078	72960	0.357428728	130644
6/1	No Treatment	27404	71820	0.381565024	132696
6/1	P123	25194	74100	0.34	131328
6/1	JSK	26962	77520	0.347807018	130644
6/1	P123/JS-K	31382	77520	0.404824561	123804
6/1	p-JNK Control	28288	160740	0.175986064	786600
6/1	JNK Control	26520	109440	0.242324561	119700
0/2	No Treatment	67716	179860	0.376492828	66640
4/2	No Treatment	52668	173604	0.303380106	81340
4/2	P123	45828	159528	0.287272454	69090
4/2	JSK	47196	162656	0.290158371	70070
4/2	P123/JS-K	46512	172040	0.270355731	66640
6/2	No T	45828	176732	0.259307879	72520
6/2	P123	49932	189244	0.263849845	70560
6/2	JSK	51300	204884	0.250385584	79380
6/2	P123/JS-K	46512	204884	0.227016263	77420
6/2	p-JNK Control	75240	273700	0.274899525	25480
6/2	JNK Control	65664	237728	0.276214834	75950